Tópicos en la evolución de Cetacea

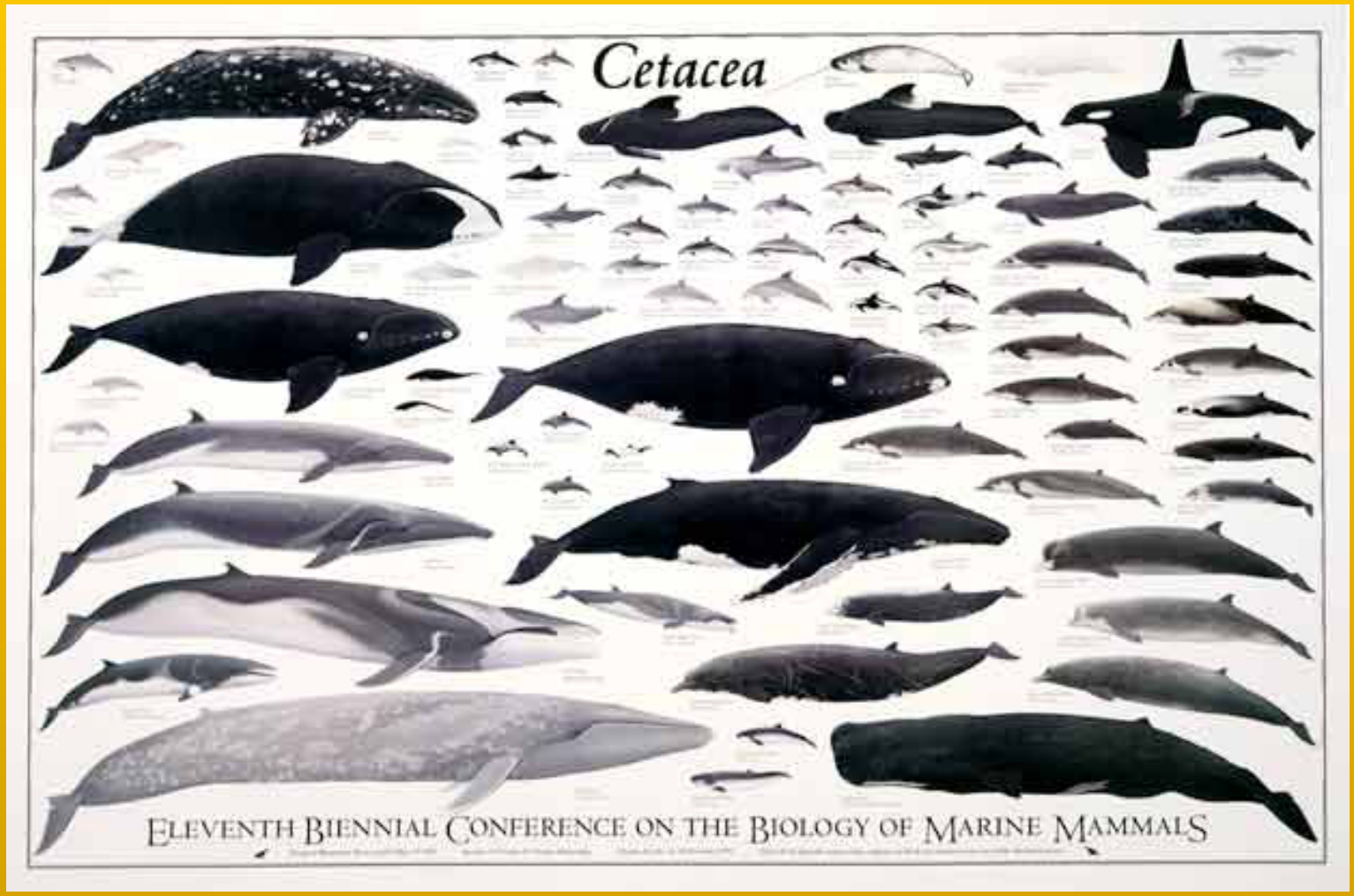

Carolina S. Gutstein

Lab. Ontogenia y Filogenia

Origen de los Cetaceos

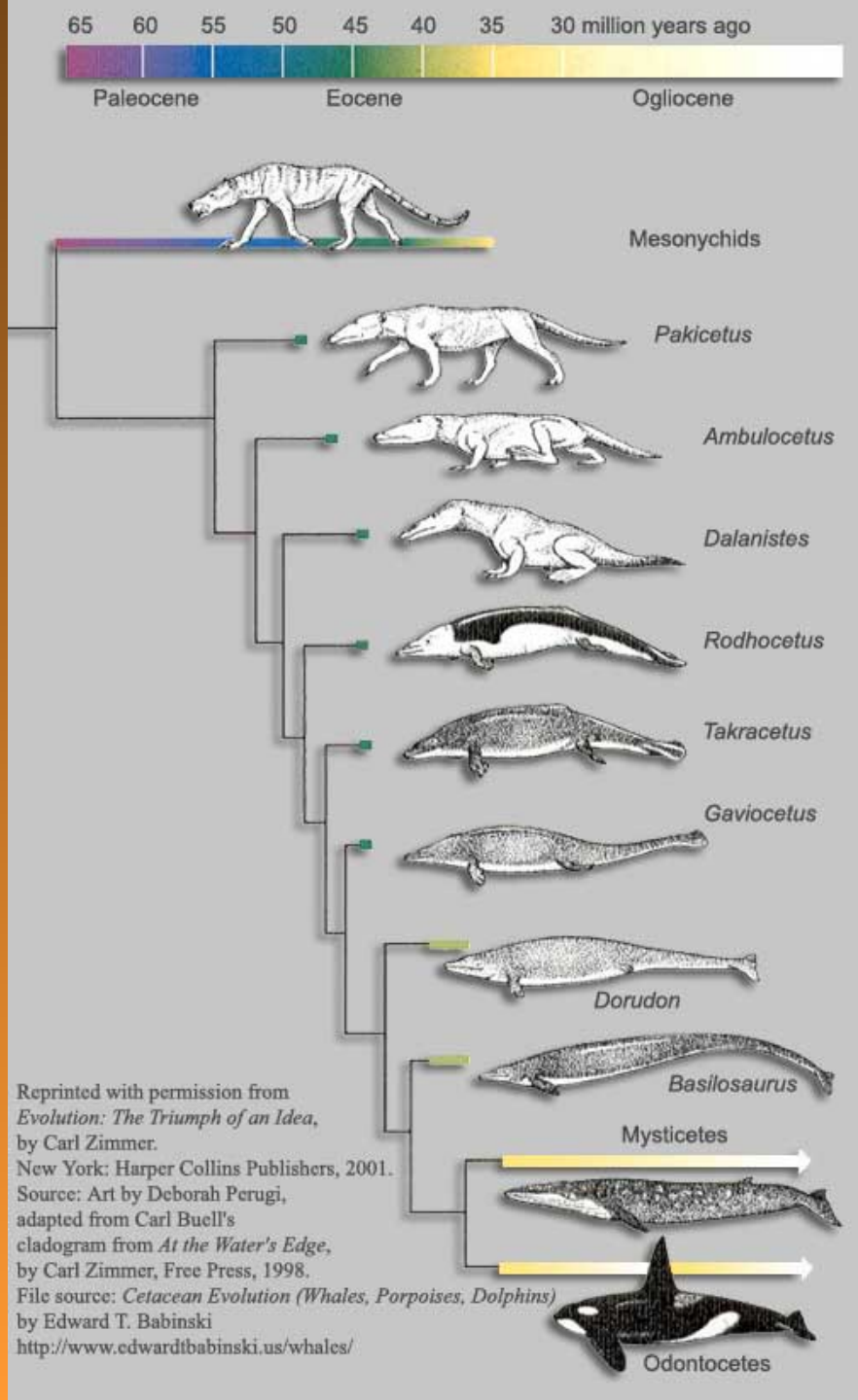

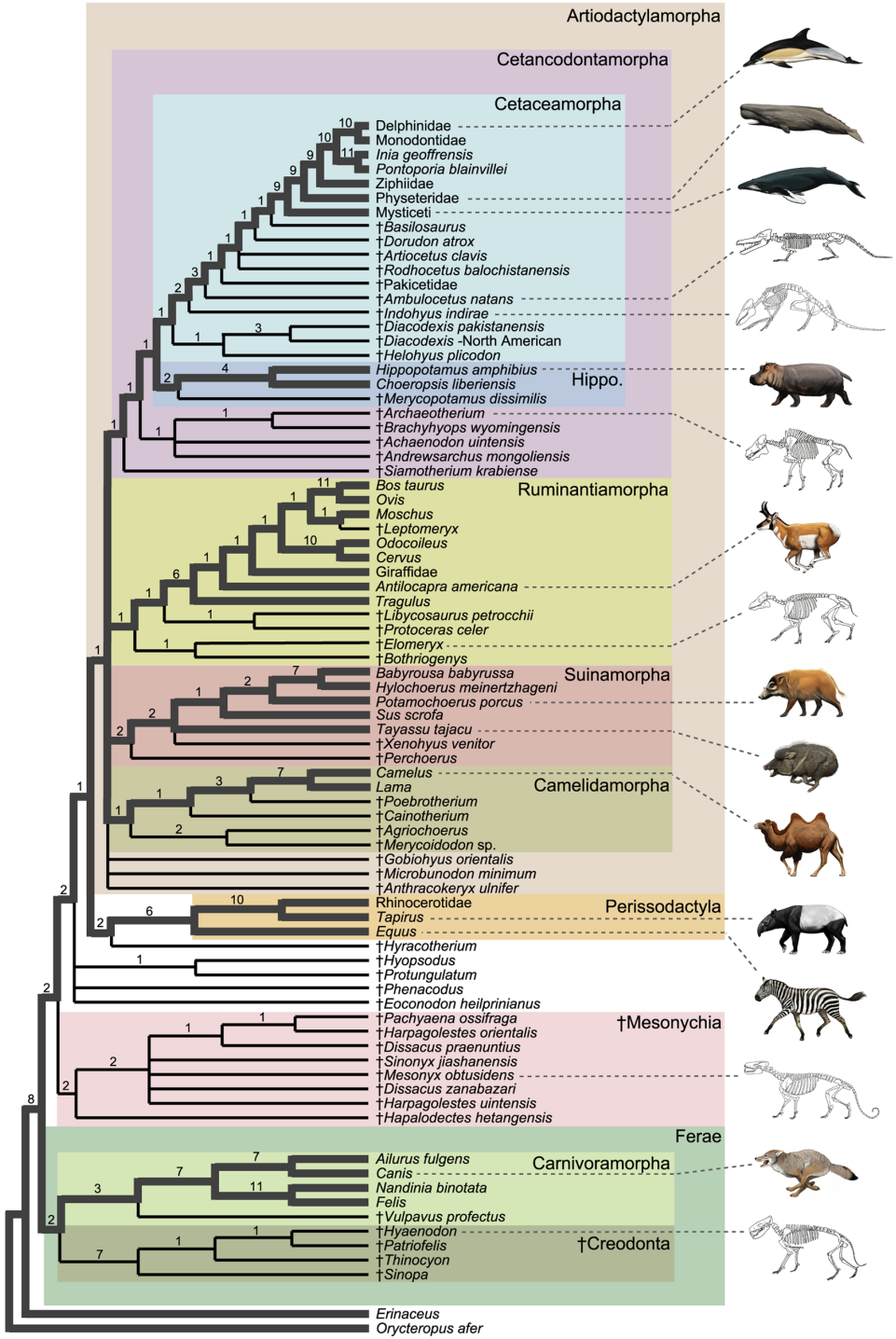

Figure 2. Strict consensus of 20 minimum length trees for the equally-weighted parsimony analysis of the combined data set (57,269 steps).

Mesonichidae+Cetacea
Proporcion escamoso-petrosal
Talonido m2 comprimido
Ausencia dientes bunodontes
Trigonido mas alto que talonido
Ausencia entoconido y postentocristido

Cetacea
Facetas molares inferiores alargadas verticalmente

Figure 3. Comparison of one minimum length tree with agreement subtree superimposed (A) and a topology that is two steps beyond minimum length (B).

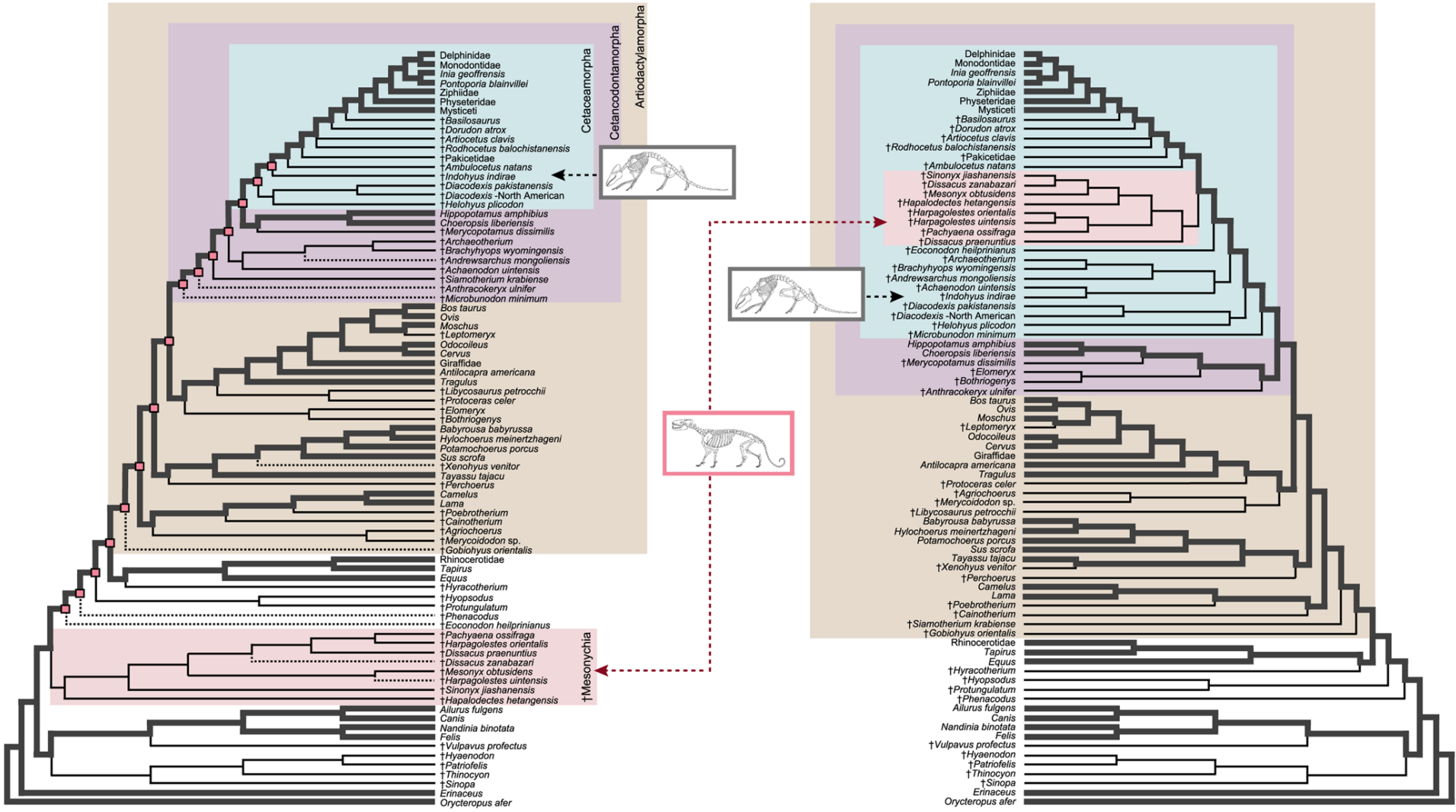

A) A most parsimonious tree; 57,269 steps

B) Two steps beyond minimum length; 57,271 steps

Spaulding M, O'Leary MA, Gatesy J (2009) Relationships of Cetacea (Artiodactyla) Among Mammals: Increased Taxon Sampling Alters Interpretations of Key Fossils and Character Evolution. PLOS ONE 4(9): e7062. https://doi.org/10.1371/journal.pone.0007062 https://journals.plos.org/plosone/article?id=10.1371/journal.pone.0007062

Thewissen et al. 2007

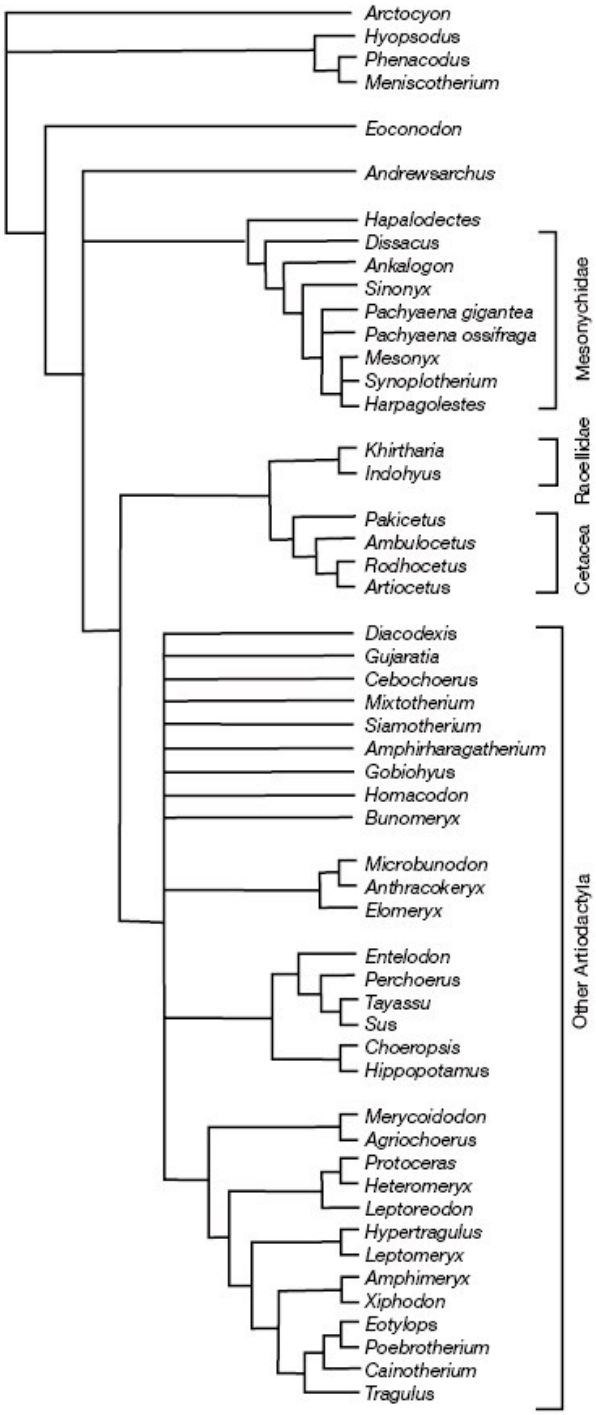

Cladograma de consenso resultante del análisis de parsimonia (búsqueda heuristica en PAUP; secuencia de adición aleatoria, 1,000 repeticiones),)

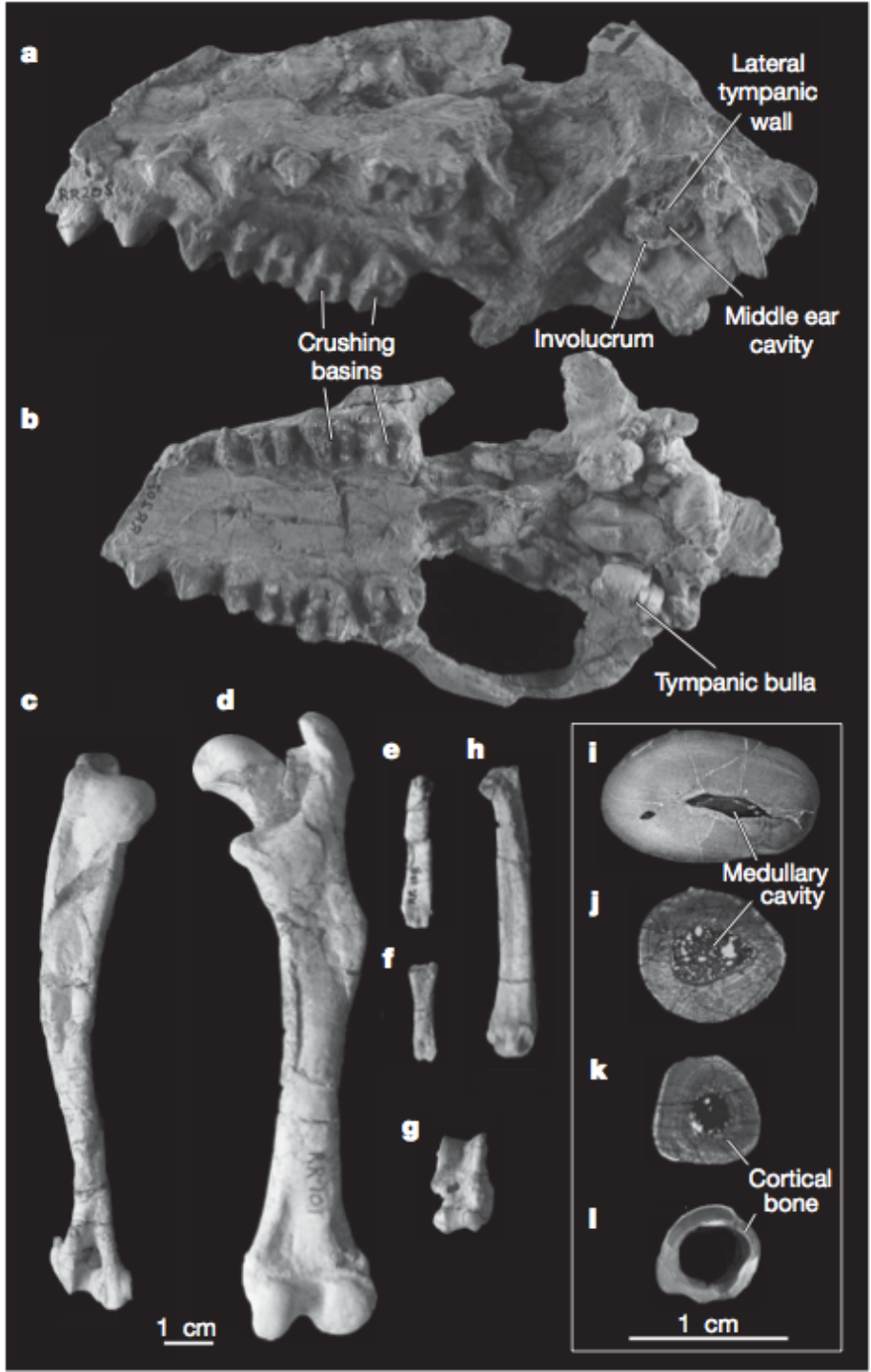

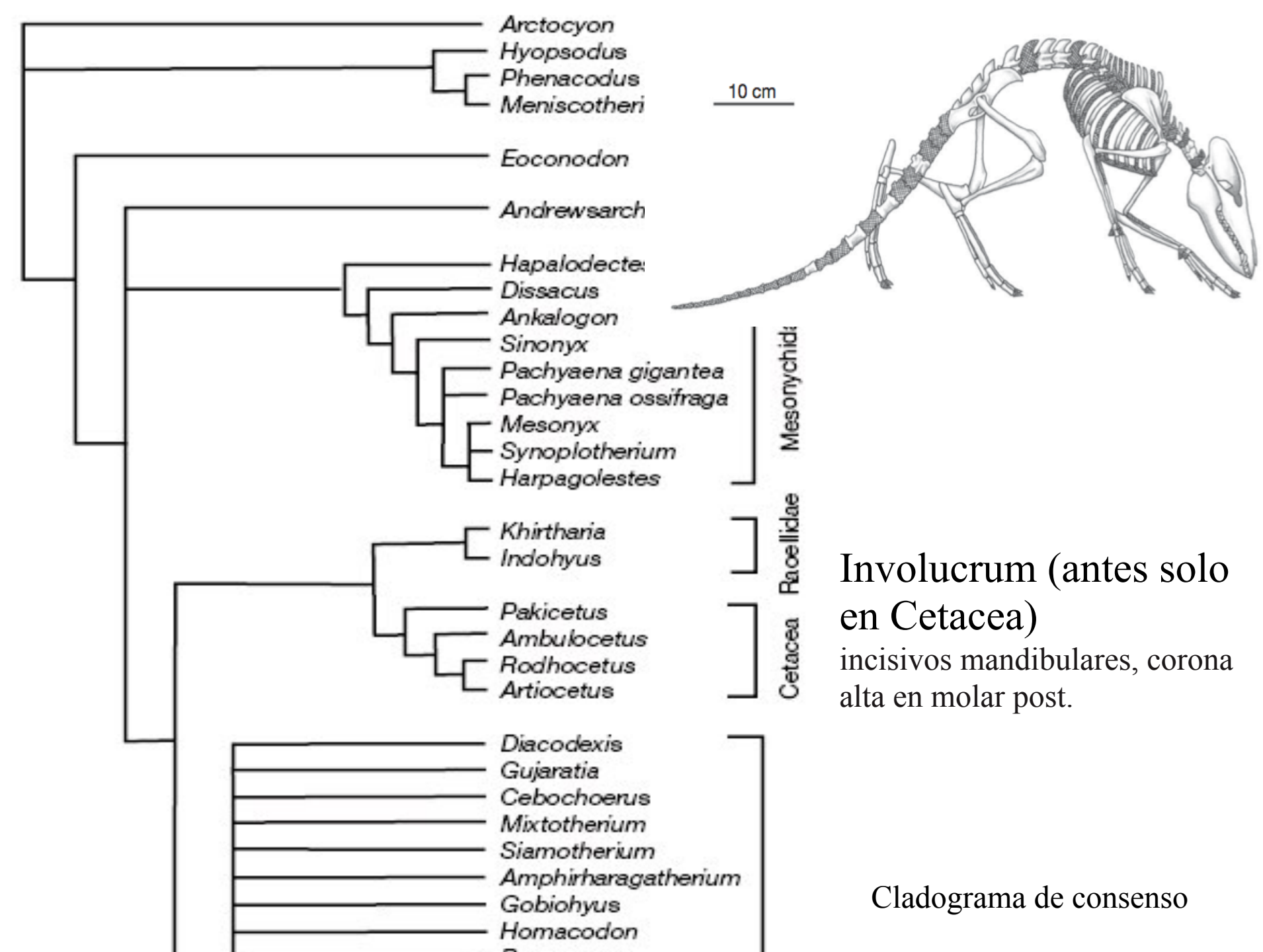

Involucrum (antes solo en Cetacea)

incisivos mandibulares, corona alta en molar post.

Cladograma de consenso

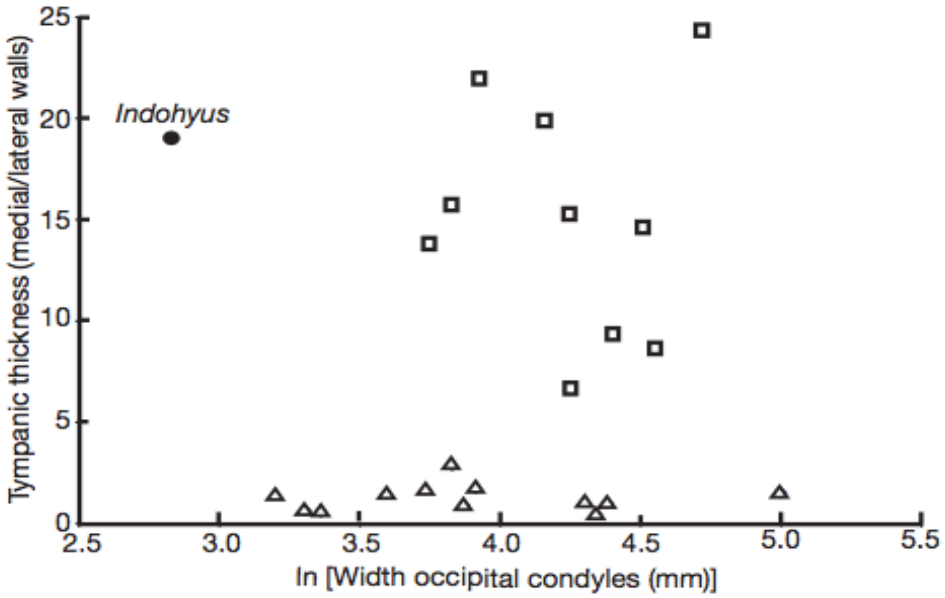
Tympanic thickness (medial/lateral walls)
25
20
15
10
5
0
Indohyus
2.5
3.0
3.5
4.0
4.5
5.0
5.5
ln [Width occipital condyles (mm)]

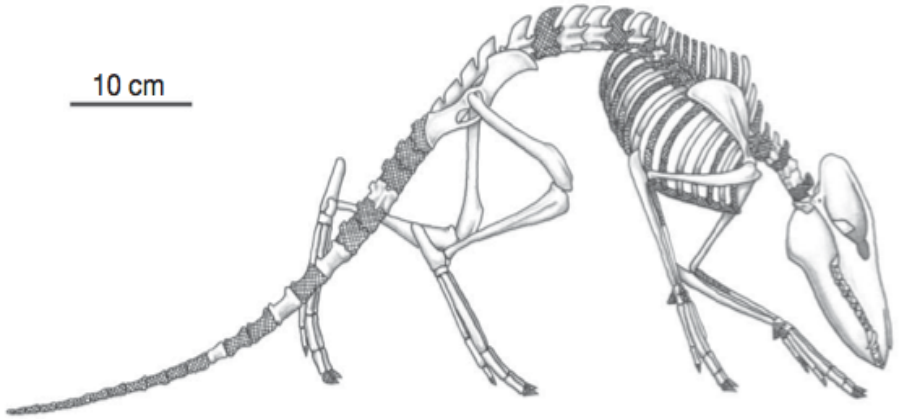
10 cm

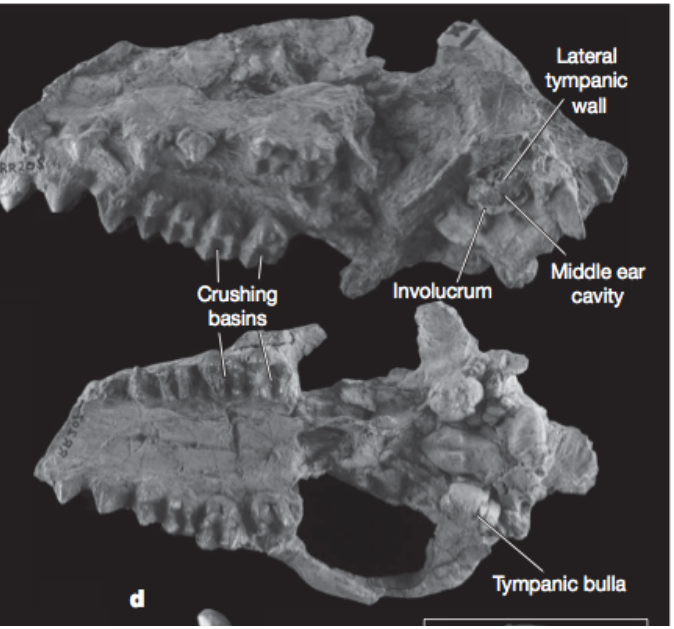
Lateral tympanic wall
Middle ear cavity
Involucrum
Crushing basins
Tympanic bulla
d

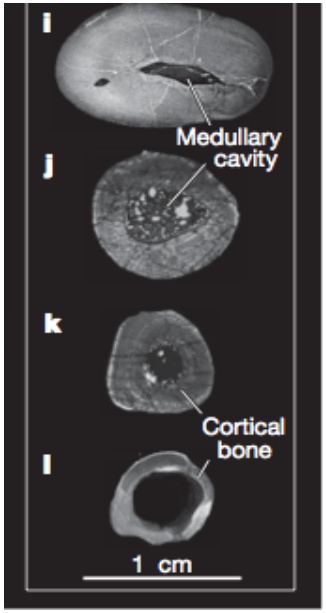
i
Medullary cavity
j
k
Cortical bone
l
1 cm

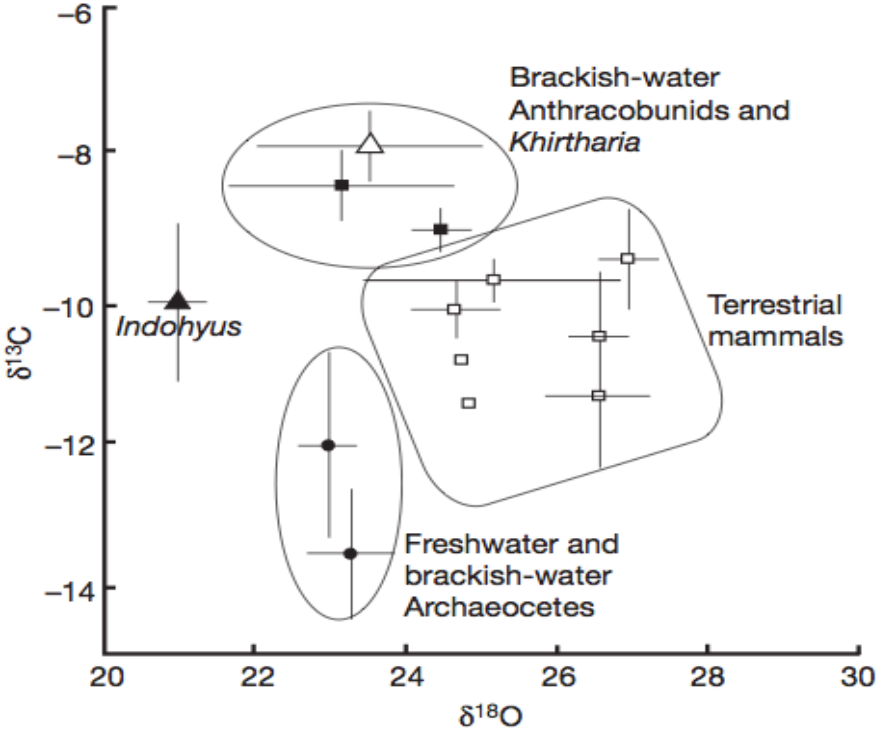
−6
−8
−10
−12
−14
δ13C
Brackish-water Anthracobunids and Khirtharia
Indohyus
Terrestrial mammals
Freshwater and brackish-water Archaeocetes
20
22
24
26
28
30
δ18O

Región ótica: Paquiostosis

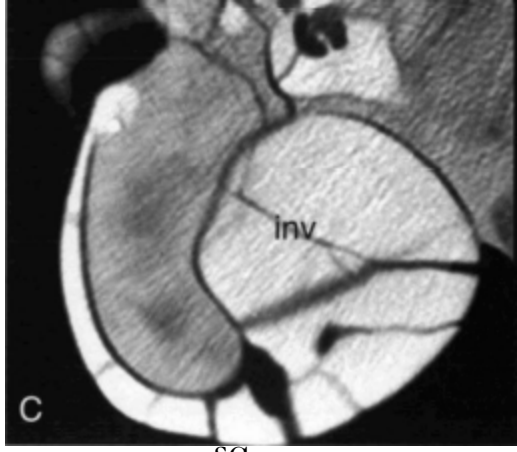

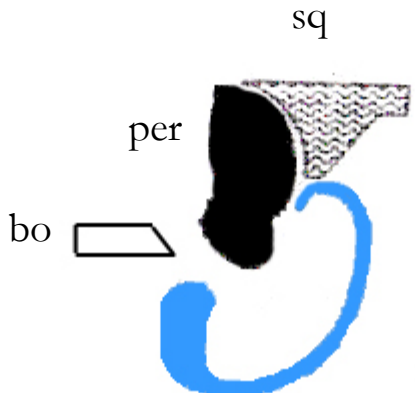

Basilosaurideos

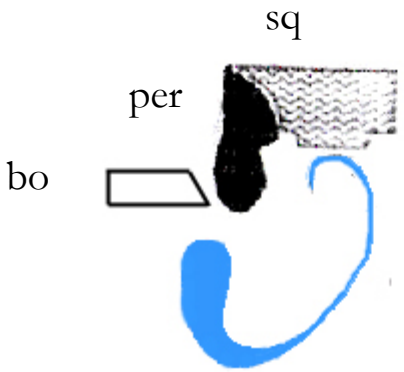

Paquicetideos

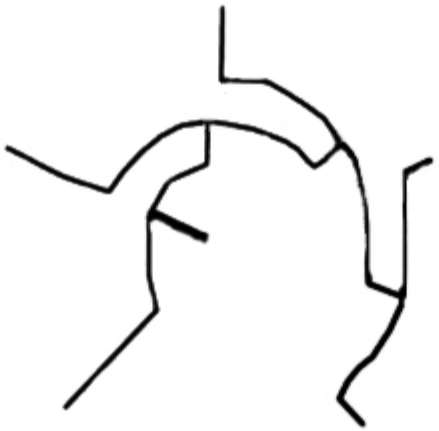

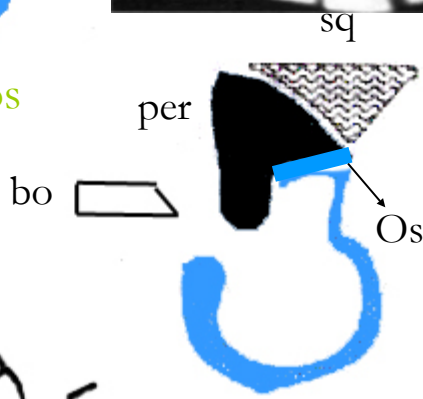

Baleanopterideos

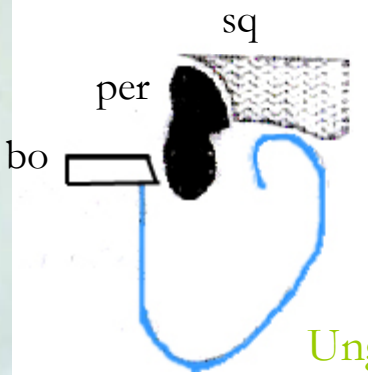

Ungulados

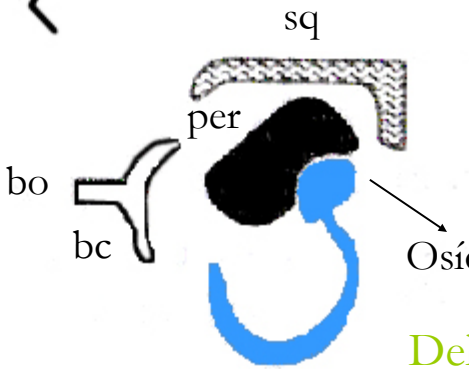

Delfinideos

Transición Tierra-mar

Aprox. 10-12 M.a. en el Eoceno

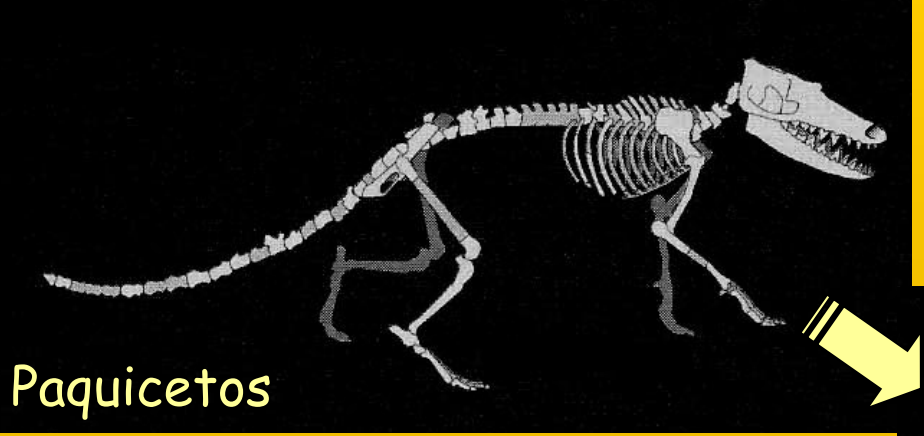

Paquicetos

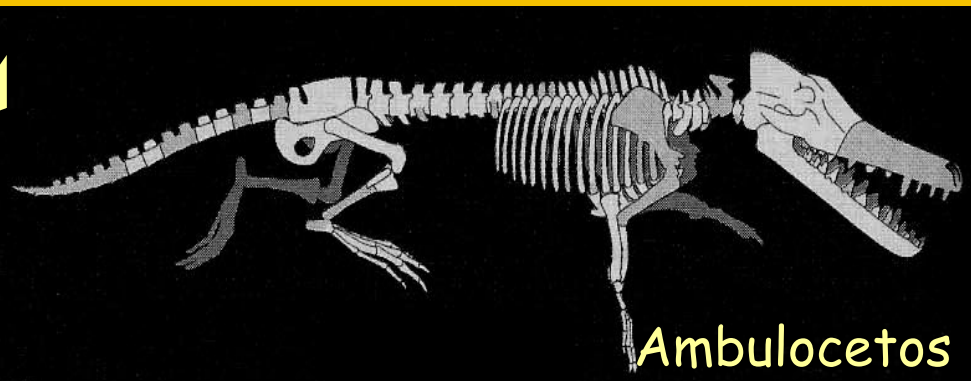

Ambulocetos

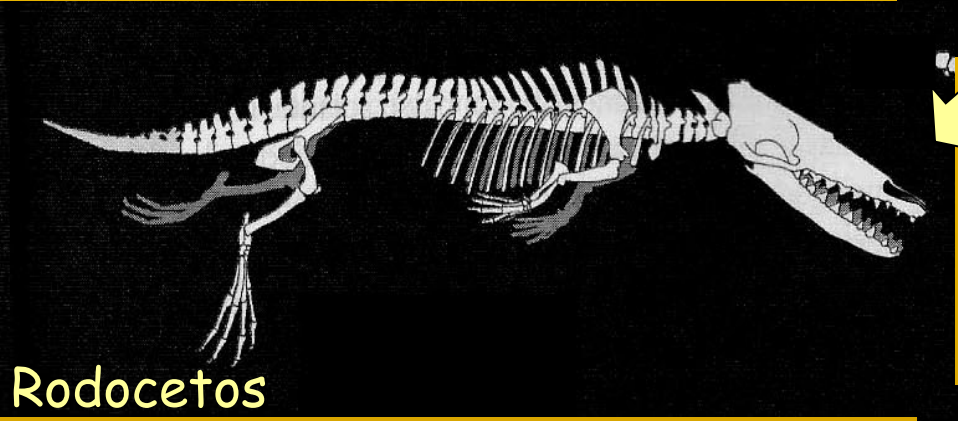

Rodocetos

Scanner batial

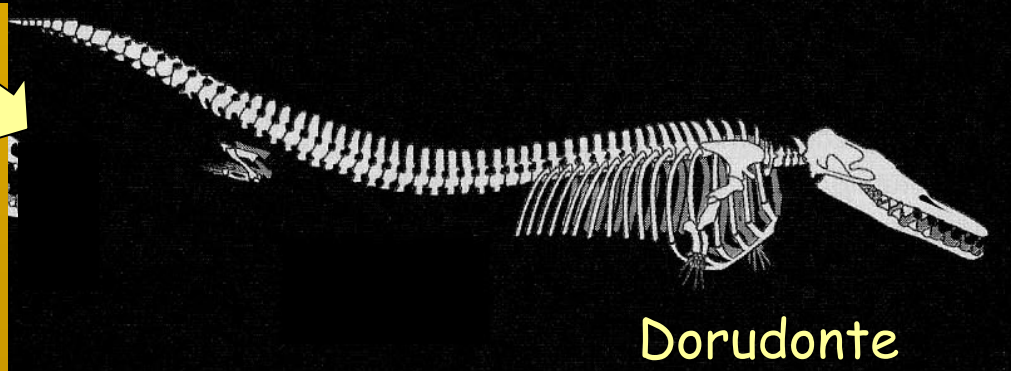

Dorudonte

Reducción miembros posteriores desde el Eoceno (50 m.a.)

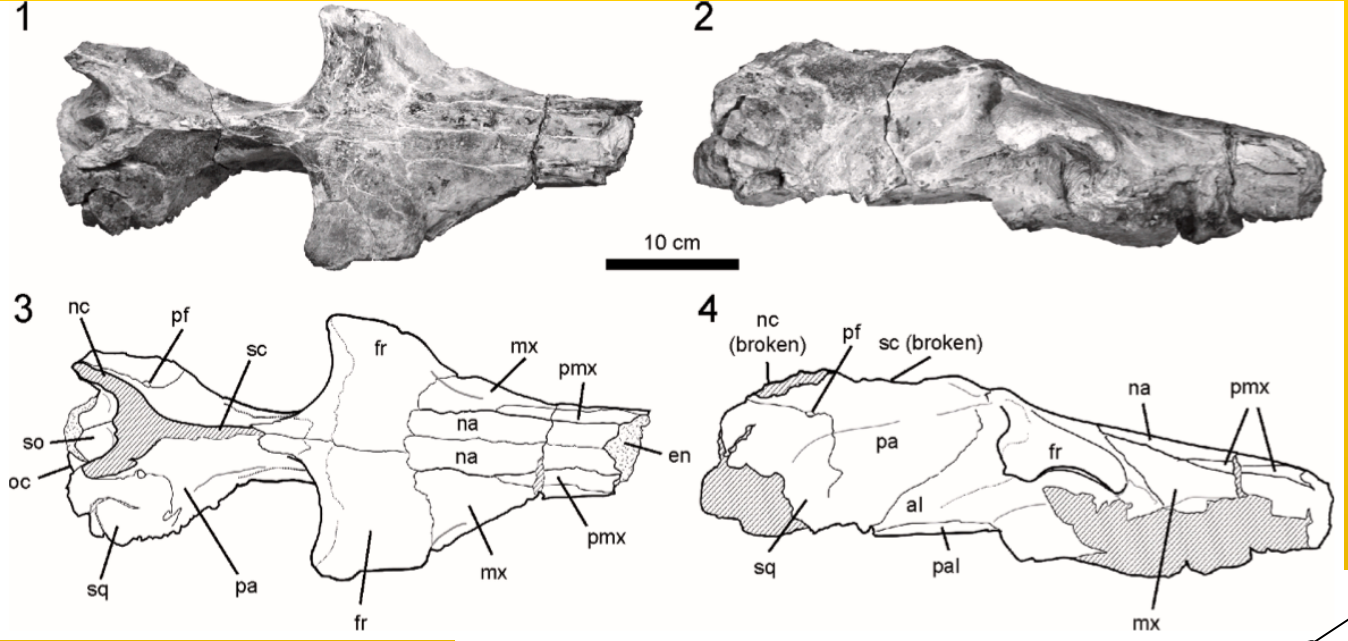

Ocucajea pickling
Eoceno medio, Peru

Protocetidae

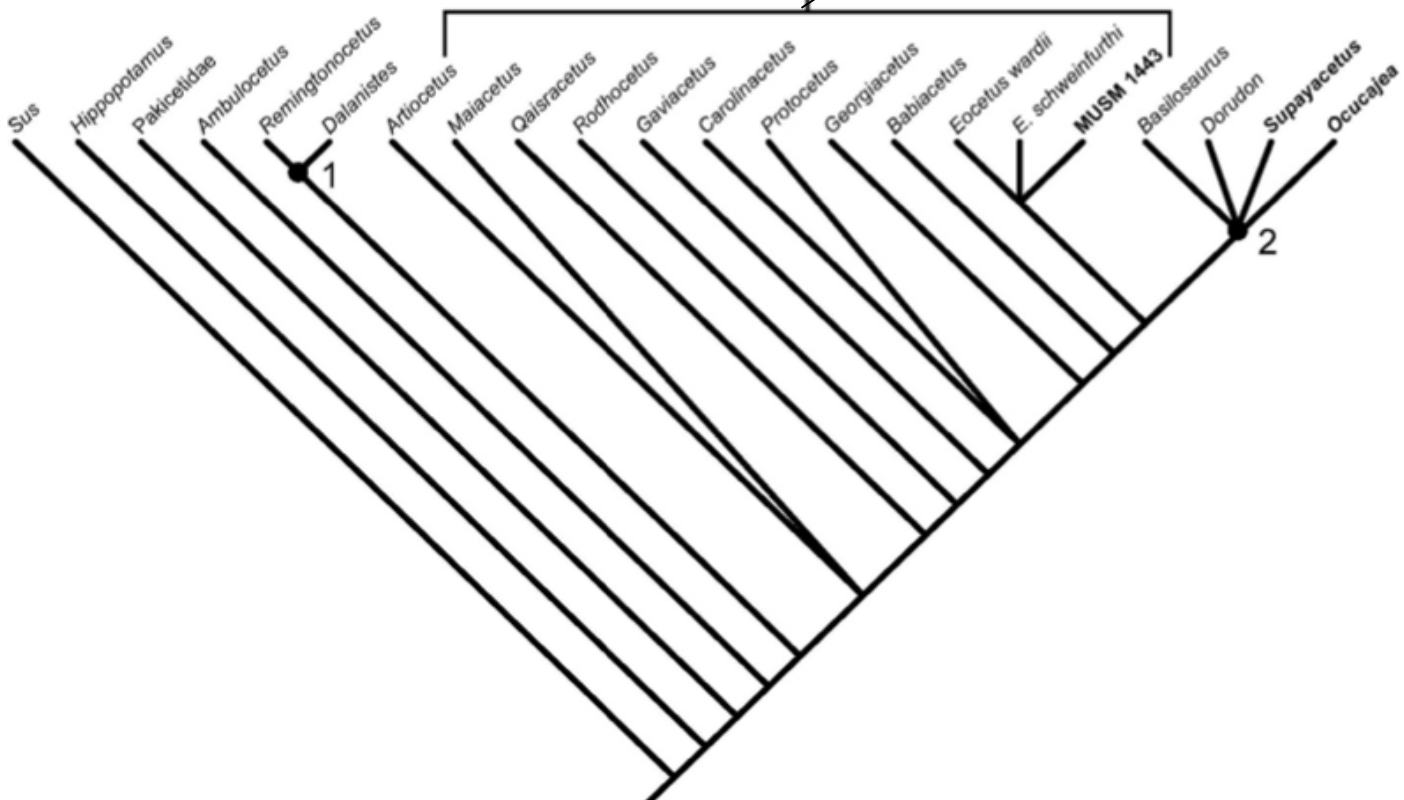

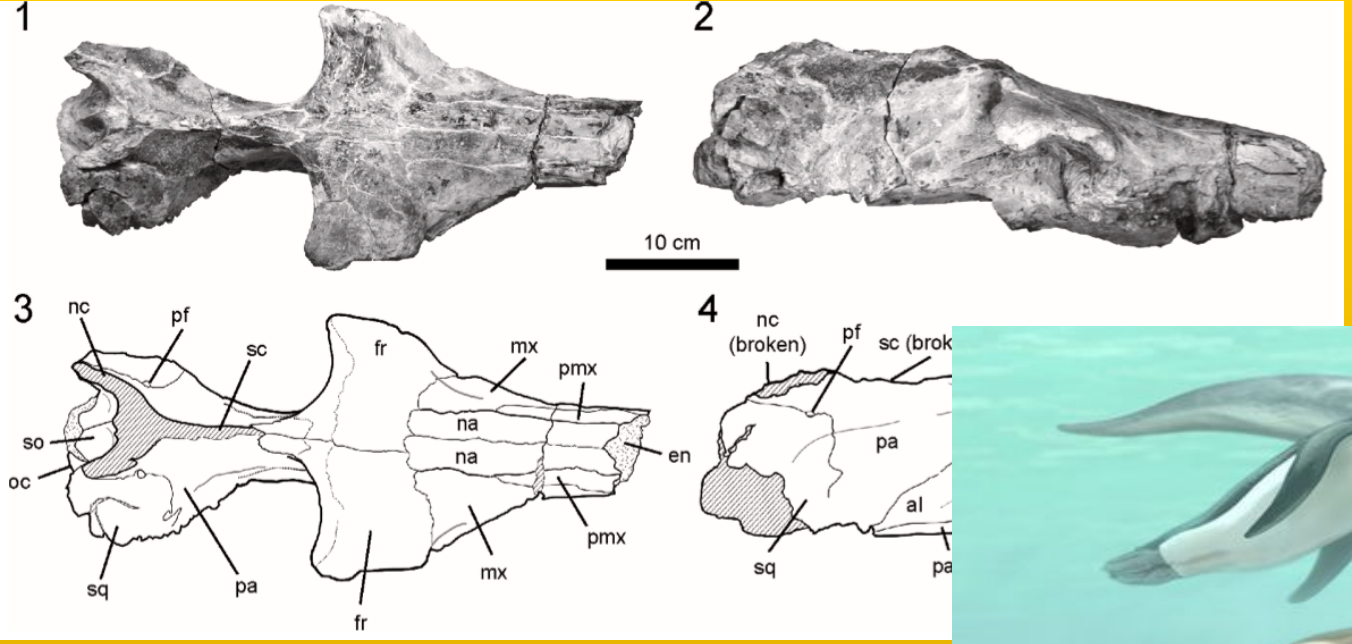
1
2
10 cm
3
nc
pf
sc
fr
mx
pmx
na
na
so
oc
en
pmx
mx
sq
pa
fr
4
nc
(broken)
pf
sc (brok
pa
al
sq
pa

Basilosaurus isis

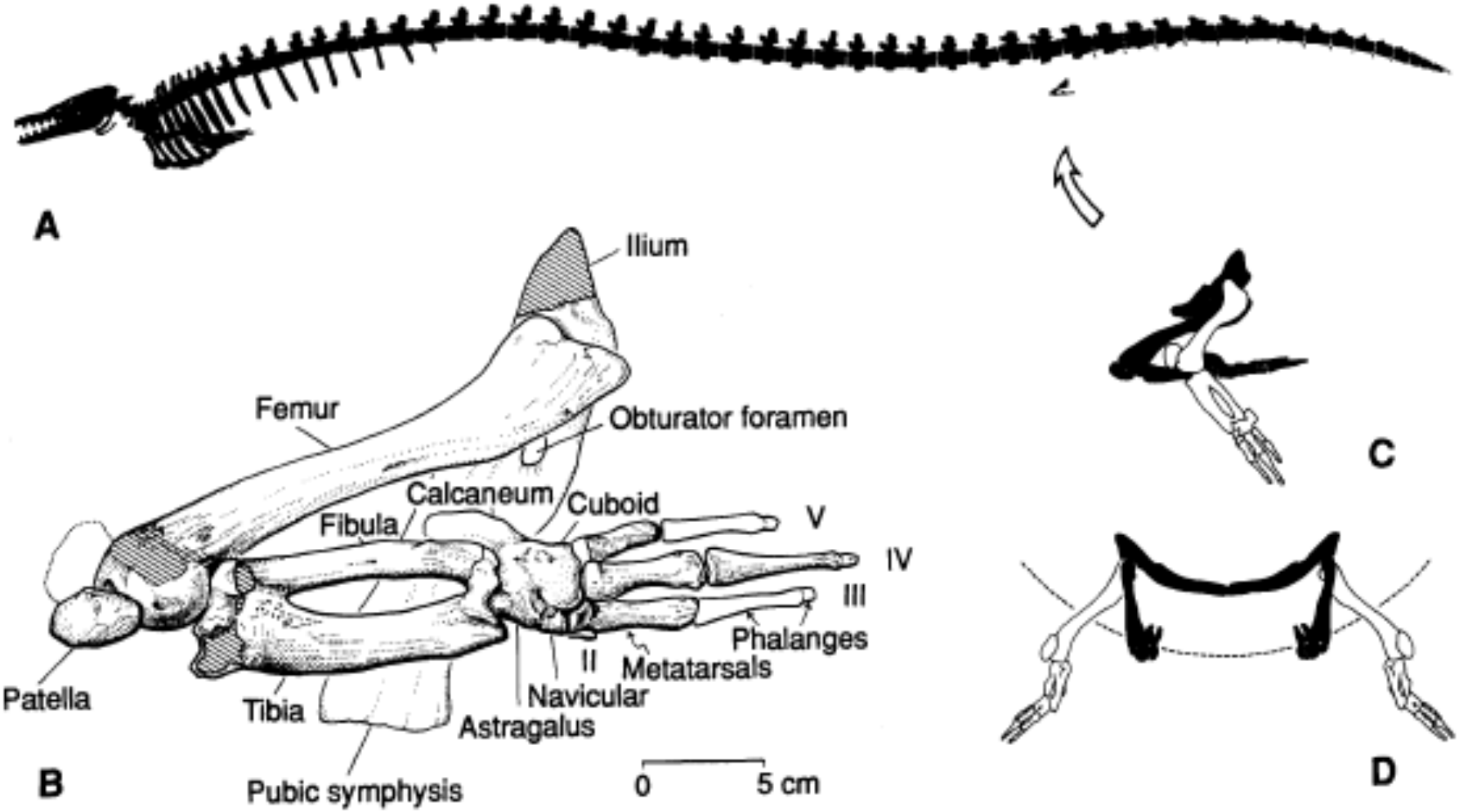

Cintura Pélvica sin función locomotora

perdida de conexión con vértebras sacrales

(Gingerich *et al.*, 1990; O'Leary & Uhen, 1999; Hulbert *et al.* 1998)

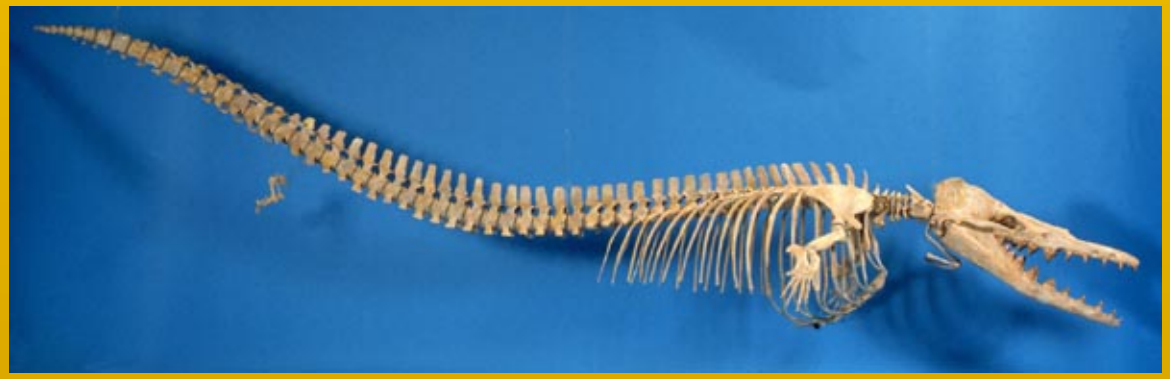

Dorudon, con miembros desconectados

Limbs in whales and limblessness in other vertebrates: mechanisms of evolutionary and developmental transformation and loss

Lars Bejder* and Brian K. Hall[1]

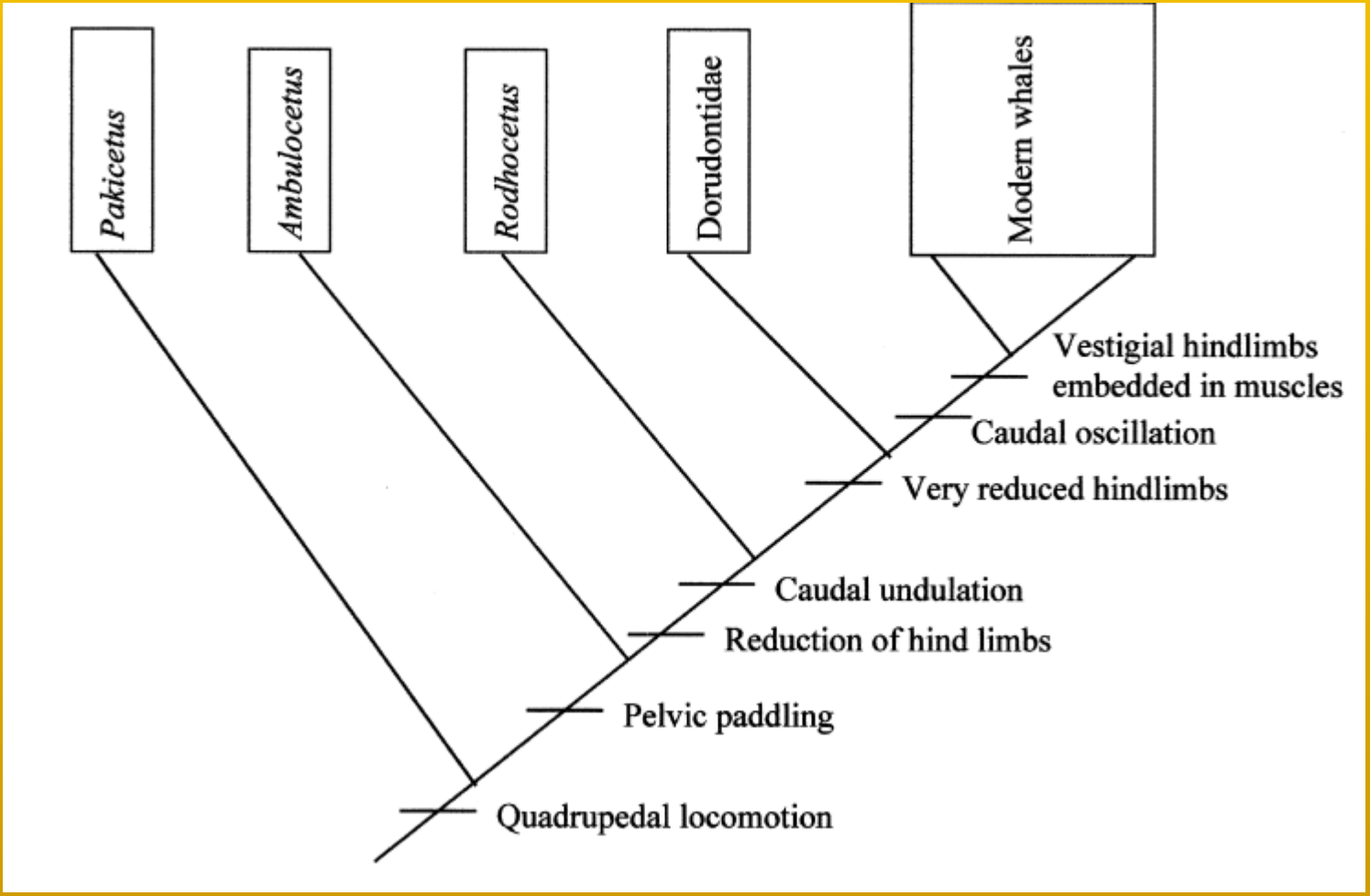

EVOLUTION & DEVELOPMENT Vol. 4, No. 6, November–December 2002

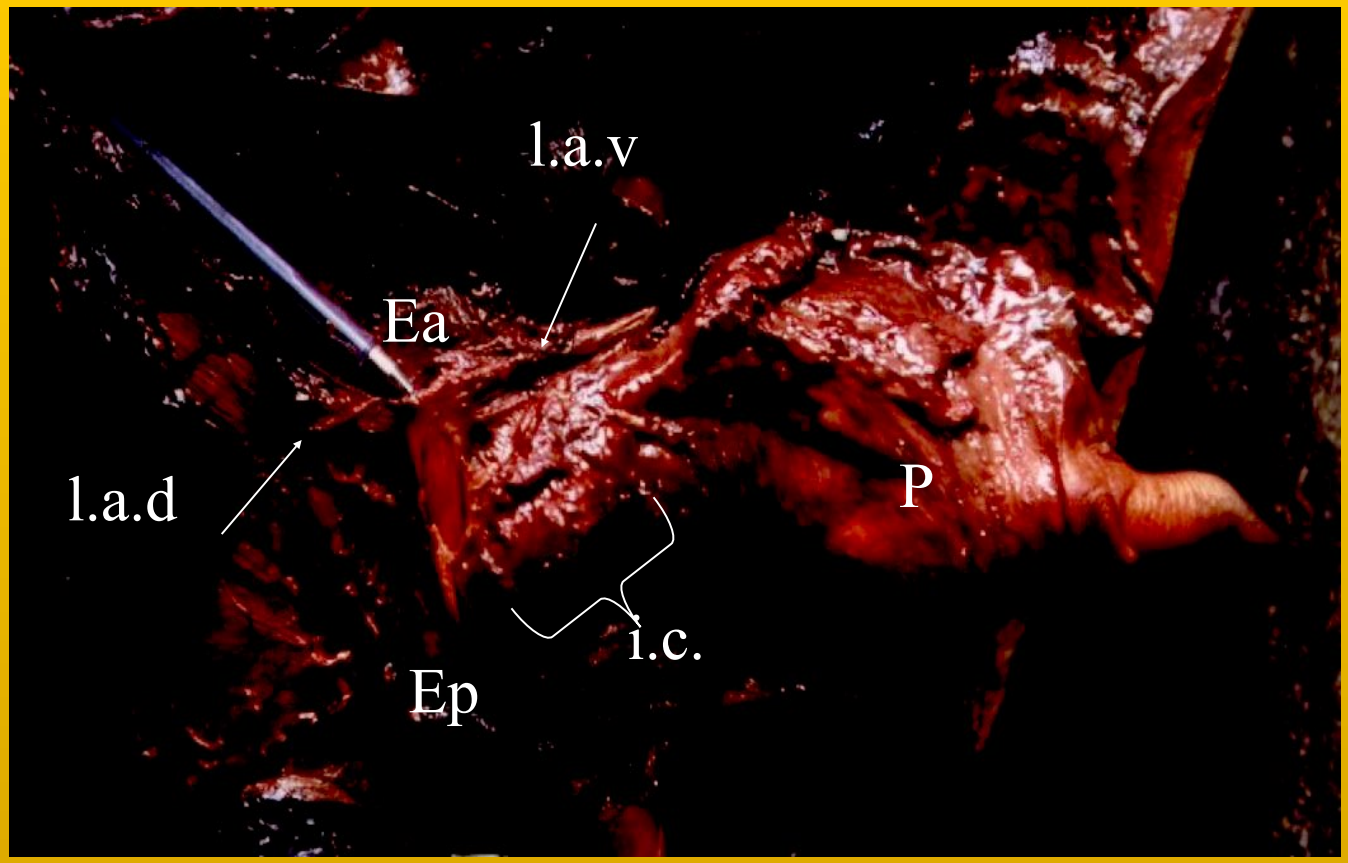

T. truncatus (imagen: Simoes-Lopes y Gutstein, 2004)

✓ Fetos y neonatos poseen huesos pélvicos no mineralizados

Bejder & Hall (2002); Hall (1984)

≠ Arvy (1976 *apud* Arvy, 1979)

Hox genes specify axial patterning and limb position during tetrapod embryonic development (Burke et al. 1995; Carroll 1995; Shubin et al. 1997).

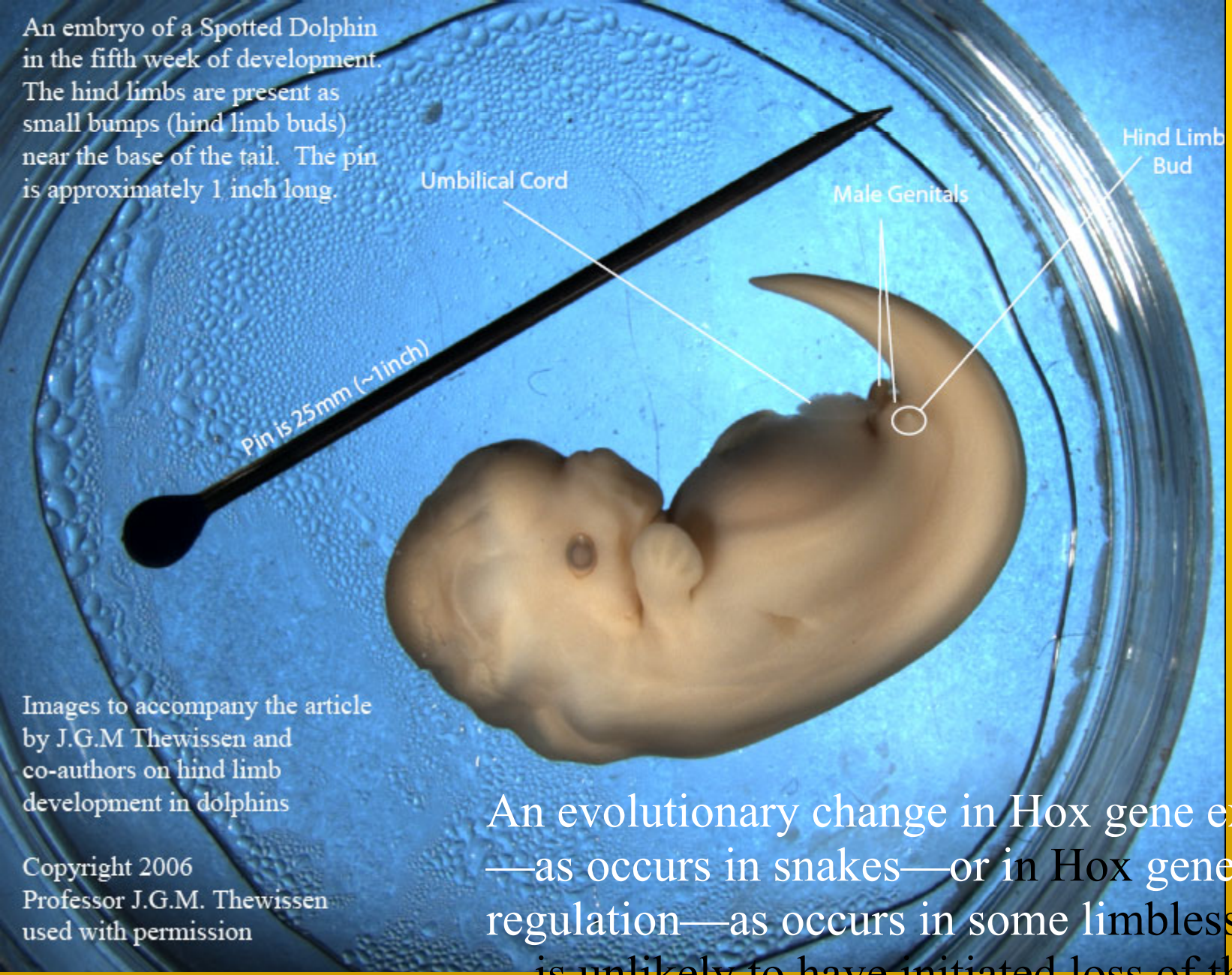

An evolutionary change in Hox gene expression —as occurs in snakes—or in Hox gene regulation—as occurs in some limbless mutants —is unlikely to have initiated loss of the hindlimbs in cetaceans.

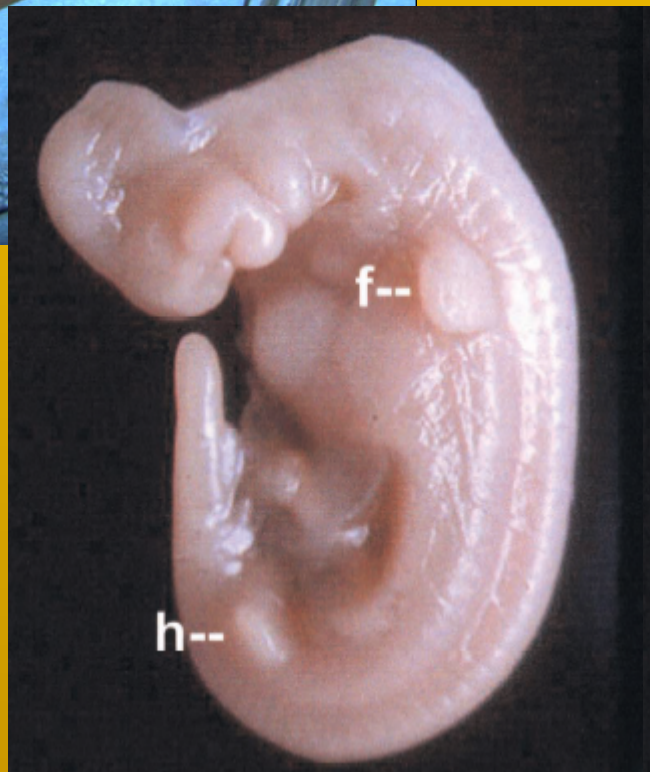

Stenella attenuata

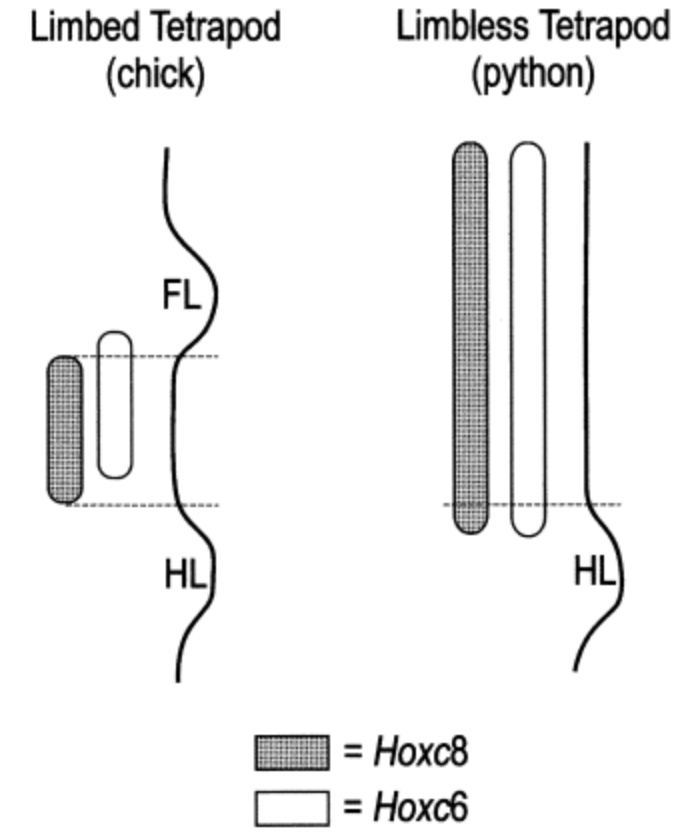

Fig. 6. The distribution of *HoxC-8* and *HoxC-6* in a limbed tetrapod (embryos of the common fowl) and a snake (embryos of the python). The expression boundaries are extended slightly more posteriorly and much more anteriorly in python than in chick embryos. FL, forelimb buds; HL, hindlimb buds.

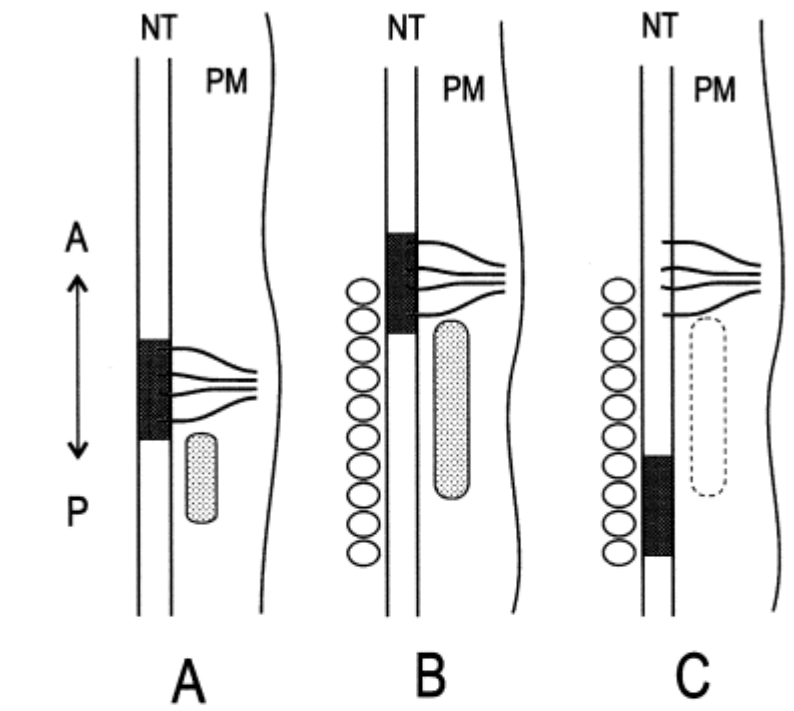

Fig. 7. Expression boundaries of *HoxC-8* in (A) chick and (B) murine embryos to show the more anterior expression in the neural tube of the mouse than in the chick and the anterior extension of expression in the mesoderm of the mouse in comparison with the chick. In both species, the anterior extent of expression coincides with the brachial nerves that innervate the limbs (shown as black lines from the neural tube). (C) Expression in mouse embryos of *HoxC-8* driven by the *cis*-regulatory enhancer of baleen whale *HoxC-8*. Expression in the neural tube is shifted the equivalent of four-somite lengths posteriorly (cf. B with C) and so is out of phase with the site of the brachial nerves. No expression is initiated in the mesoderm; the normal expression boundary is shown by the dotted oval (cf. B). A ↔ P, anterior-posterior body axis;

A simple evolutionary change in *Hox* gene expression or *Hox* gene regulation is unlikely to have driven loss of the hindlimbs in cetaceans, which occurred concurrent with various other morphological and physiological changes associated with the transition from a terrestrial to an aquatic environment and adaptation to that aquatic environment.

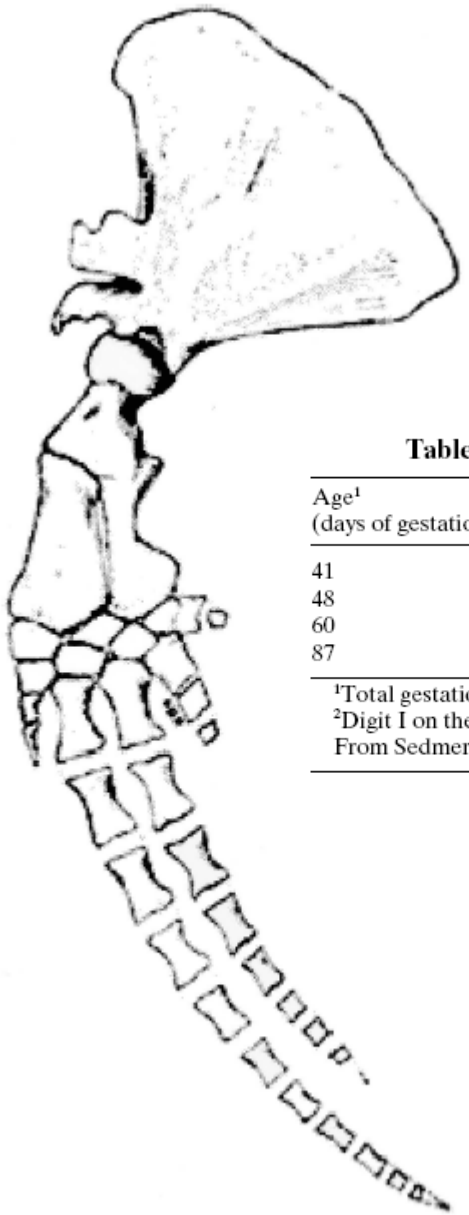

ig. 4. Polyphalangy of digits II and III of the flipper of the long-
nned pilot whale, *Globicephala melas*. Reproduced from Howell

Table 1. Changes in phalangeal formulae during embryonic life of the spotted dolphin, *Stenella attenuata*

Age[1] (days of gestation)	Stage	Crown-Rump Length (mm)	Phalangeal Formula[2]
41	36	22	2-3-3-3-0
48	44	30	3-4-4-3-1
60	54	44	3-5-5-4-2
87	75	101	3-7-7-5-3

[1]Total gestation time is 280 days (Sterba et al. 1994).
[2]Digit I on the left, digit V on the right; see Padian (1992) for phalangeal formulae.
From Sedmera et al. (1997b).

14 phalanges in digits II and III in the pilot whale *Globicephala melas*

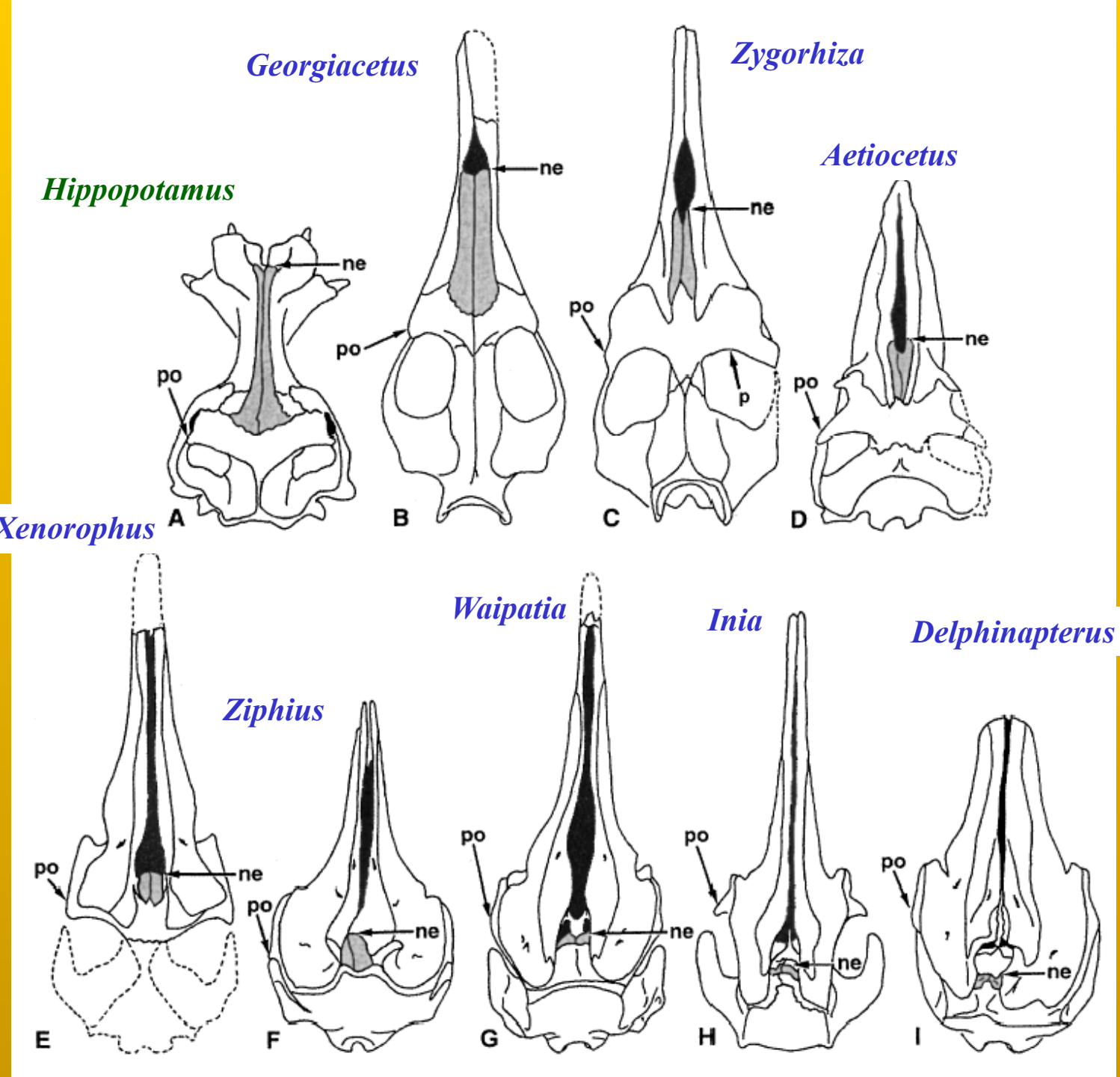

Archaeoceti

Odontoceti

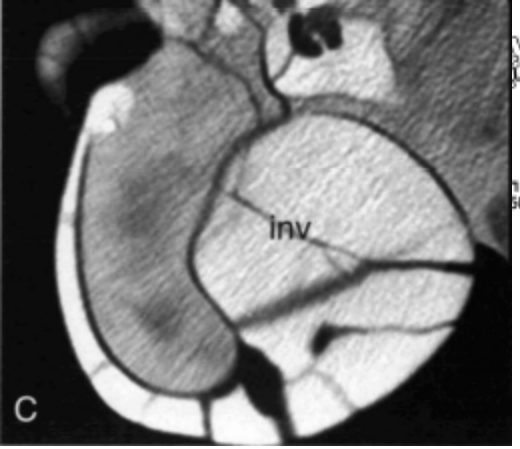
inv
C

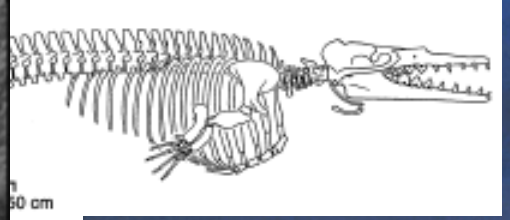
50 cm

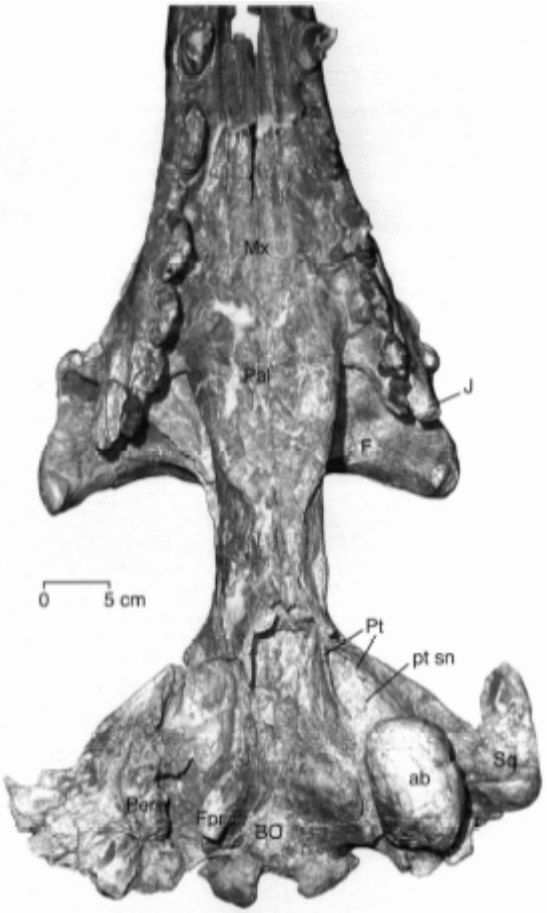
Mx
Pal
J
F
0
5 cm
Pt
pt sn
ab
Sq
Perio
Fpr
BO

Dorudon atrox

Mysticeti

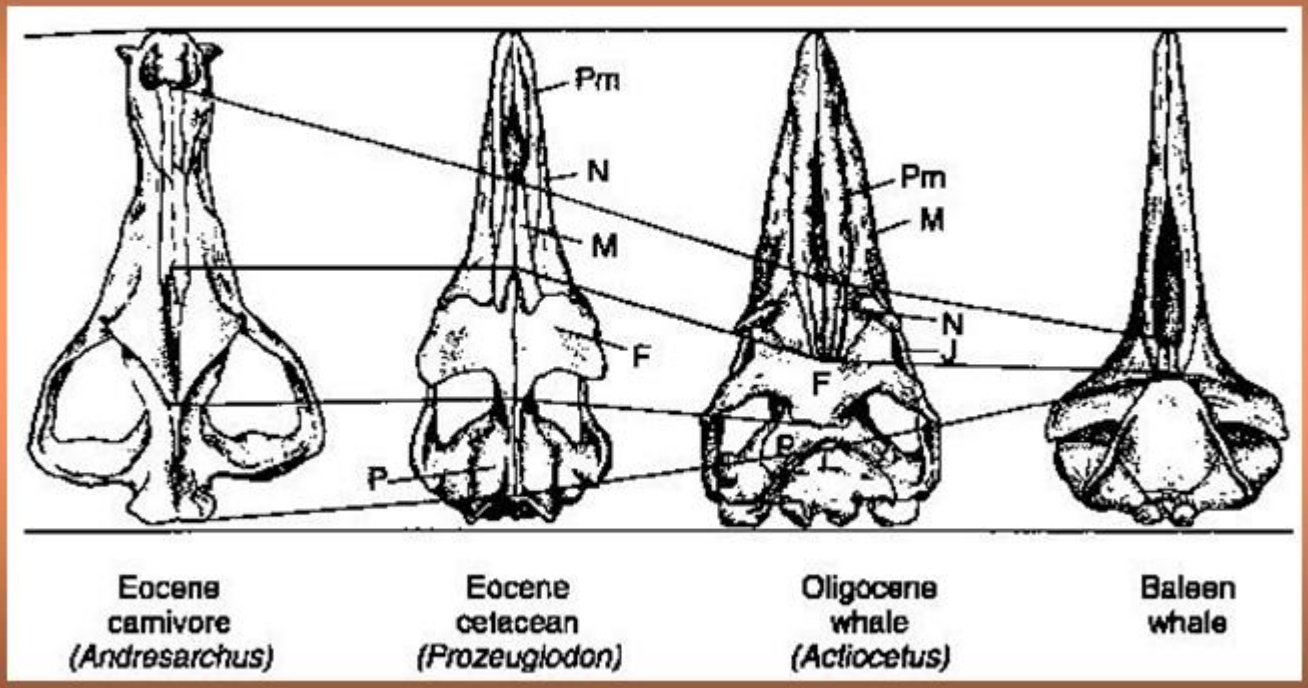
Pm
N
M
F
P
Pm
M
N
J
F
P
Eocene carnivore (Andresarchus)
Eocene cetacean (Prozeuglodon)
Oligocene whale (Actiocetus)
Baleen whale

Janjucetus hunderi

Oligoceno Tardio

Fitzgerald 2006

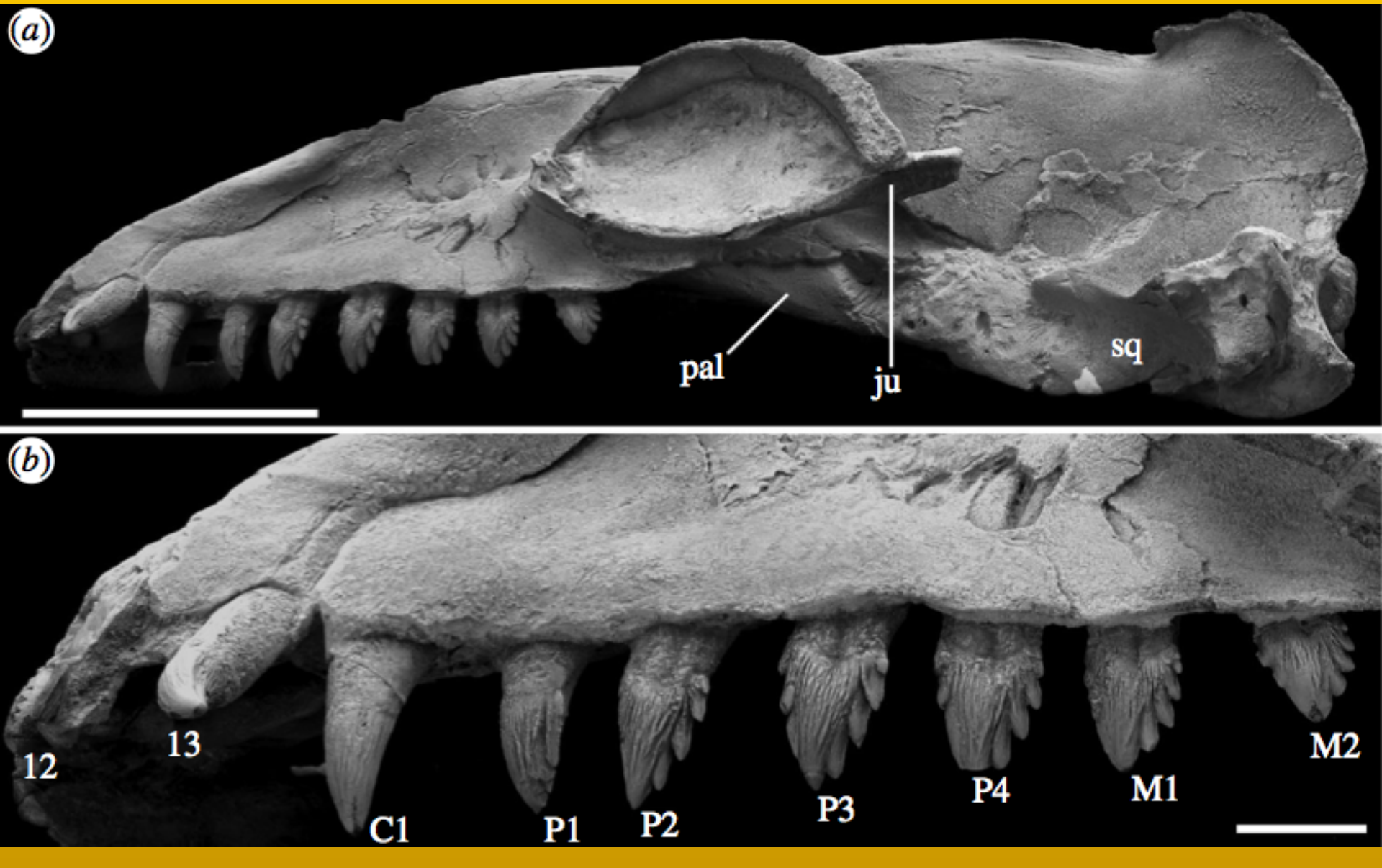

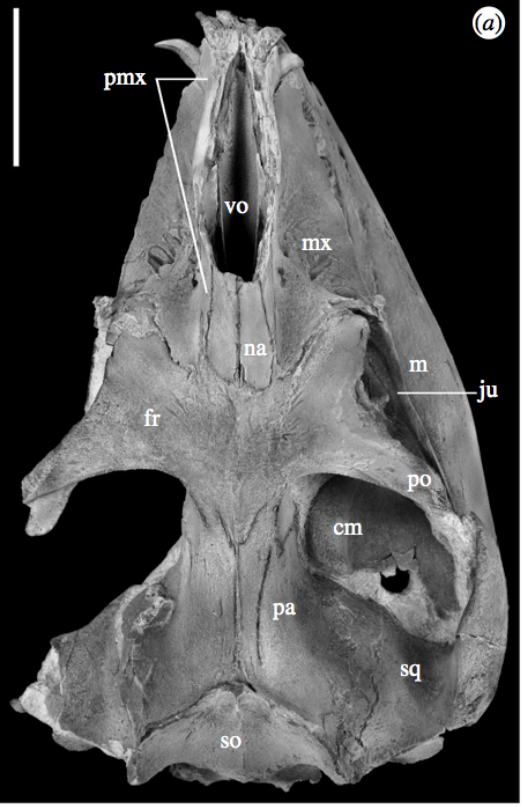

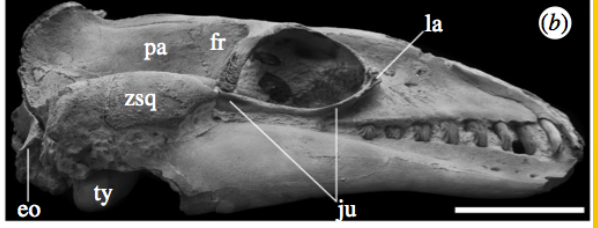

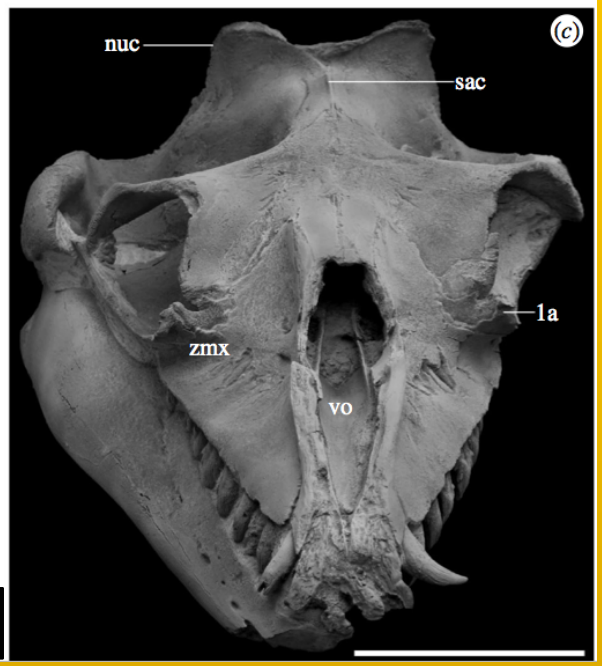

Fitzgerald 2006

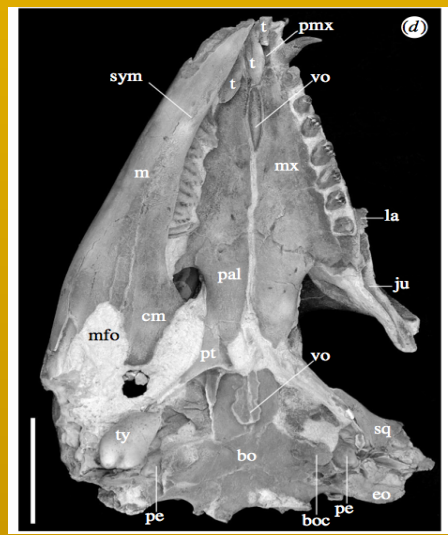

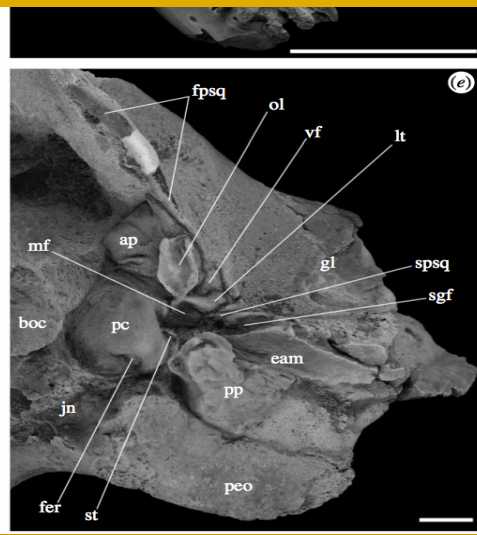

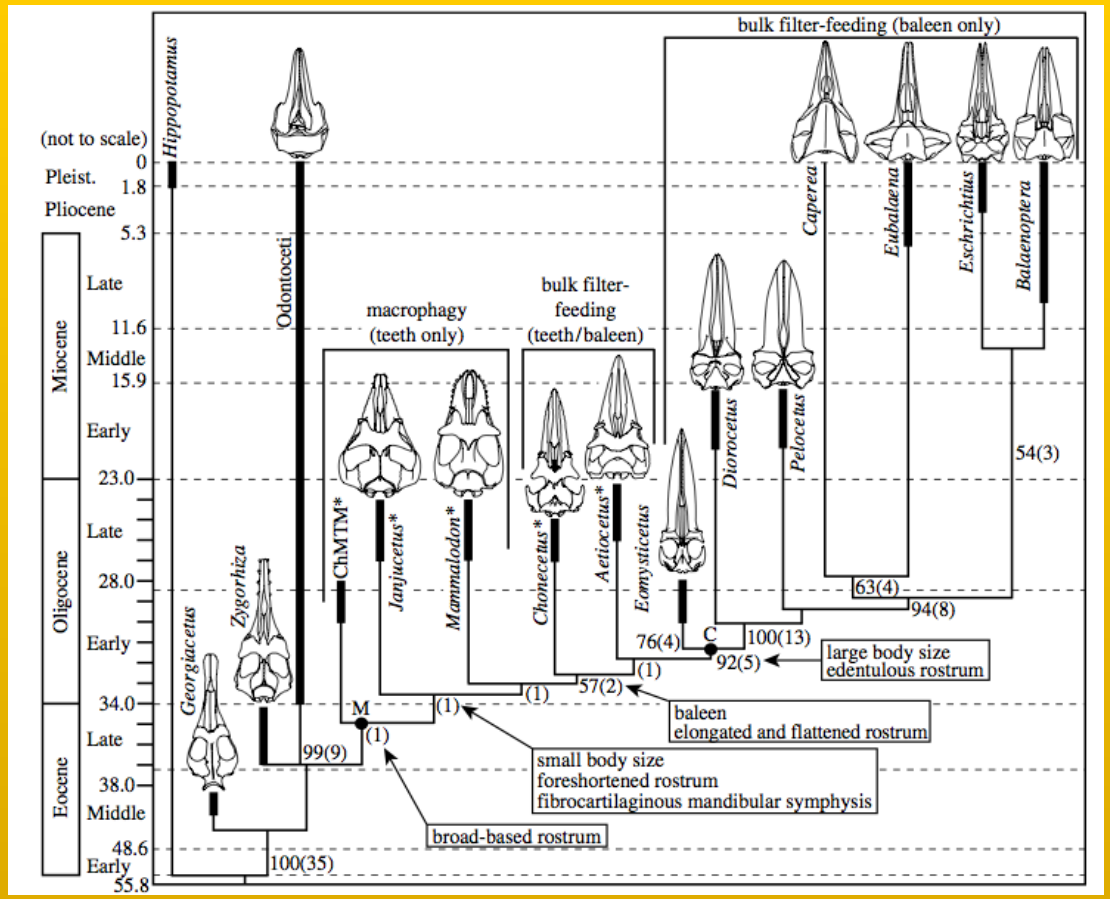

Fitzgerald 2006

Figure 3. Phylogeny and stratigraphic record of Mysticeti, including Janjucetus, and the evolution of feeding ecology in mysticetes. Phylogenetic relationships of Janjucetus based on strict consensus of three trees derived from parsimony analysis of 266 characters in 26 genera (some taxa pruned from tree). Cetacean skull reconstructions shown in dorsal view. Characters relevant to the evolution of feeding in mysticetes are optimized on to the tree at nodes where they appear. Taxa marked with * represent toothed mysticetes. Numbers, and numbers in parentheses, at nodes represent bootstrap and branch support values, respectively. Solid circles denote named clades. Solid black bars on branches represent stratigraphic range error bars of their respective clade. Ages are in millions of years, with the time-scale being linear only for Late Eocene through Oligocene. Time- scale after Gradstein et al. (2004). Abbreviations: ChM TM, Charleston Museum toothed mysticetes; C, Chaeomysticeti; M, Mysticeti. (See electronic supplementary material for further information.)

Morphological and Molecular Evidence for a Stepwise Evolutionary Transition from Teeth to Baleen in Mysticete Whales

Demere et al. 2008

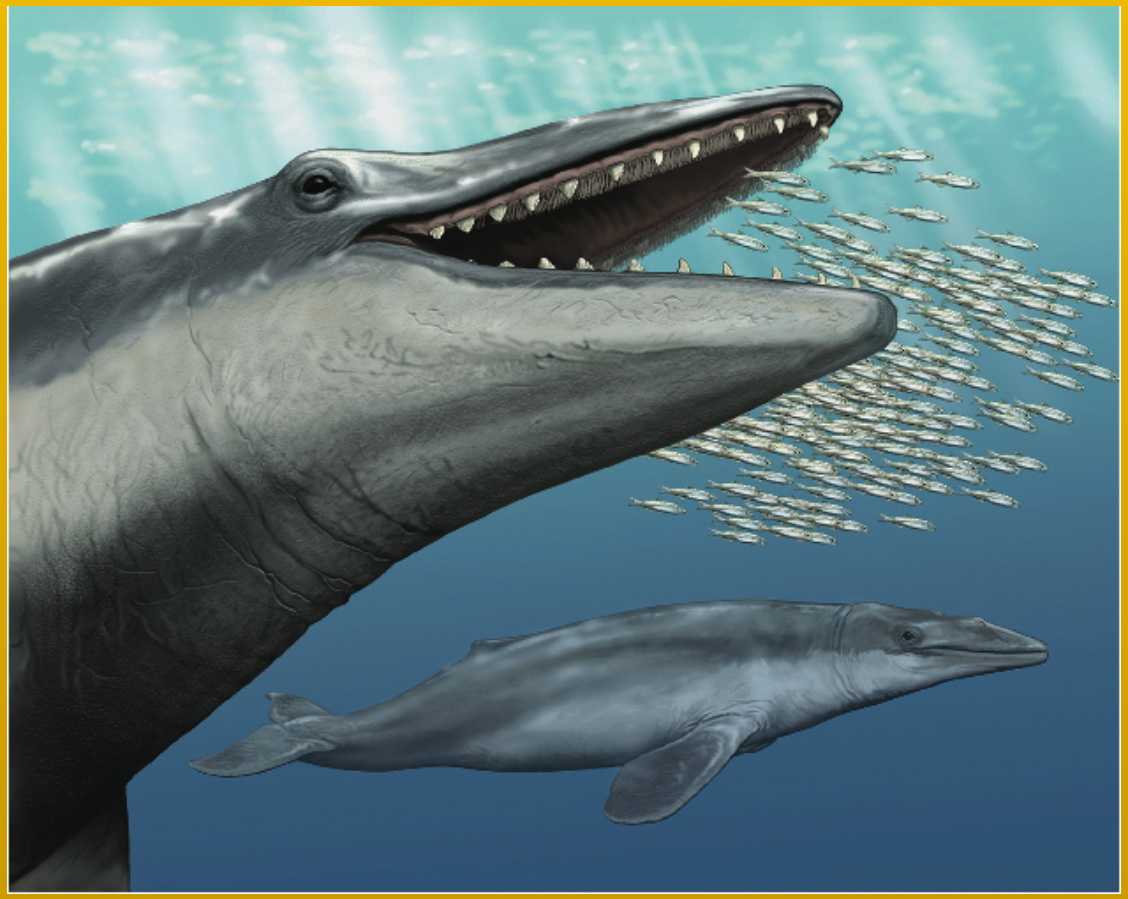

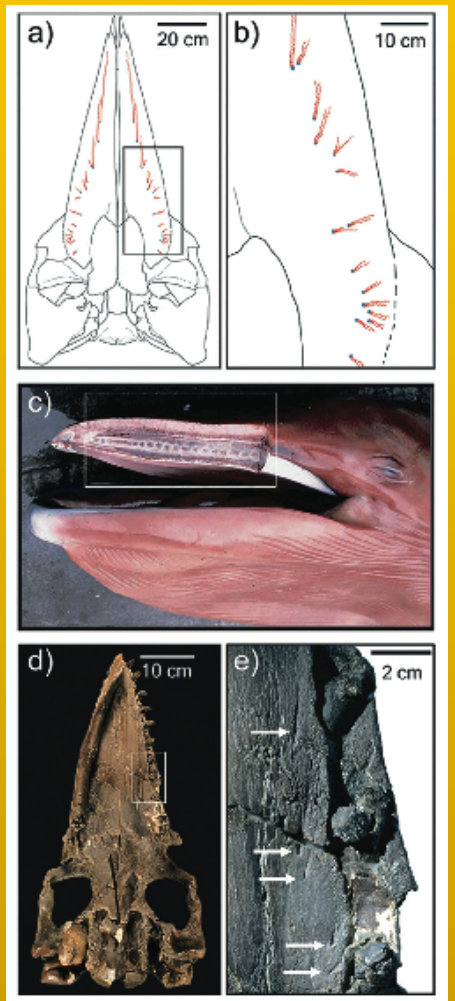

FIGURE 1. Mysticete palates and dentitions. (a, b) sketch of palate from an extant edentulous mysticete (*Balaenoptera acutorostrata*—minke whale); (c) lateral view of a mysticete fetus (*Balaenoptera physalus*—fin whale) with dissection showing tooth buds in upper jaw; and (d, e) palate of the holotype of *Aetiocetus weltoni* (UCMP 122900; ~24 to 28 million years old). b is an enlargement of the inset in a (blue = lateral nutrient foramen; red = sulcus). e is an enlargement of the inset in d; white arrows point to nutrient foramina and associated sulci. Photo of *Balaenoptera physalus* is by Alex Aguilar (GRUMM/FDS).

Gigantism Precedes Filter Feeding in Baleen Whale Evolution

R. Ewan Fordyce[1,2] and Felix G. Marx[3,4,5,6,*]

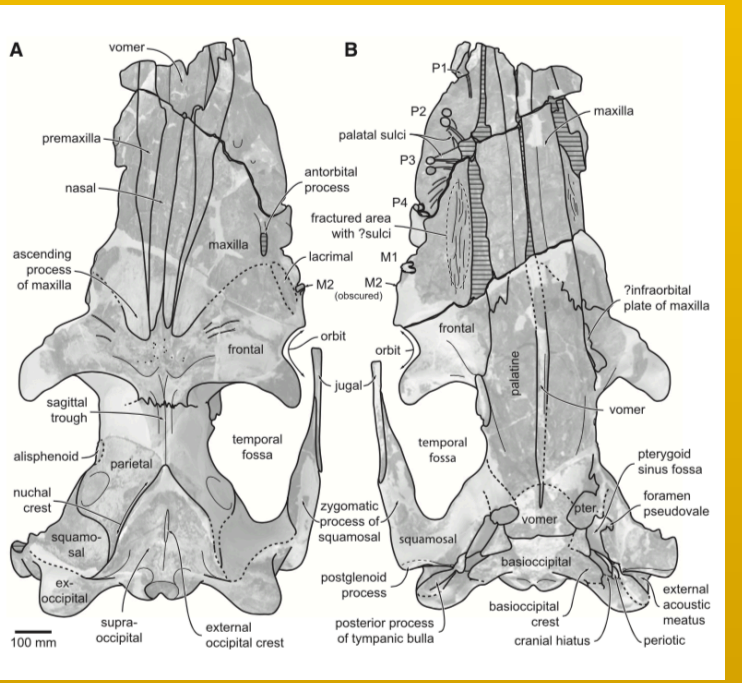

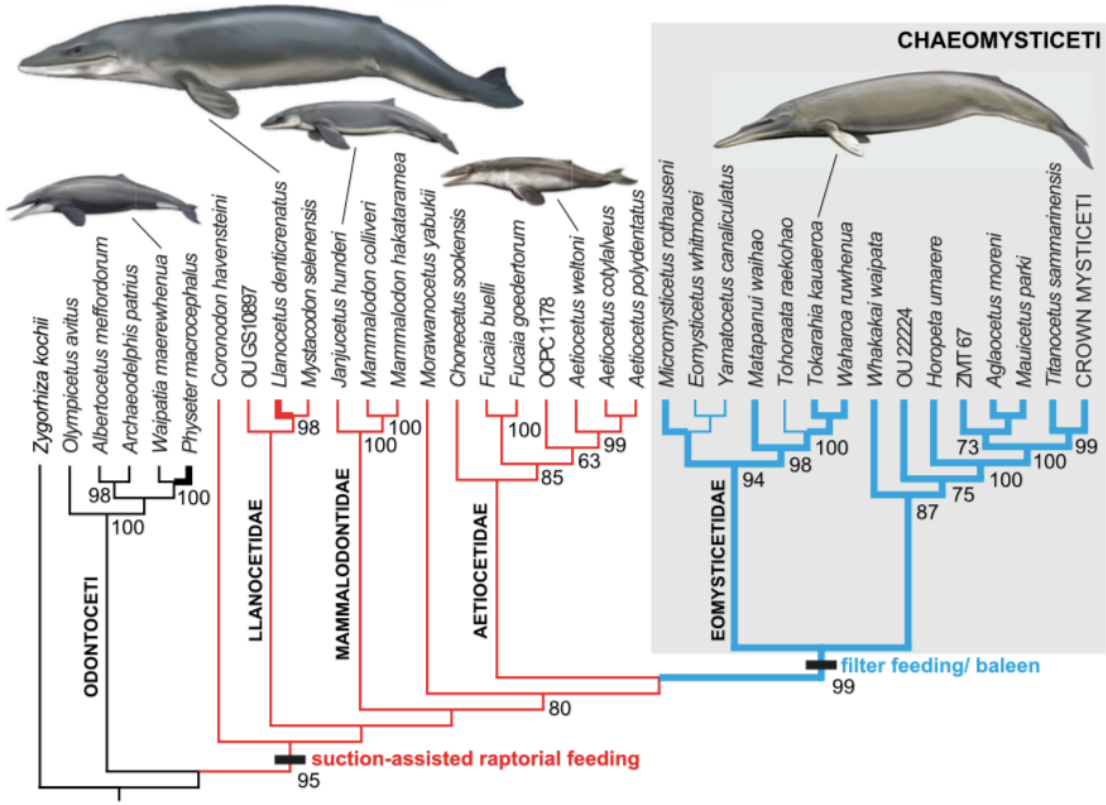

Figure 4. Phylogenetic Relationships of *Llanocetus denticrenatus*

Numbers next to nodes represent posterior probabilities (only values ≥50 are shown). Thick lines indicate large body size (>5 m), with ancestral states reconstructed based on parsimony (likelihood yields equivalent results). Note the markedly larger size of *Llanocetus* relative to other stem mysticetes. Reconstructions by Carl Buell.

Fordyce and Marx, Gigantism Precedes Filter Feeding in Baleen Whale Evolution, Current Biology (2018),

https:// doi.org/10.1016/j.cub.2018.04.027

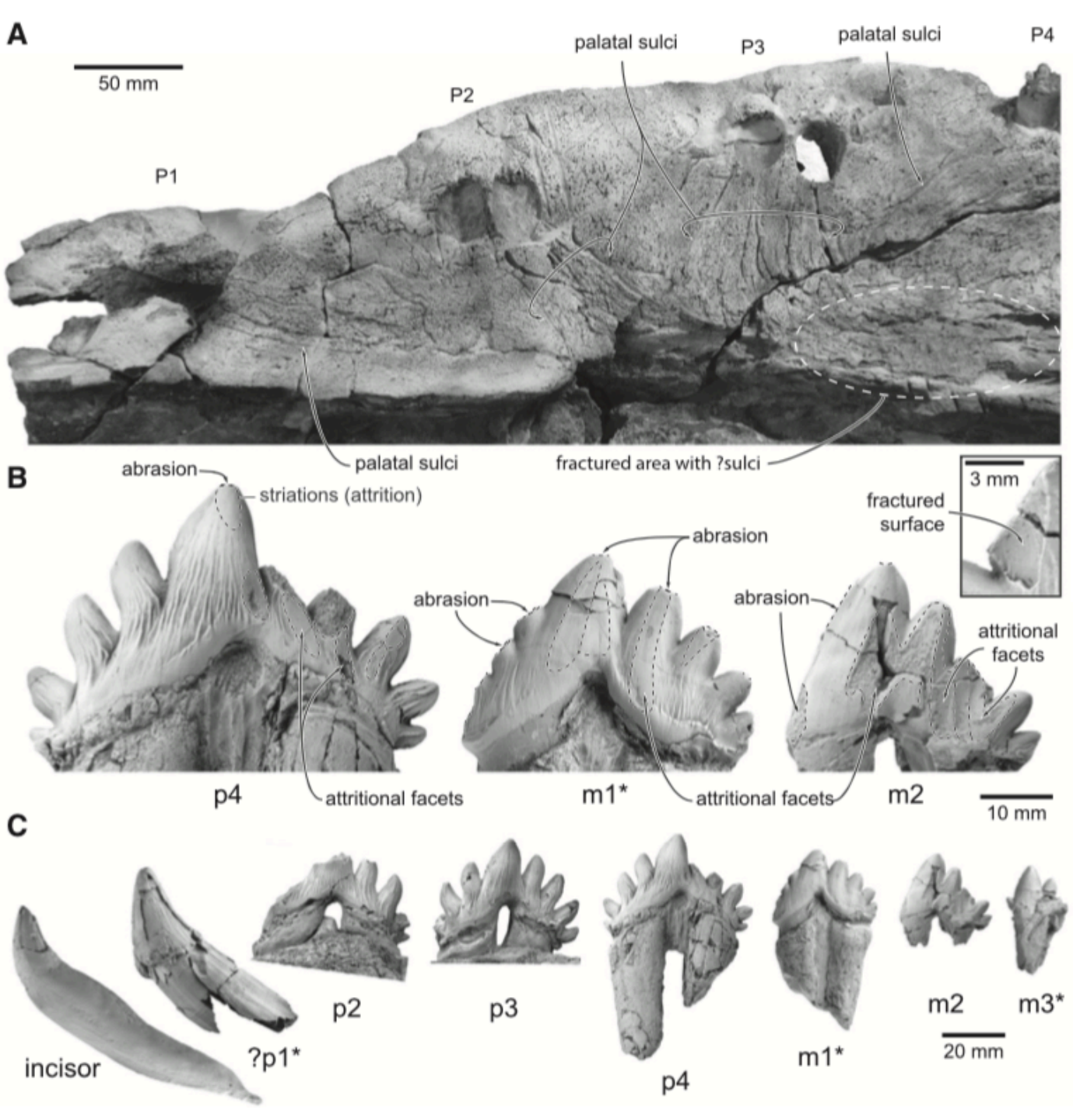

Figure 2. Feeding Apparatus of *Llanocetus denticrenatus*, USNM 183022

(A) Left palate in ventral view, showing alveoli and palatal sulci.

(B) Lower posterior check teeth, in labial view, showing abrasion and attrition.

(C) Lower dentition, in labial view.

Photographs marked by an asterisk have been mirrored to facilitate comparisons. See Data S1 for additional details.

Archaeocete-like jaws in a baleen whale

(Fitzgerald, 2011)

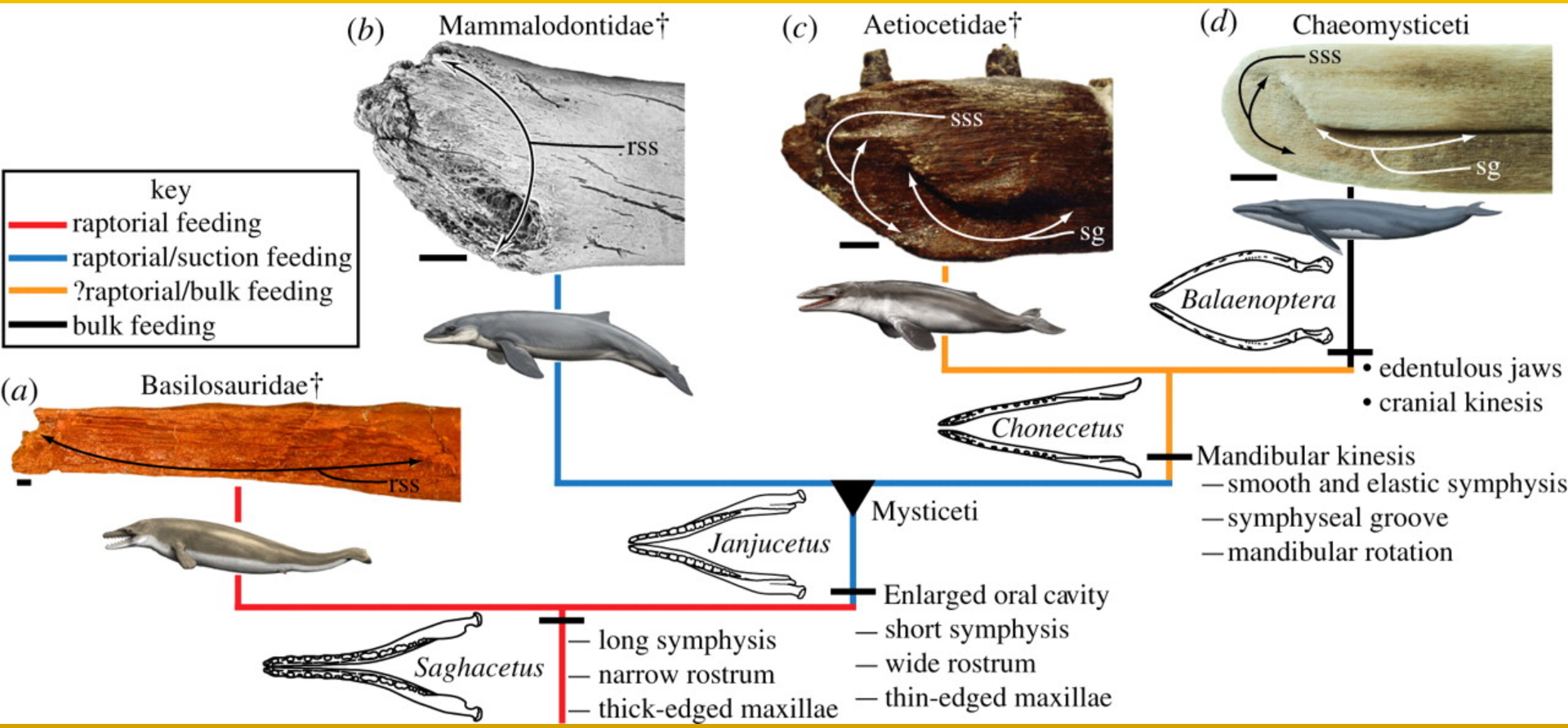

Current Biology

Tooth Loss Precedes the Origin of Baleen in Whales

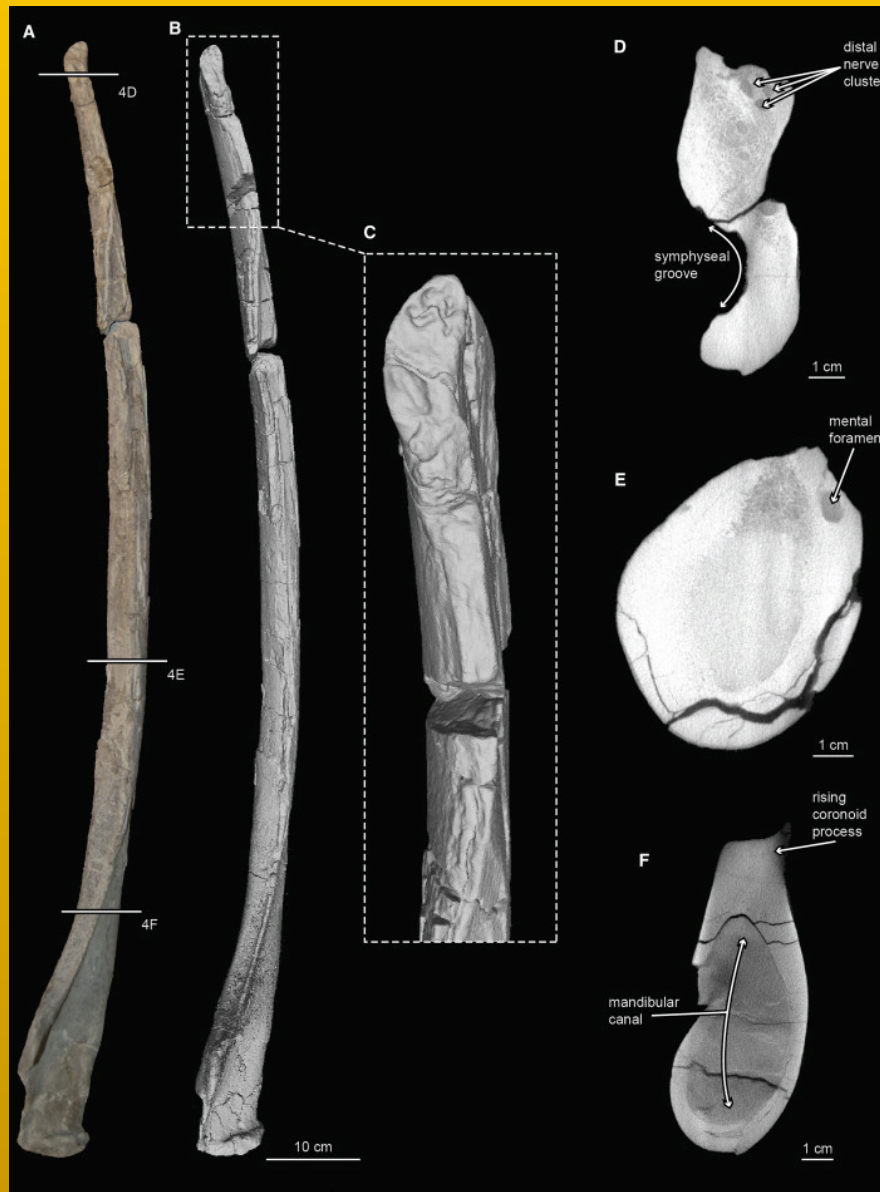

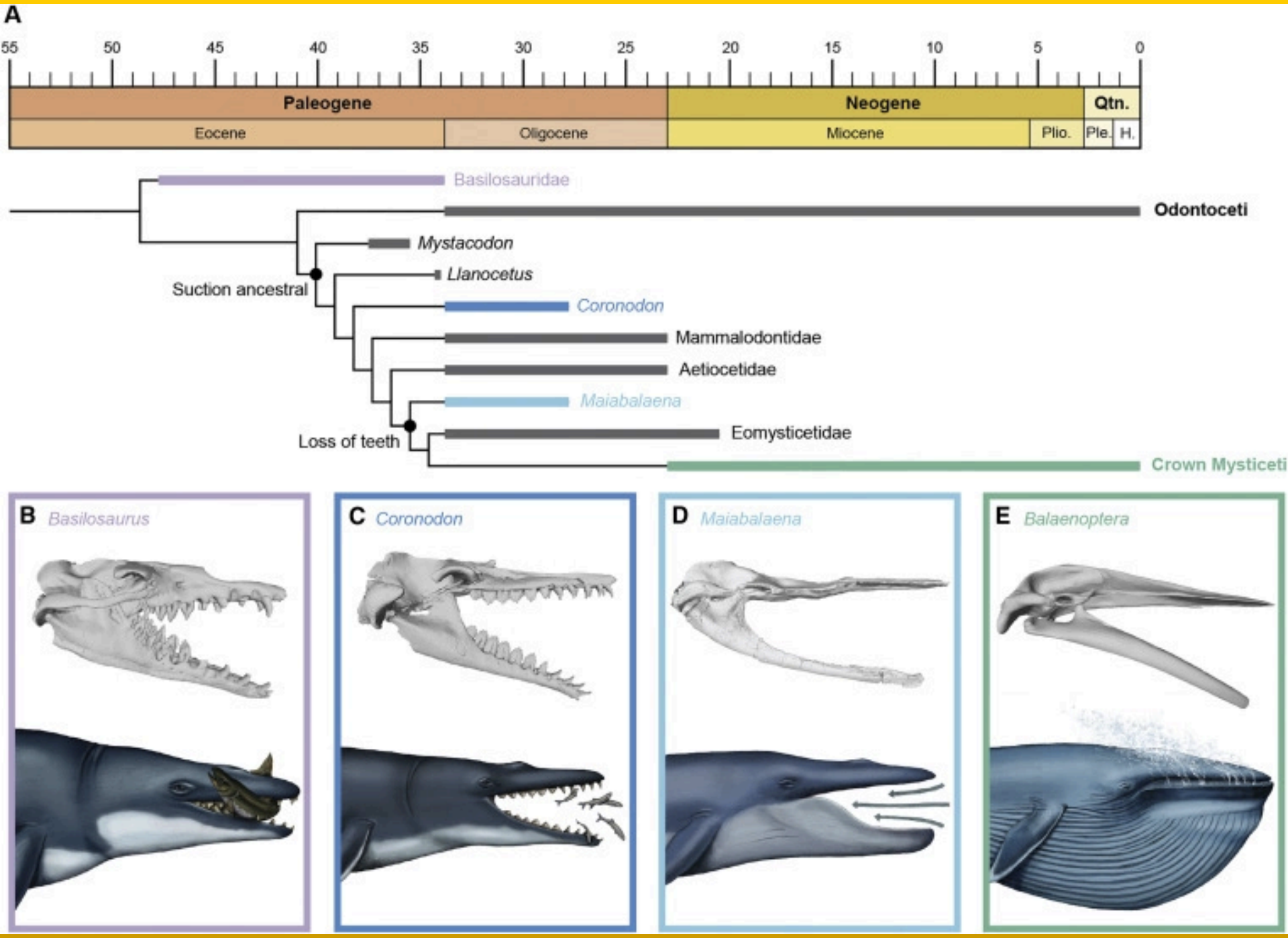
A
55
50
45
40
35
30
25
20
15
10
5
0
Paleogene
Neogene
Qtn.
Eocene
Oligocene
Miocene
Plio.
Ple.
H.
Basilosauridae
Odontoceti
Mystacodon
Llanocetus
Suction ancestral
Coronodon
Mammalodontidae
Aetiocetidae
Maiabalaena
Loss of teeth
Eomysticetidae
Crown Mysticeti
B Basilosaurus
C Coronodon
D Maiabalaena
E Balaenoptera

Report

Current Biology

Tooth Loss Precedes the Origin of Baleen in Whales

Carlos Mauricio Peredo, Nicholas D. Pyenson, Christopher D. Marshall, Mark D. Uhen - https://doi.org/10.1016/j.cub.2018.10.047

Maiabalaena nesbittae is 33 million year old fossil baleen whale from Oregon

Maiabalaena has neither teeth, nor baleen

Early whales lost teeth entirely before the evolutionary origin of baleen

Despite no teeth or baleen, these whales were effective suction feeders

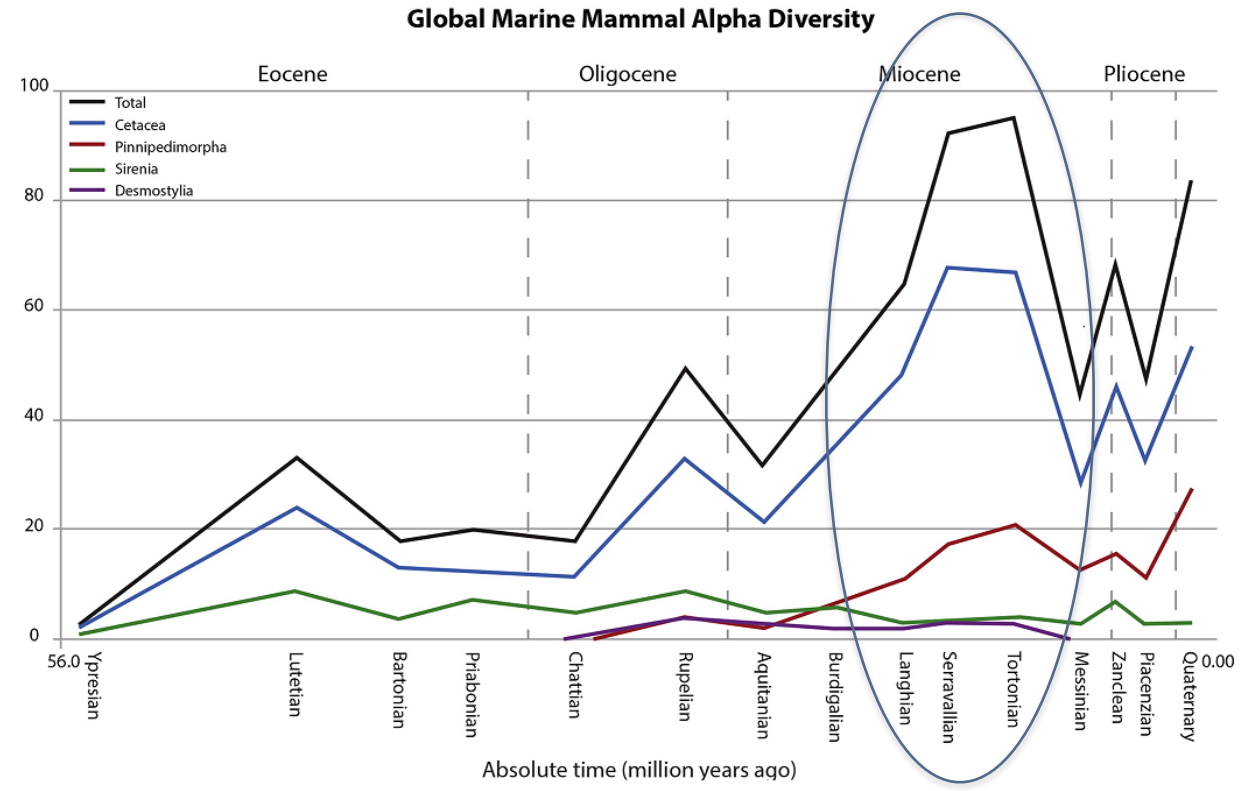

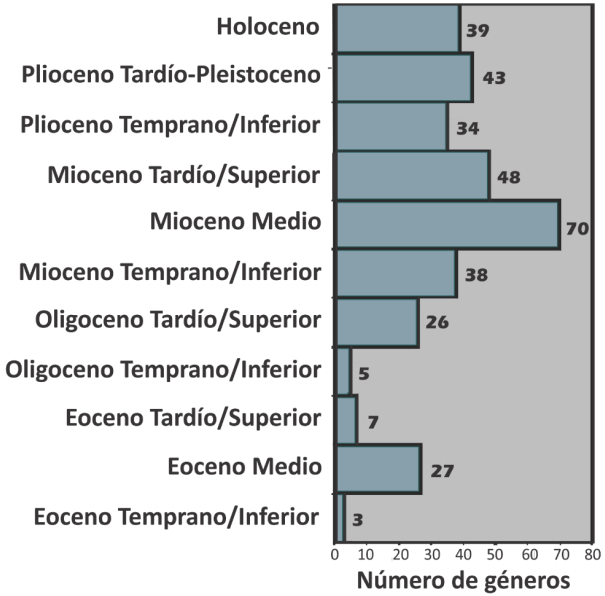

(Uhen y Pyenson 2007)

Peredo y Uhen 2016

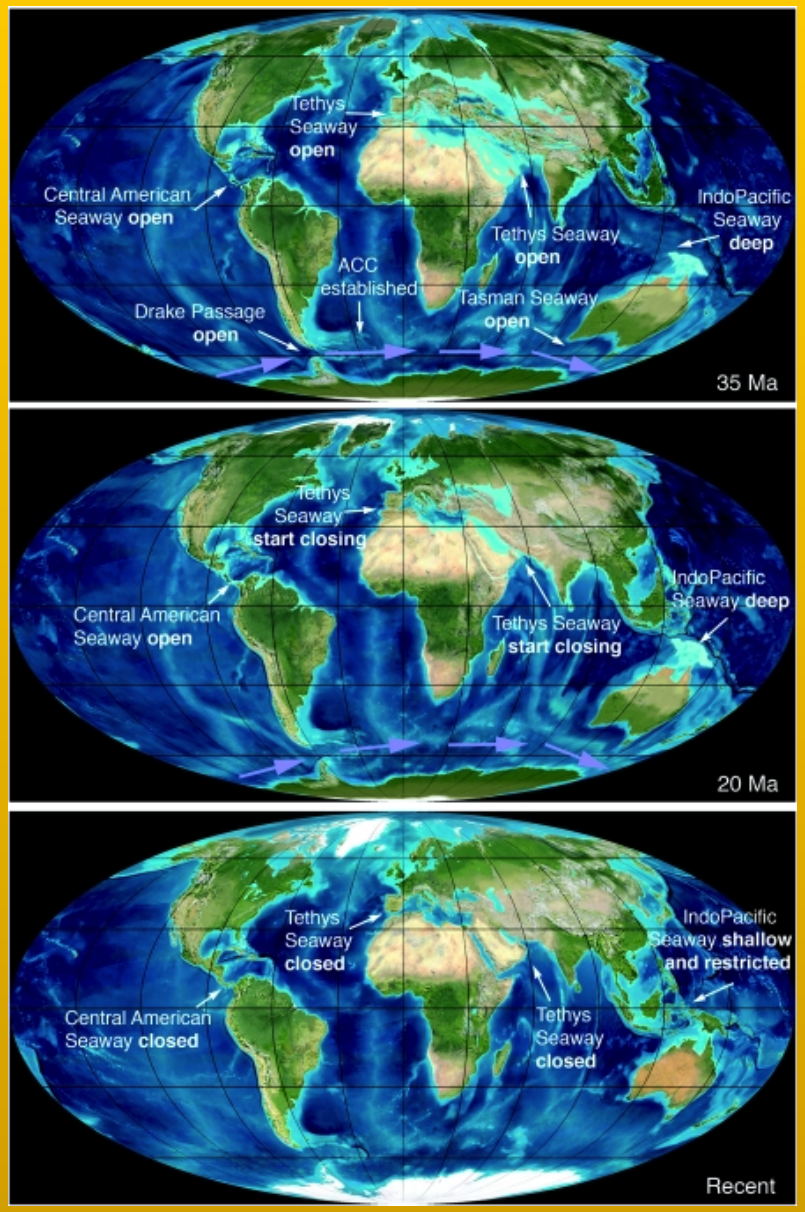

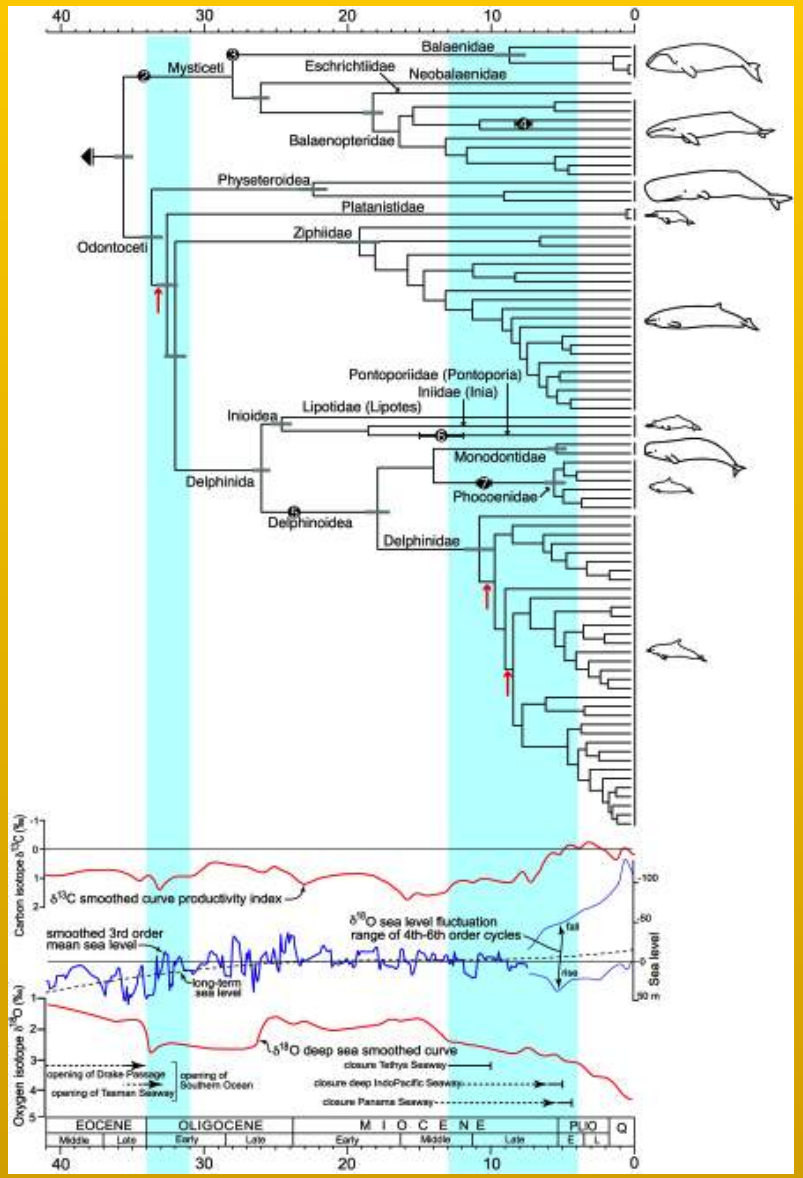

Steeman et al. 2009.
Radiation of Extant Cetaceans Driven by Restructuring of the Oceans. Syst. Biol. 58: 573-585

Se ha considerado que las primeras radiaciones comenzaron en las frías aguas del Pacífico Norte

- Gaskin (1985) → a) nuevos nichos ecológicos

  → b) nueva oferta trófica, en especial para las poblaciones de ballenas, delfines, focas y lobos marinos.

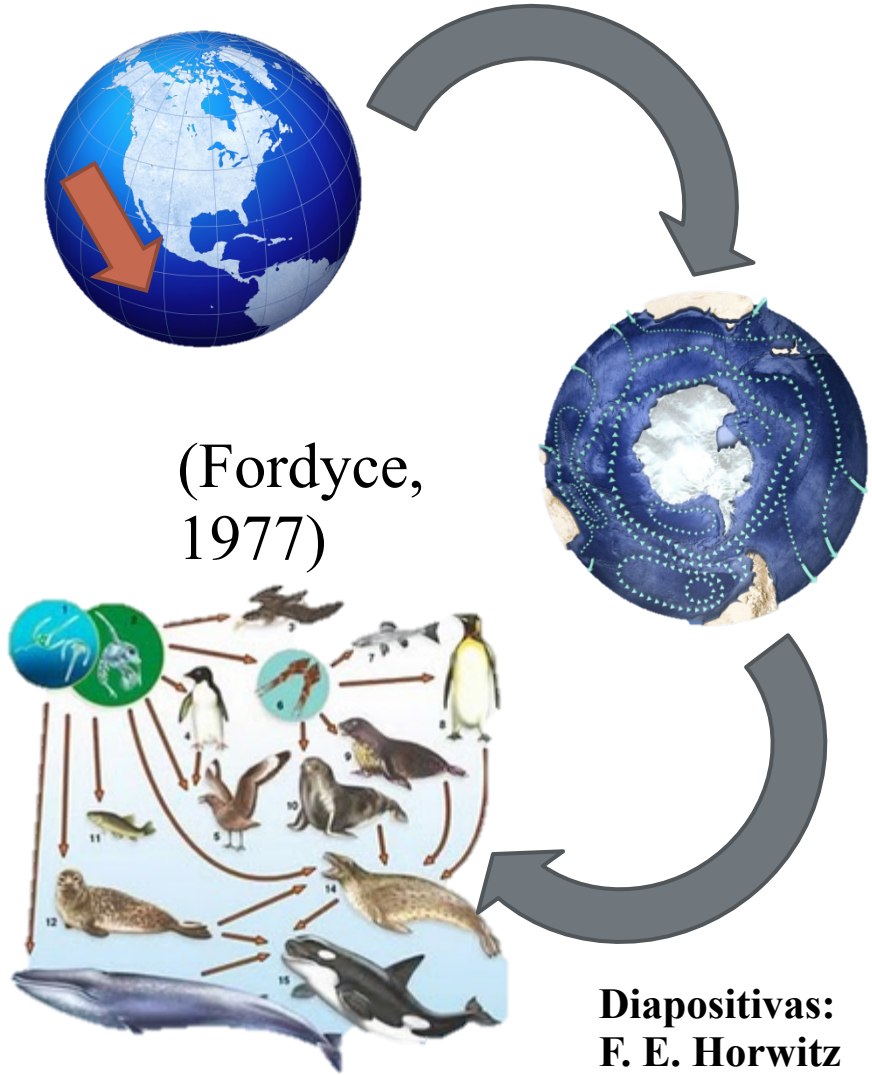

(Fordyce, 1977)

Diapositivas: F. E. Horwitz

Se ha considerado que las primeras radiaciones comenzaron en las frías aguas del Pacífico Norte

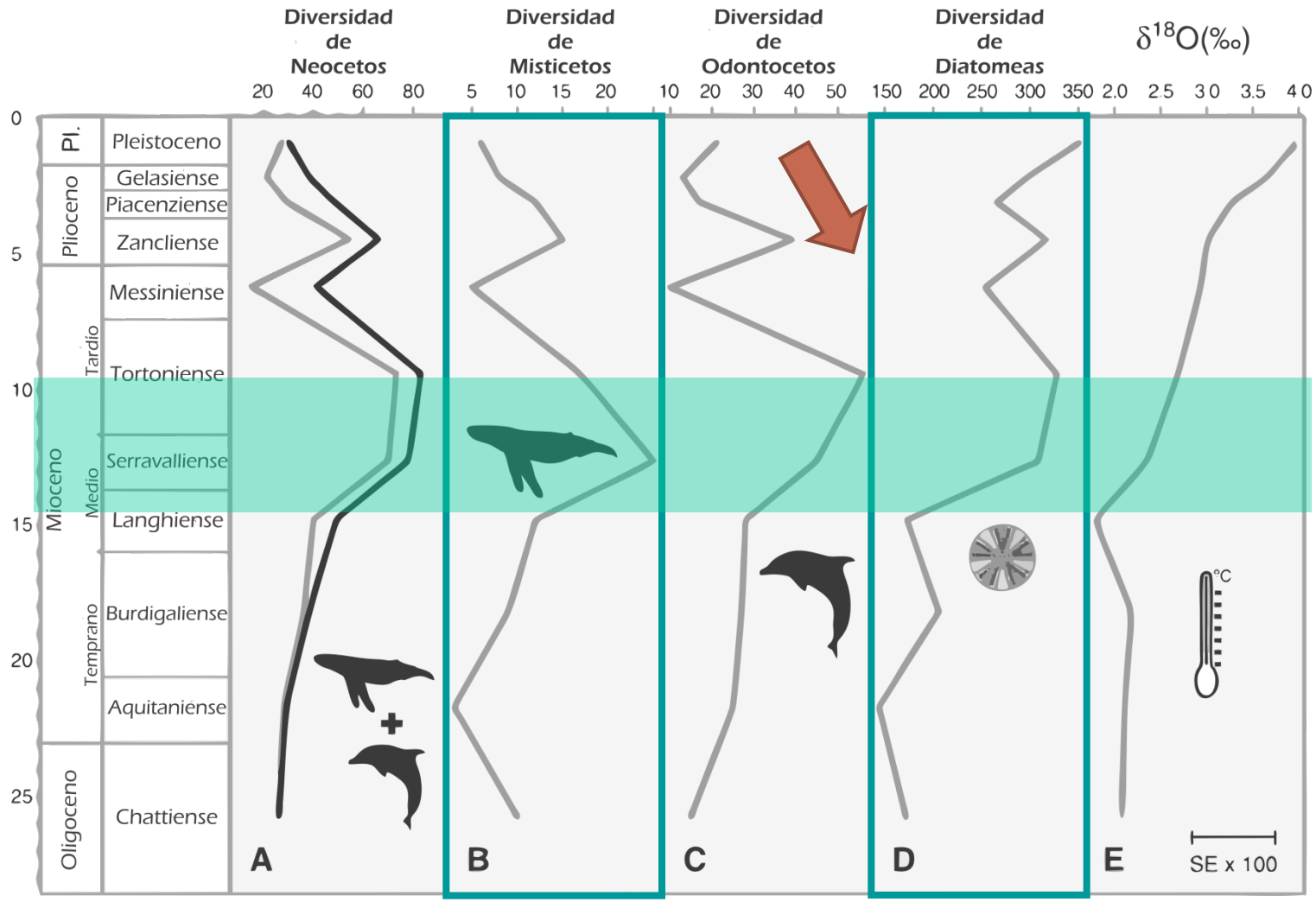

(Marx & Uhen, 2010)

Diapositivas:
F. E. Horwitz

Misticetos: las relaciones entre las familias siguen siendo a menudo objeto de acalorados debates

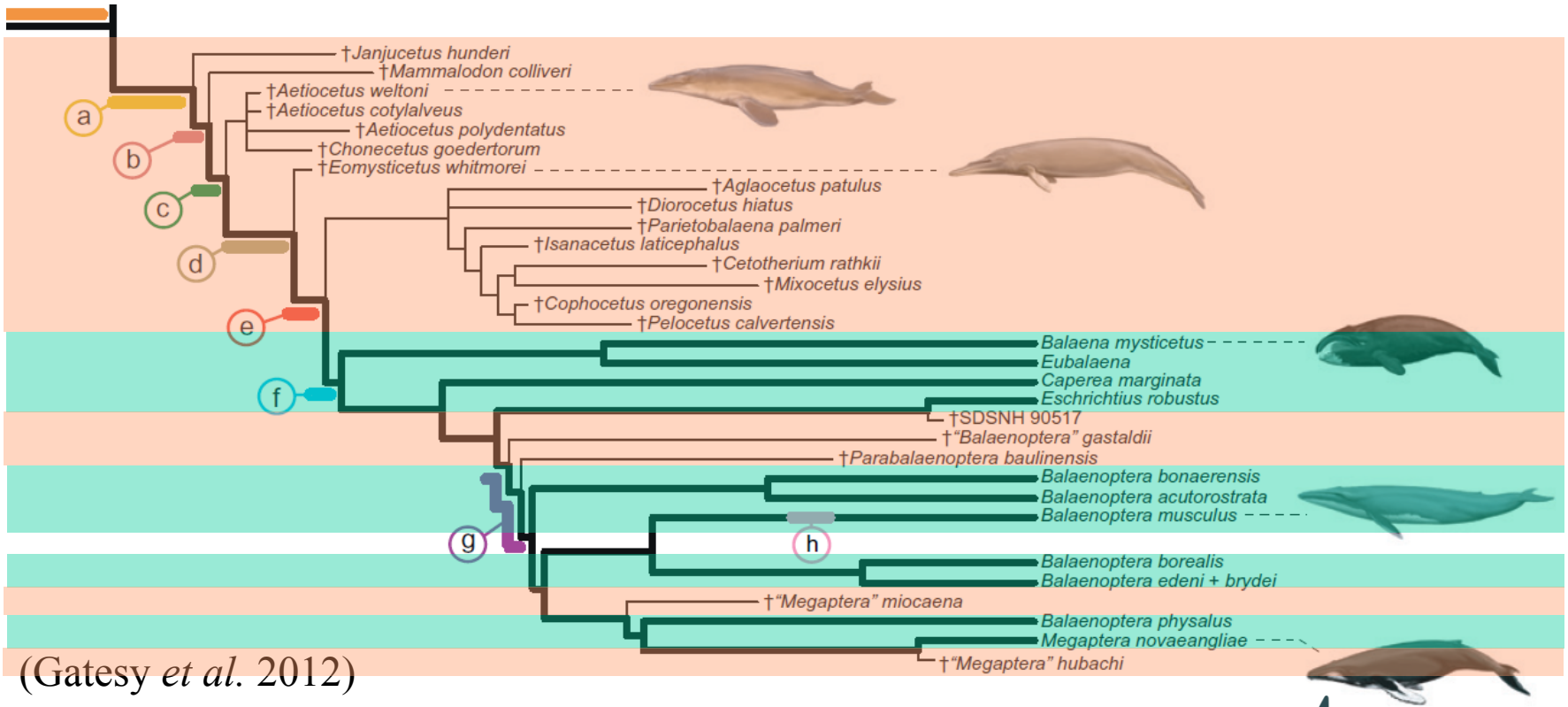

(Gatesy *et al.* 2012)

- 14 géneros extintos.
- 6 géneros vivientes.

- Chile → 8 de las 12 especies reconocidas (67%) (Capella & Gibbons, 2008)

Diapositivas:
F. E. Horwitz

En la actualidad…

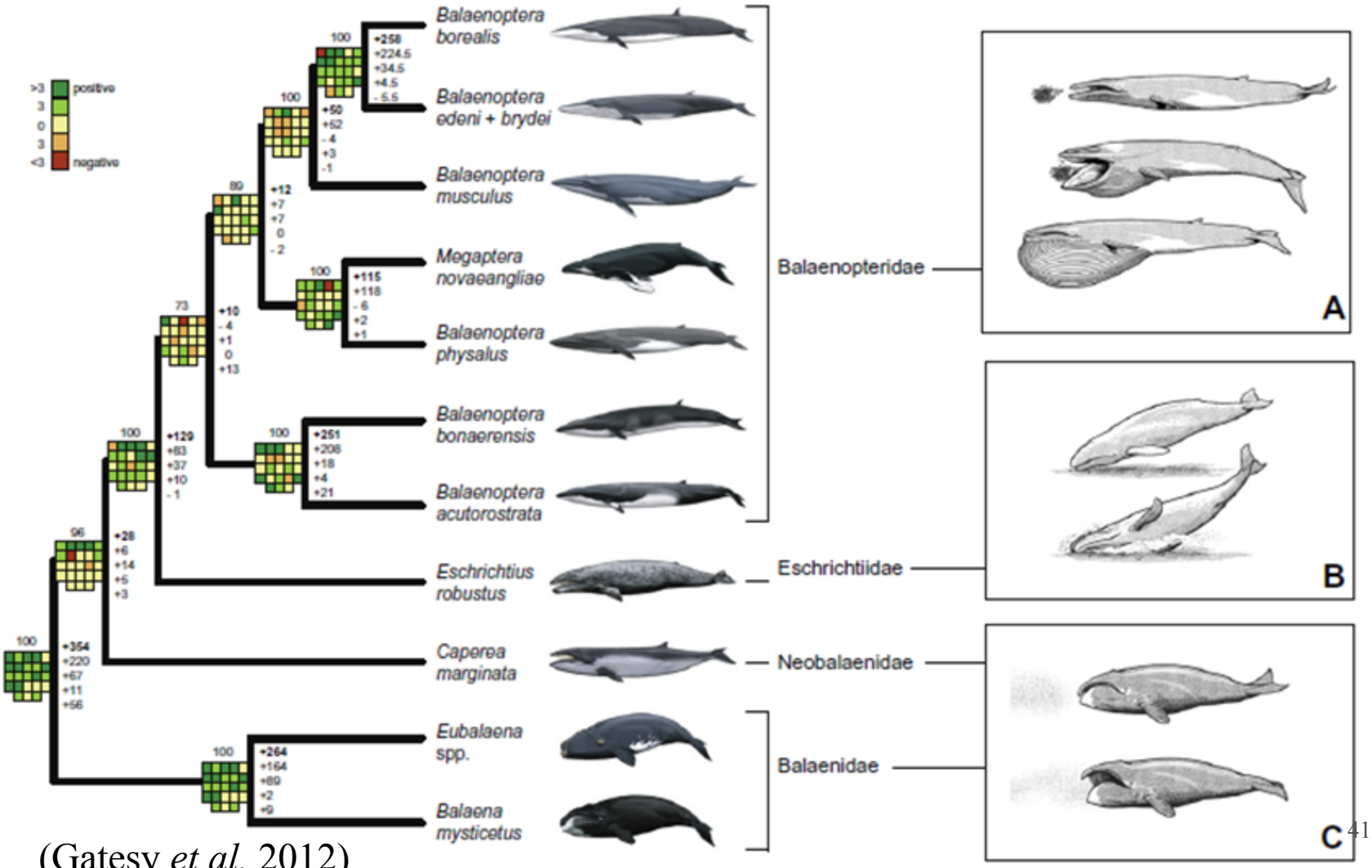

(Gatesy *et al.* 2012)

En la actualidad…

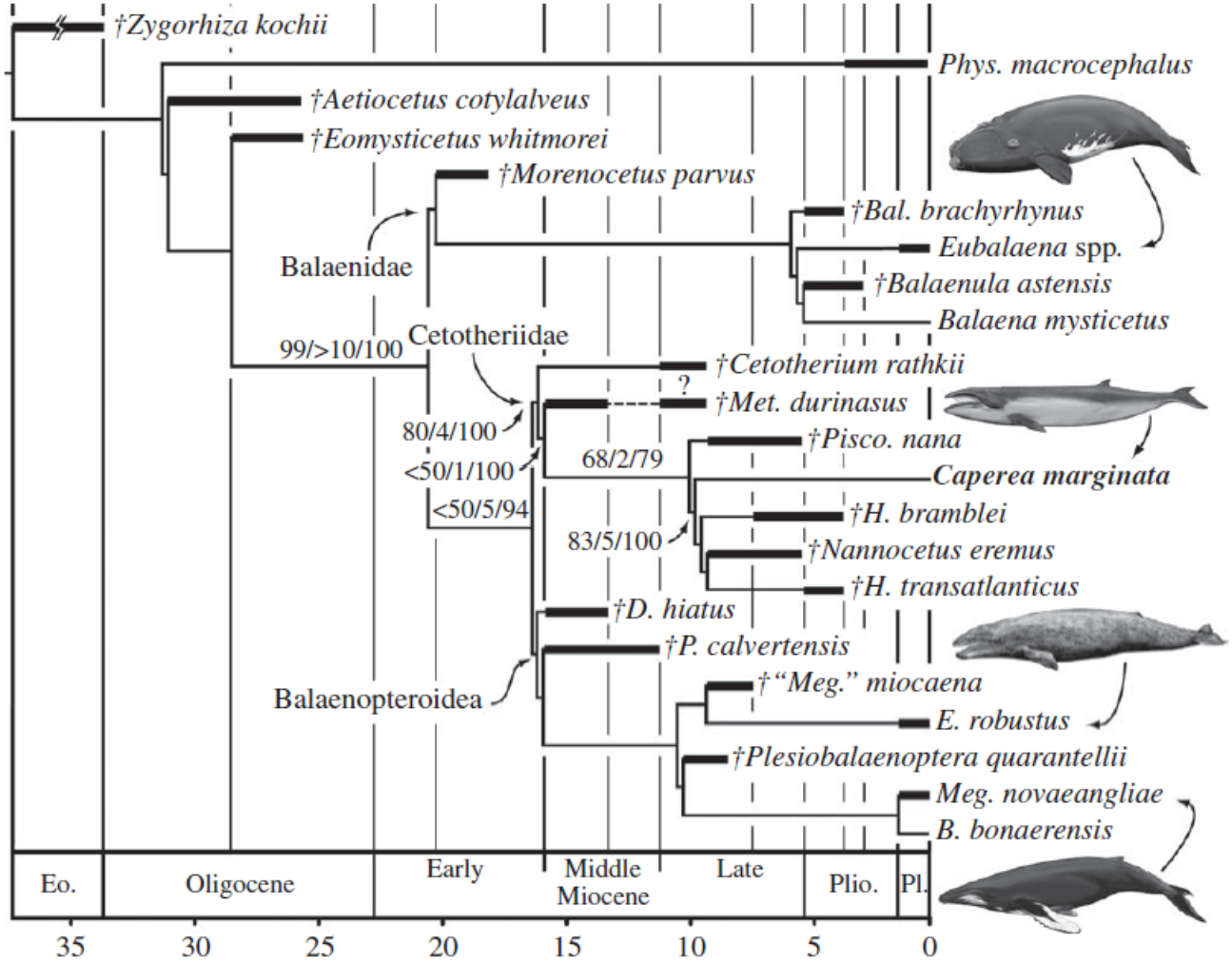

(Fordyce & Marx, 2012)

Balaenidae

Churchill et al. 2011

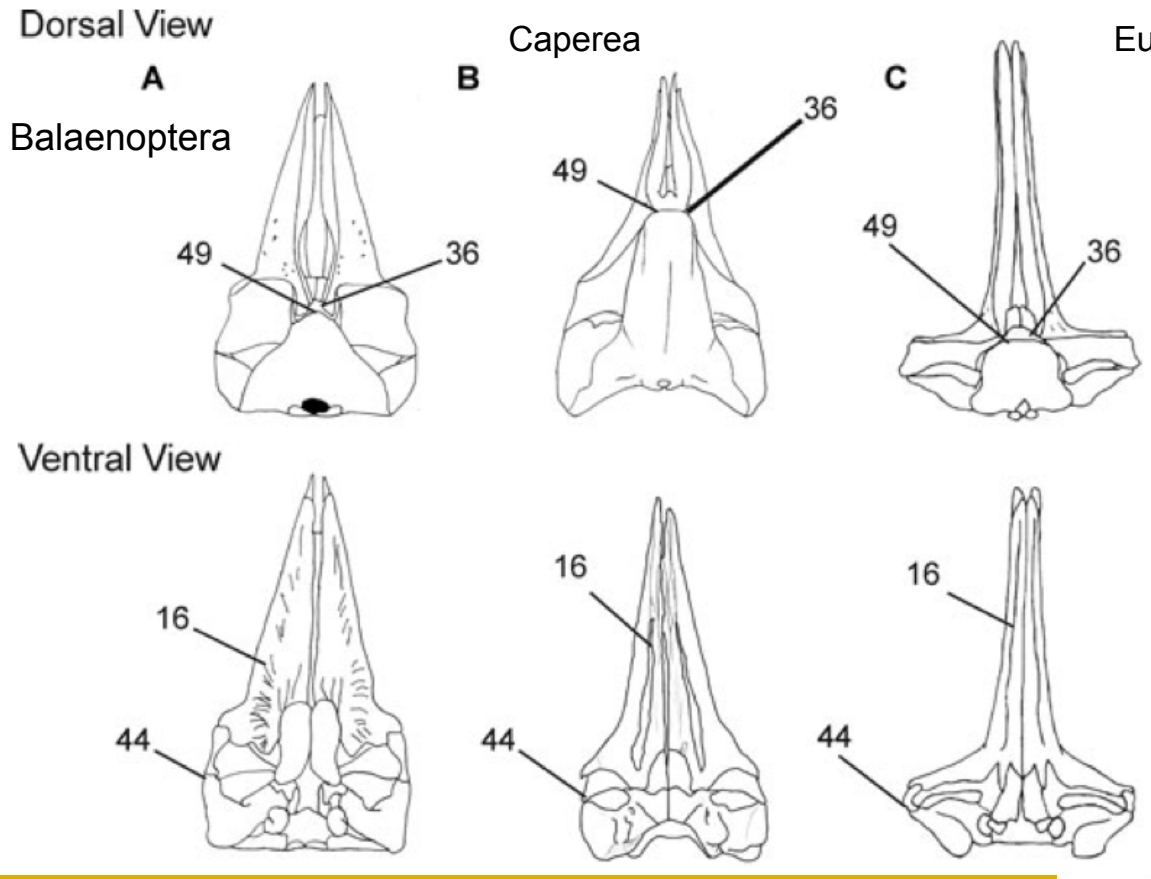

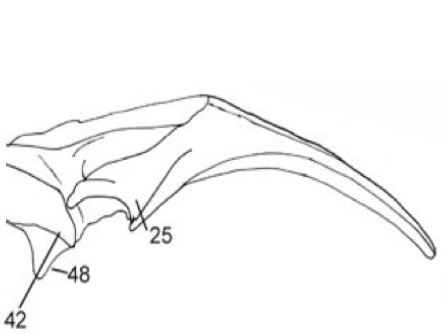

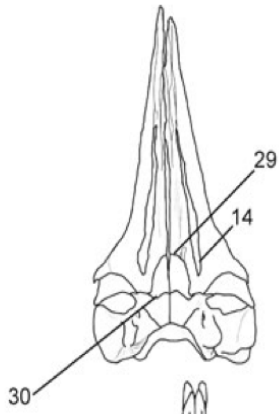

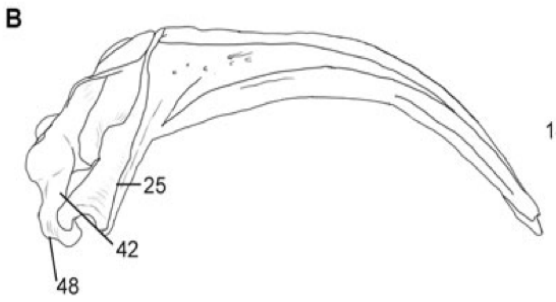

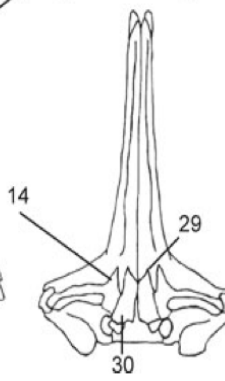

Synapomorphies Balaenidae:
ventral maxillary window that reaches the posterior margin of the maxilla (14), a ventrally developed supraorbital process with limited lateral expansion (25), M-shaped anterior margins of the palatine (29), long overlap of pterygoids by the palatine (30), and a dorsoventrally developed squamosal (42) with a reduced and bulbous postglenoid process (48). palatal maxillary sulci, which open into a long alveolar groove (16), parietal mostly excluded from view on the cranial vertex (36), a relatively short zygomatic process (44), and extension of the supraoccipital shield to the level of the frontal-maxillary suture.

Balaenidae

Churchill et al. 2011

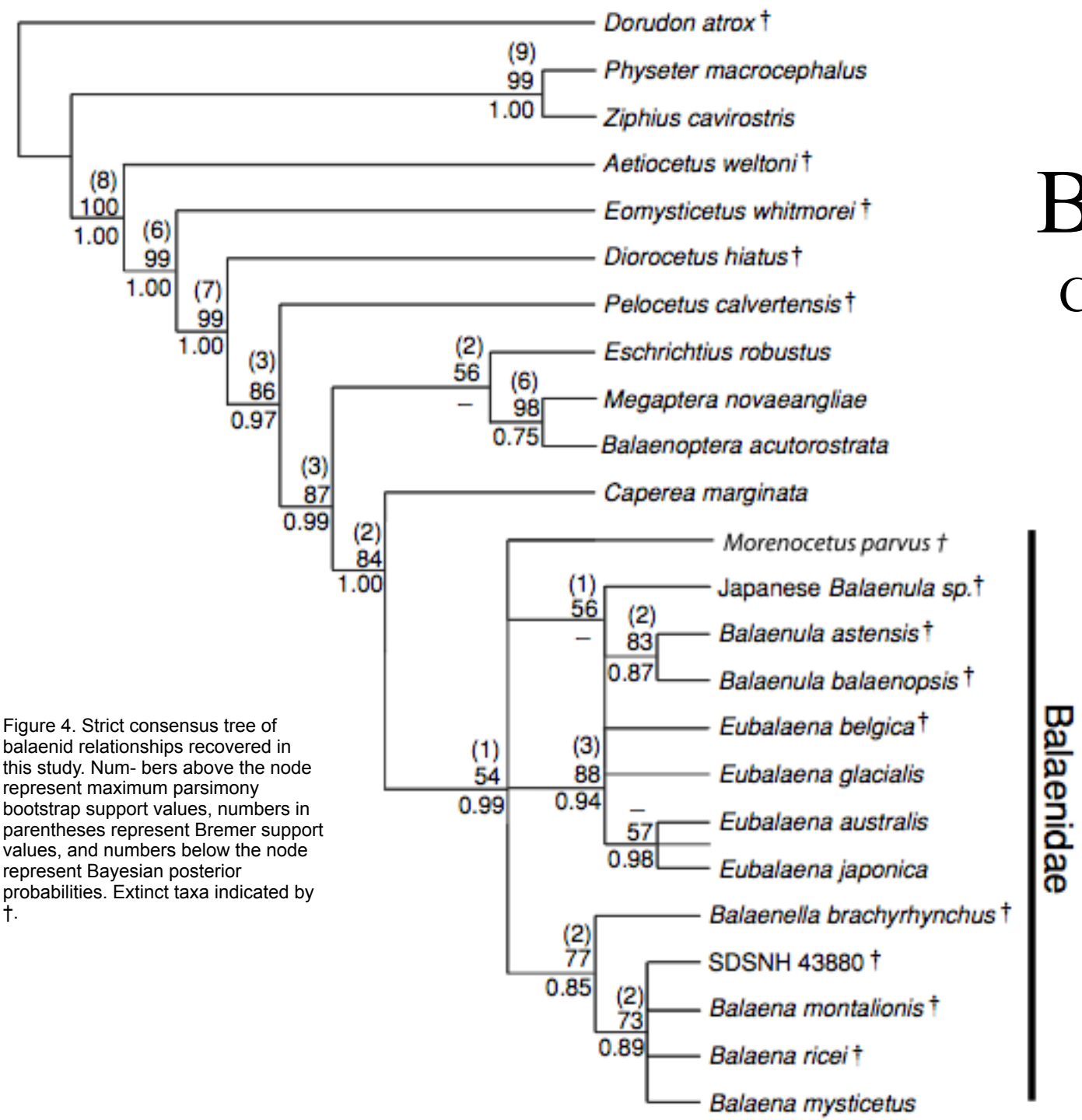

Figure 4. Strict consensus tree of balaenid relationships recovered in this study. Num- bers above the node represent maximum parsimony bootstrap support values, numbers in parentheses represent Bremer support values, and numbers below the node represent Bayesian posterior probabilities. Extinct taxa indicated by †.

Balaenidae

Baleia Franca

Balaena glacialis

Comprimento 18 metros

Massa :90.000 kg

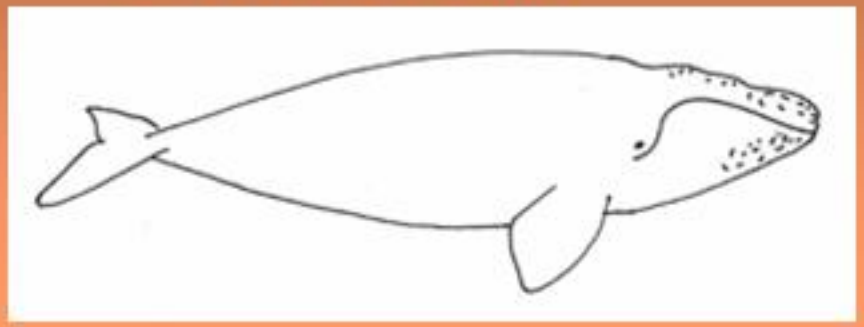

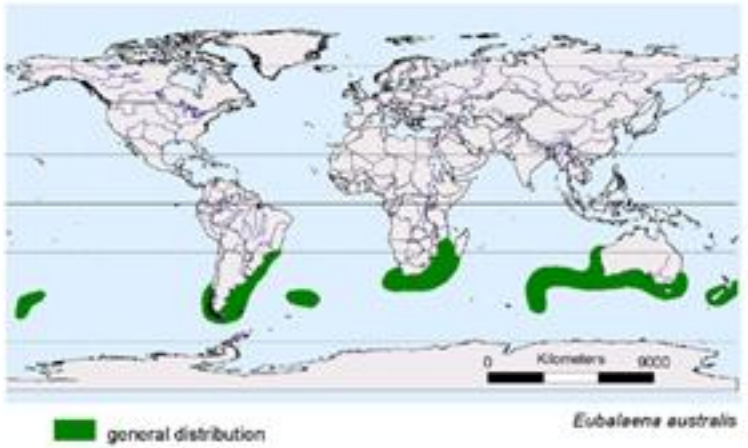

Balaenopteridae

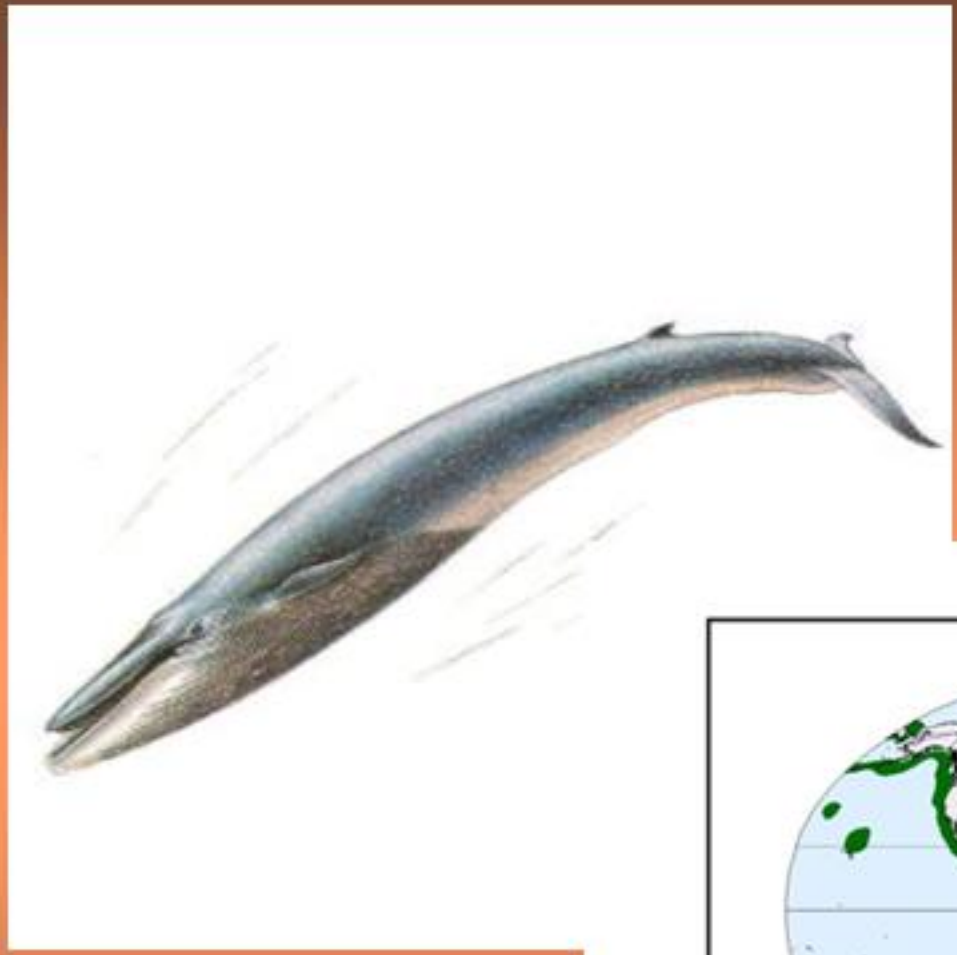

Baleia Azul

Balaenoptera musculus

Comprimento 28 metros

Massa :136.000 kg

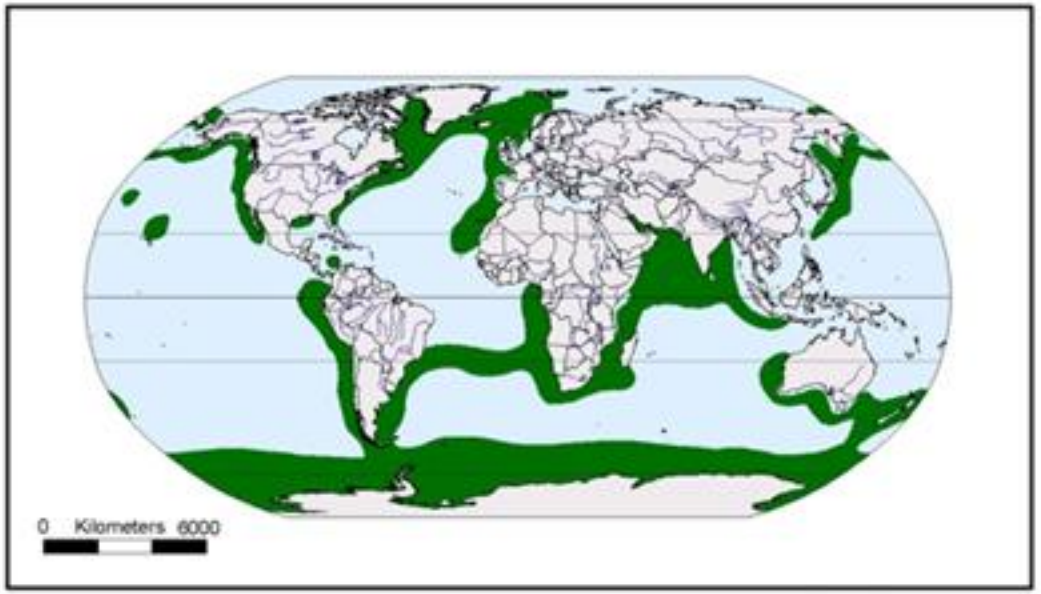

Balaenoptera musculus

general distribution


Balaenopteridae
Megaptera novaengliae

Balaenopteridae

Megaptera novaengliae

Foto: Monterrey Bay feeding ground - CSG 2013

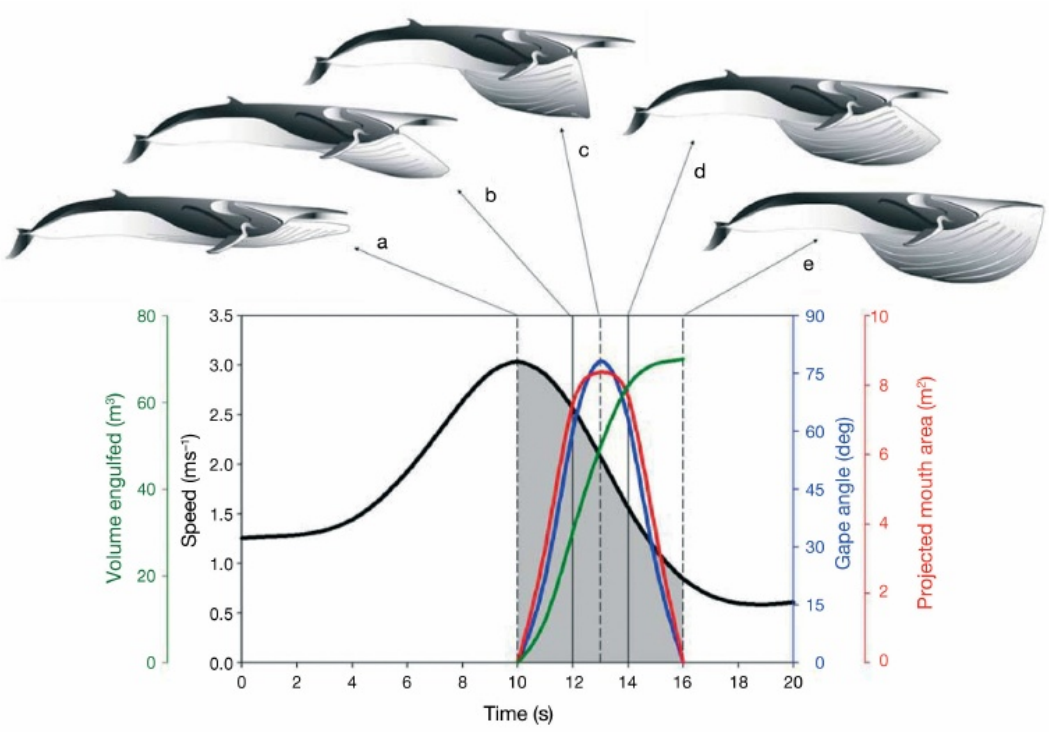

Balaenopteridae (rorcuales)

Goldbogen, J.A,. N.D. Pyenson, R.E. Shadwick.2007.
Big gulps require high drag for fin whalelunge feeding. Mar Ecol Prog Ser.
doi: 10.3354/meps07066

Balaenoptera physalus

Relationship between gape angle (red line), projected mouth area (blue line), speed (black line)and volume engulfed (green line) in the context of the mechanics of the body during a lunge. Vertical lines mark significant events throughout the lunge cycle represented by each schematic: (a) mouth begins to open, (b) ventral groove blubber (VGB)begins to expand, (c) maximum gape angle, (d) VGB is nearly fully expanded, and (e)Â mouth closes. The shaded area representsthe distance traveled during the lunge.

Modern baleen whales feed by filtering gulps of seawater through plates of baleen in their mouths.Credit: Doug Perrine/naturepl.com

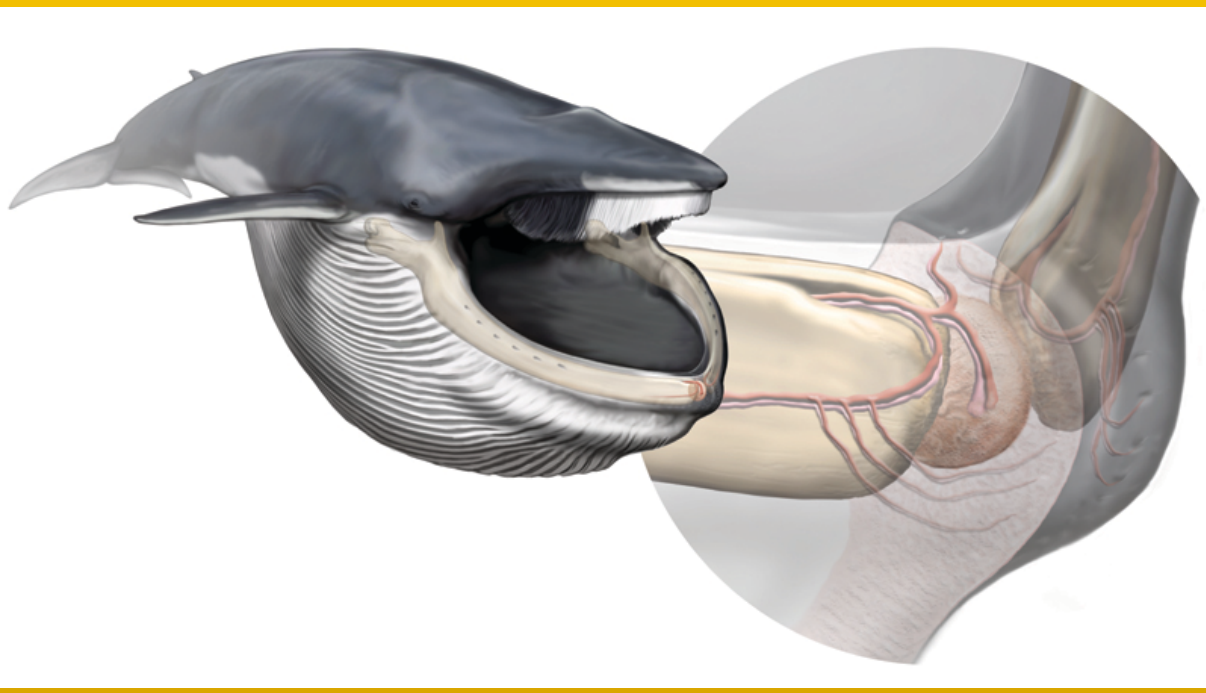

Pyenson, N. D., J. A. Goldbogen, A. W. Vogl, G. Szathmary, R. L. Drake and R. E. Shadwick. 2012. Discovery of a sensory organ that coordinates lunge-feeding in rorqual whales. Nature 485: 498-501. doi: 10.1038/nature11135

Balaenopteridae indet. Pyenson et al. 2014

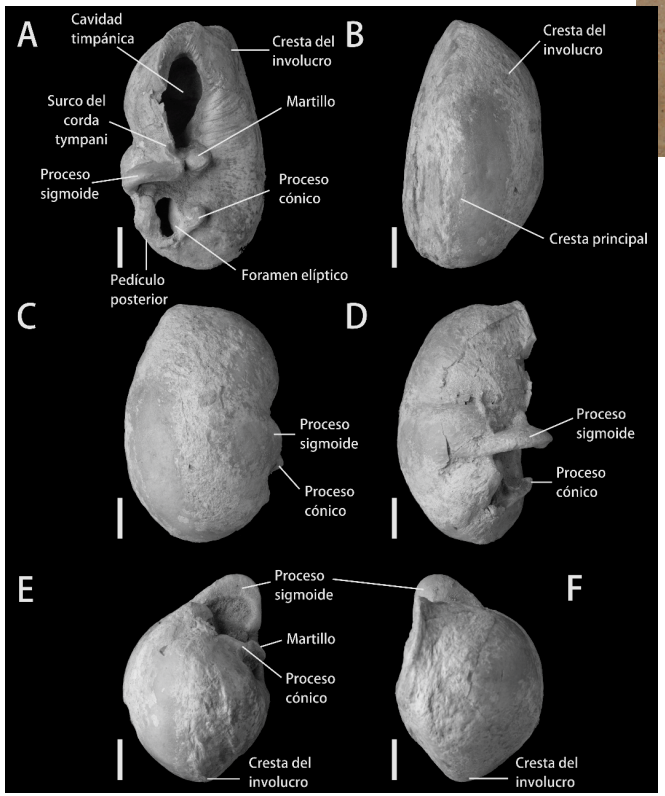

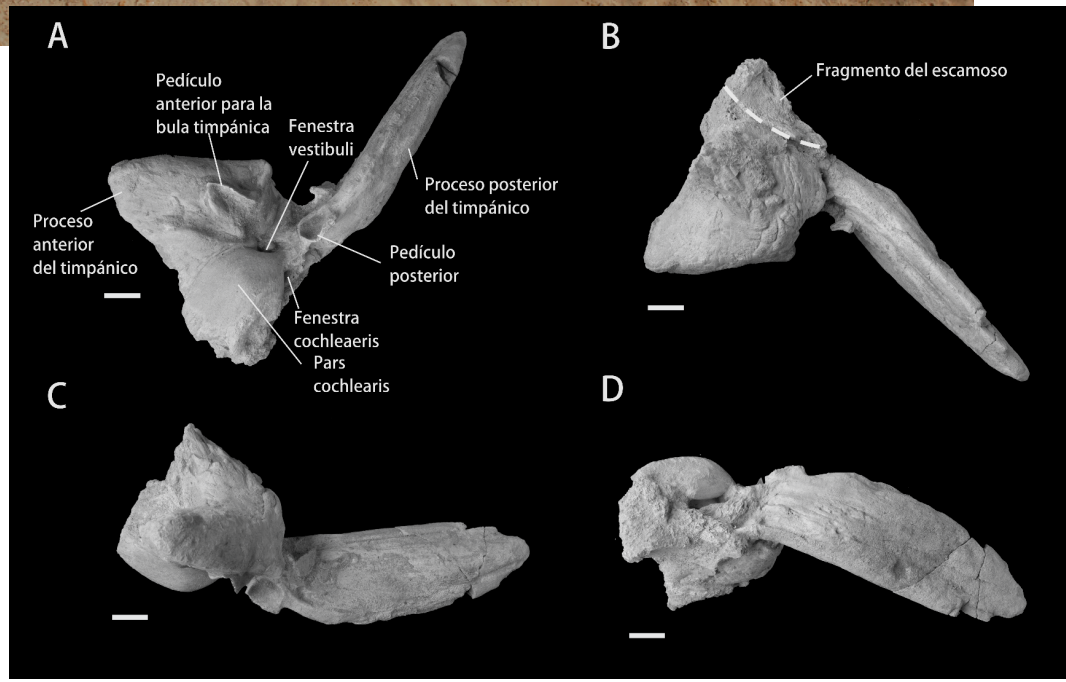

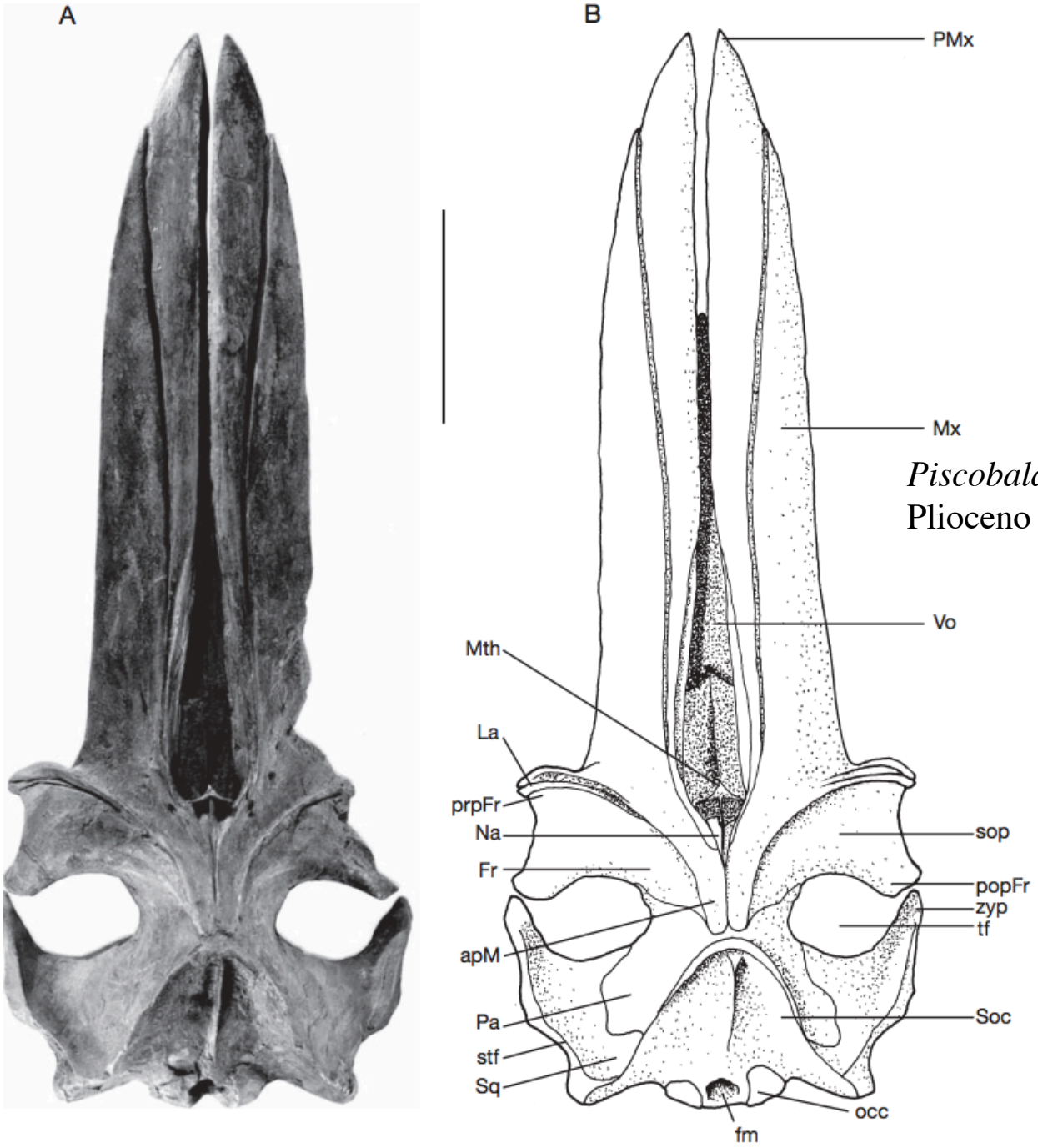

Piscobalaena nana (Cetotheridae)
Plioceno temprano (Fm. Pisco)

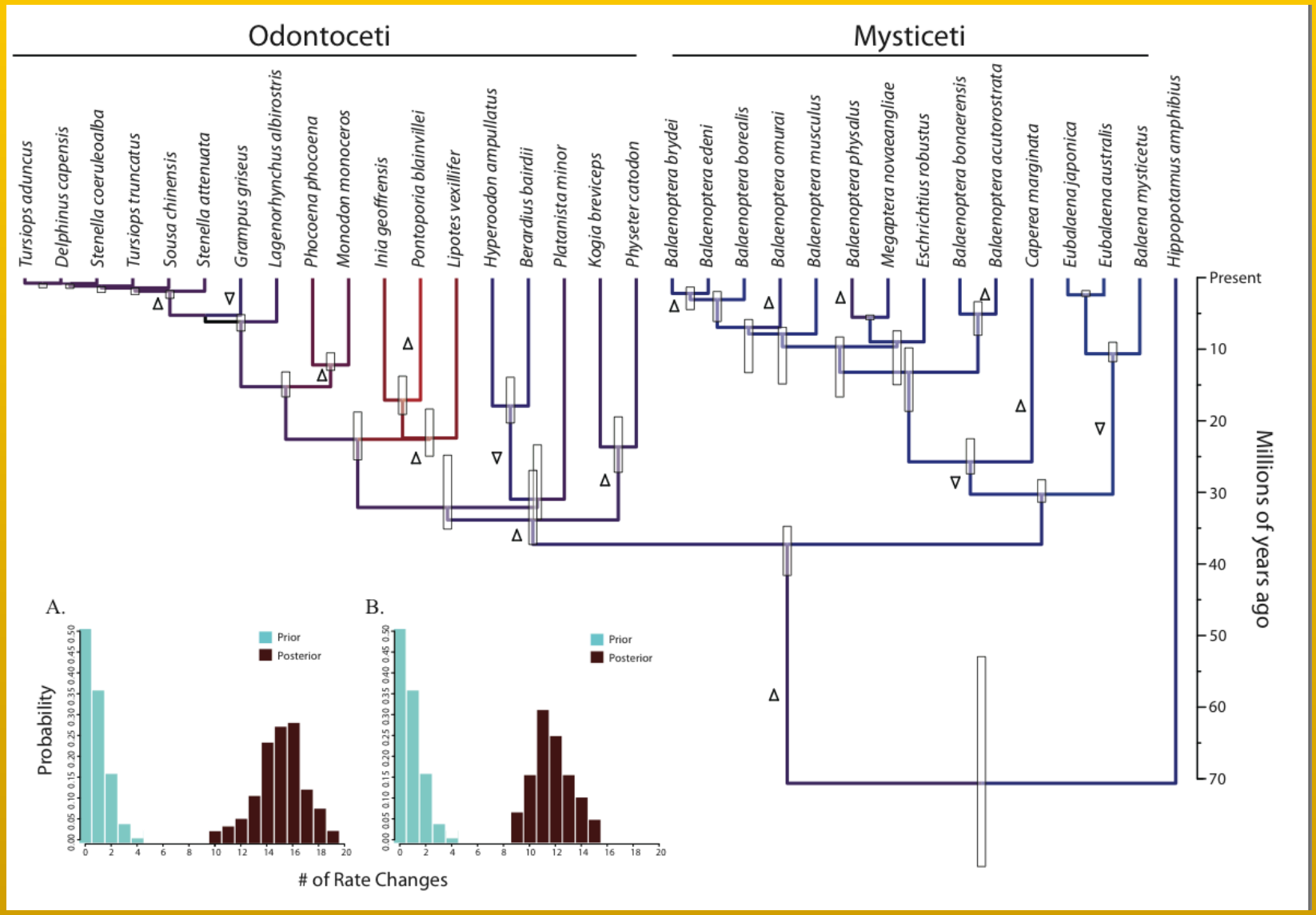
Odontoceti
Mysticeti
Tursiops aduncus
Delphinus capensis
Stenella coeruleoalba
Tursiops truncatus
Sousa chinensis
Stenella attenuata
Grampus griseus
Lagenorhynchus albirostris
Phocoena phocoena
Monodon monoceros
Inia geoffrensis
Pontoporia blainvillei
Lipotes vexillifer
Hyperoodon ampullatus
Berardius bairdii
Platanista minor
Kogia breviceps
Physeter catodon
Balaenoptera brydei
Balaenoptera edeni
Balaenoptera borealis
Balaenoptera omurai
Balaenoptera musculus
Balaenoptera physalus
Megaptera novaeangliae
Eschrichtius robustus
Balaenoptera bonaerensis
Balaenoptera acutorostrata
Caperea marginata
Eubalaena japonica
Eubalaena australis
Balaena mysticetus
Hippopotamus amphibius
Present
10
20
30
40
50
60
70
Millions of years ago
A.
B.
Prior
Posterior
Probability
# of Rate Changes

Odontoceti: Ecolocalización

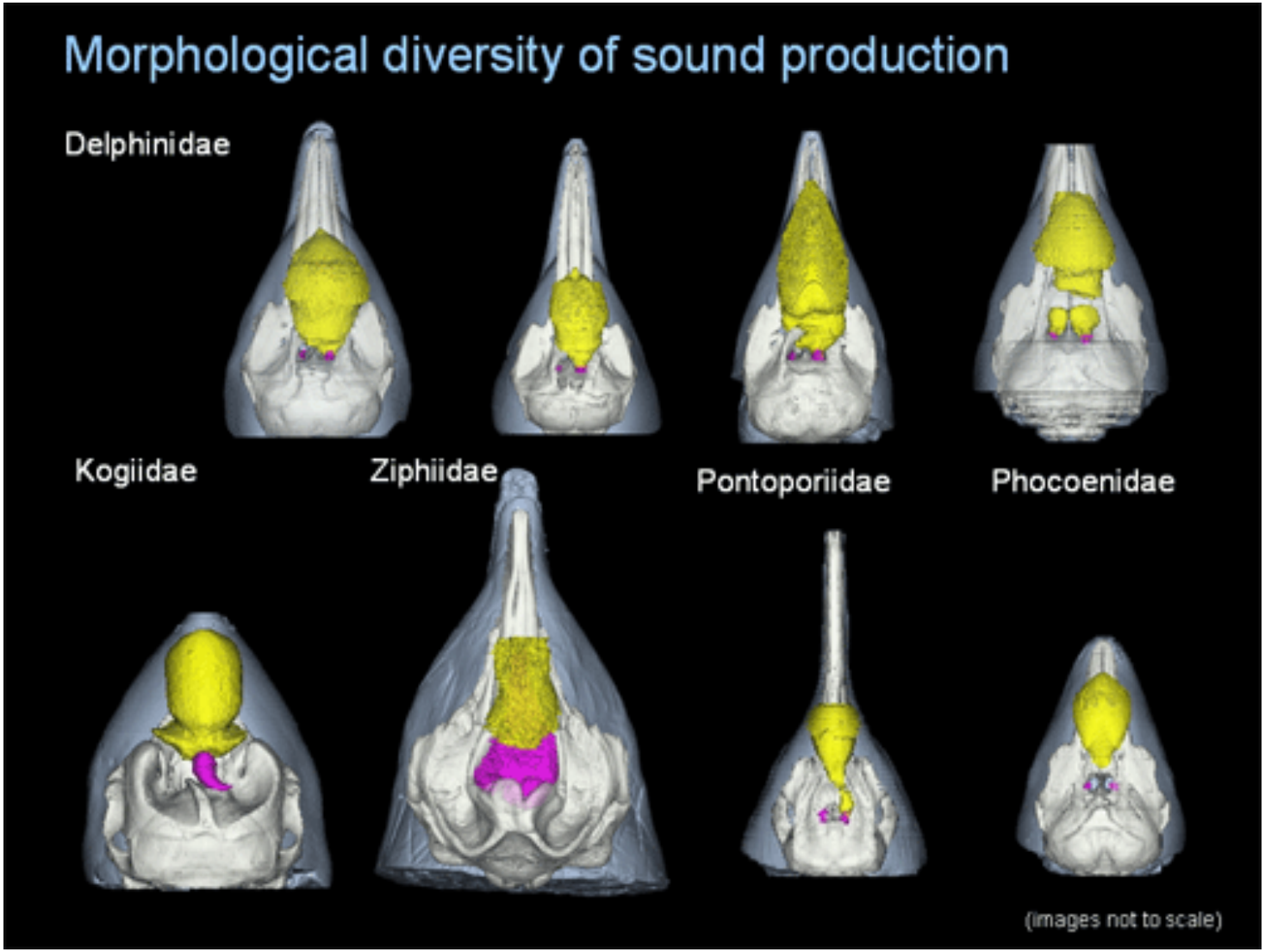

Uhen 2007

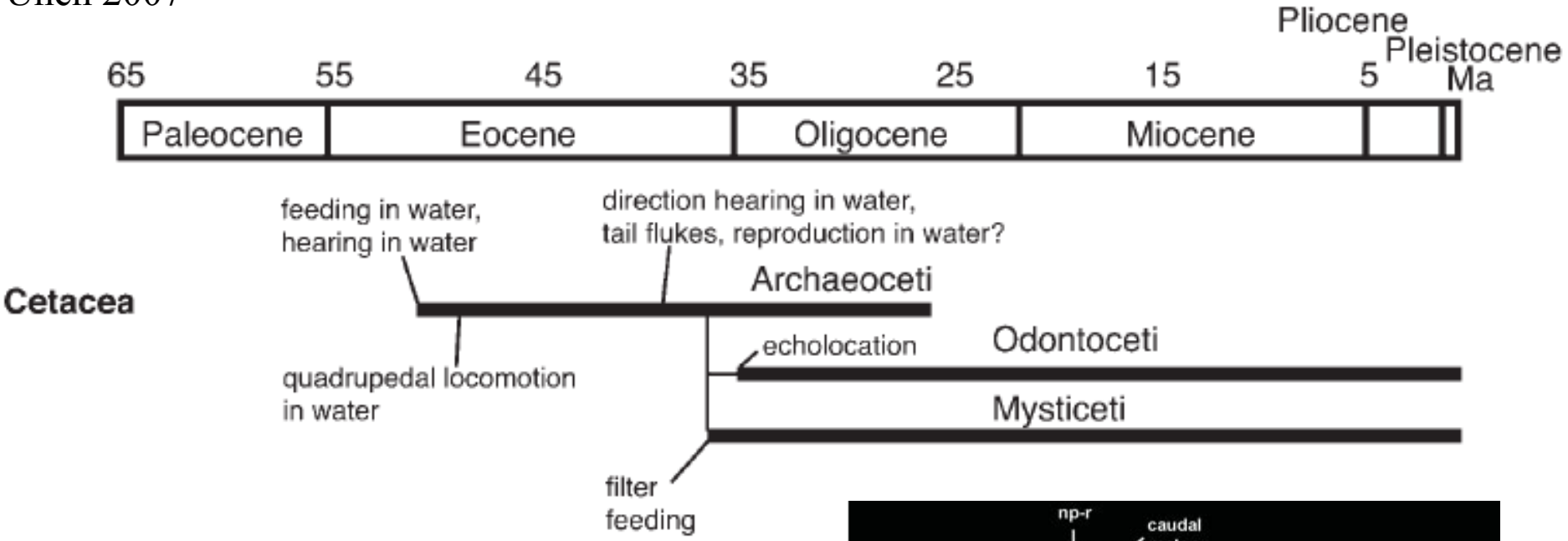

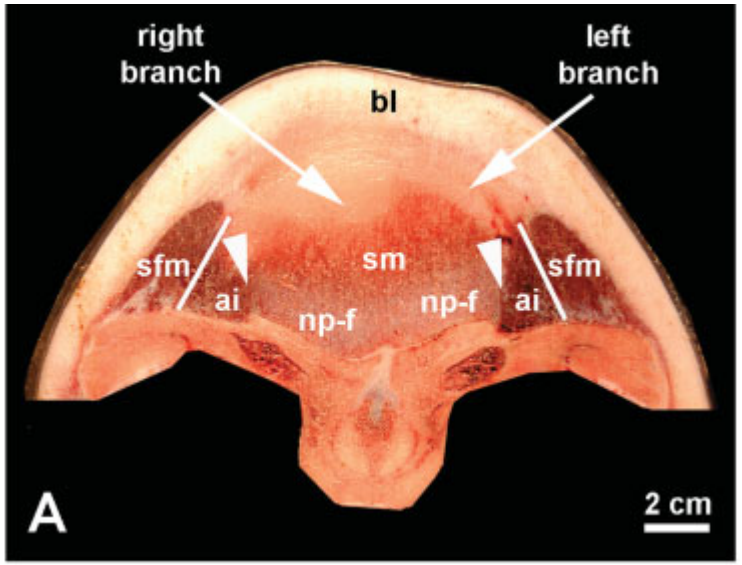

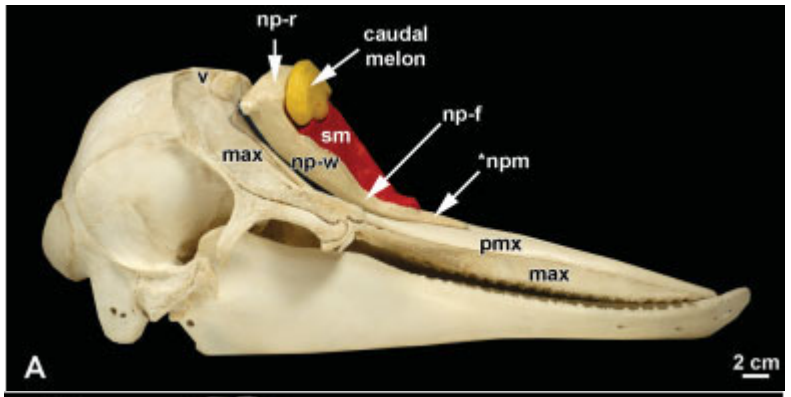

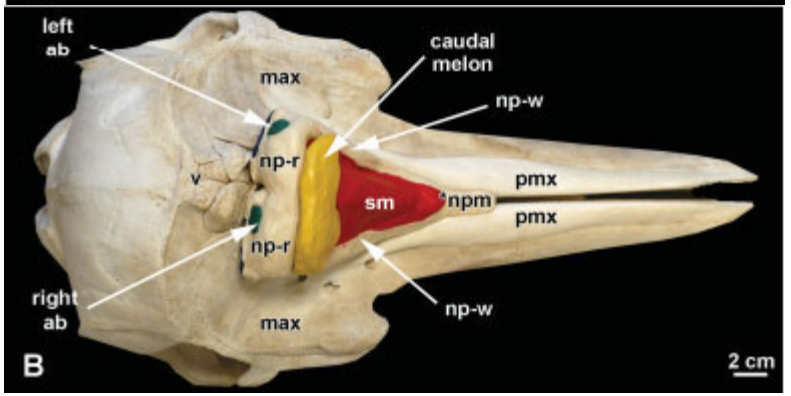

Harper et al. 2008

Mecanismo de la transmisión de sonido en mamíferos terrestres y en cetáceos

mamíferos terrestre (a)
pakicetídeo (b)
remingtonocetídeo/
protocetídeo (c)
odontoceto moderno (d)

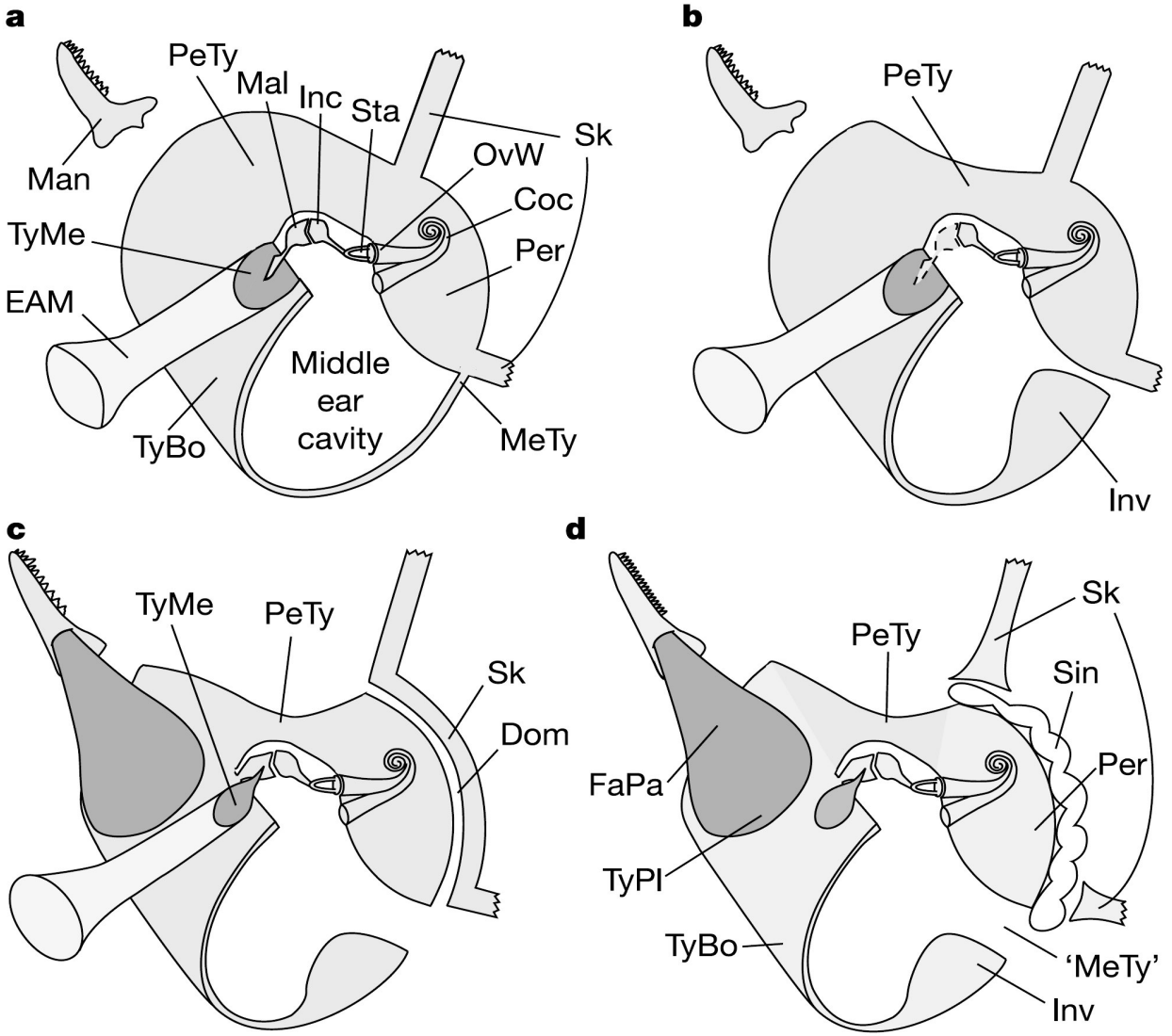

Figure 2 Sound transmission mechanisms in land mammals and whales. Diagram of the

Desarrollo tardío de la cápsula nasal

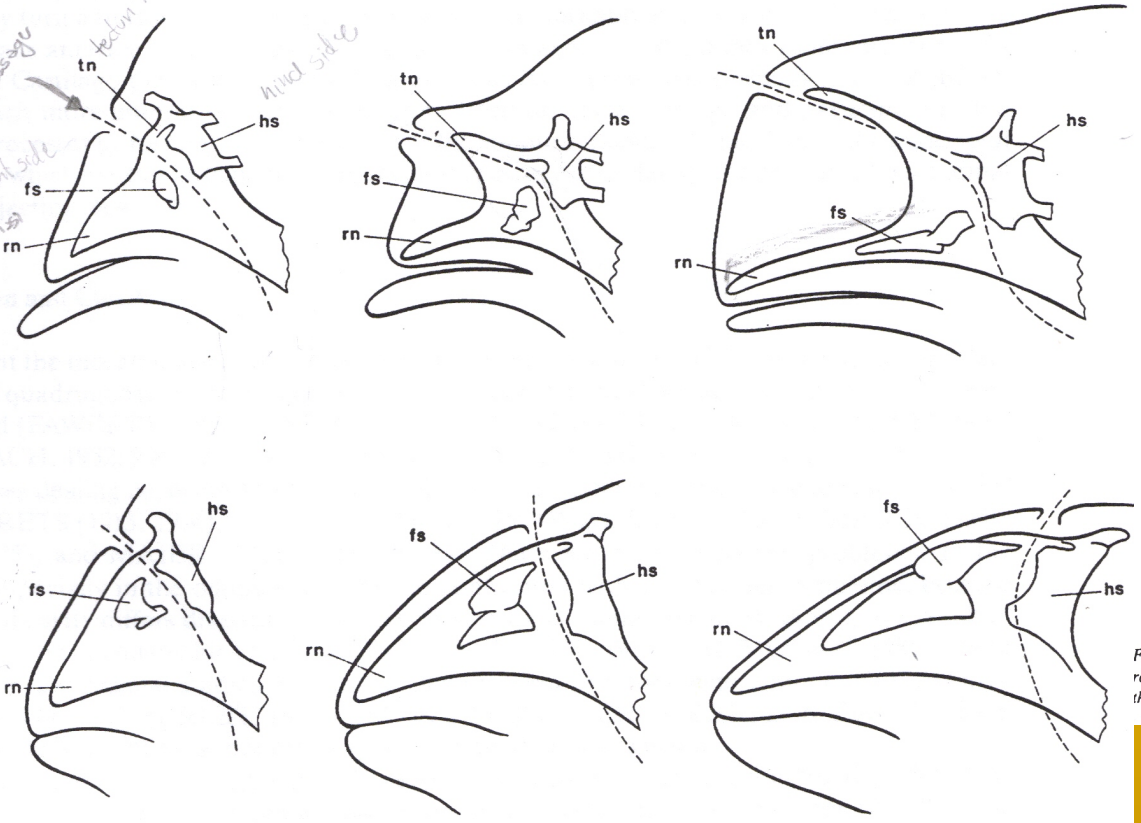

Fig. 9 : Schematic representation of developmental changes of the nasal structures during early ontogeny in Physeter macrocephalus *(upper row) and in* Phocoena phocoena *(lower row). The schemes show a sequence of embryonal stages of both species of about 40, 90, and 170 mm body length. For labelling see list of abbreviations. Broken line shows the nasal passage.*

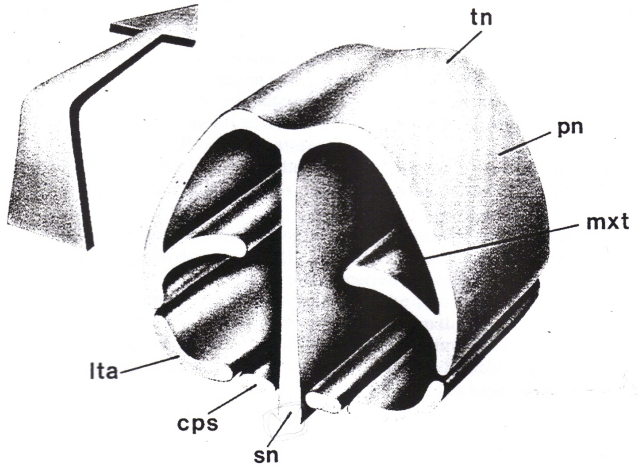

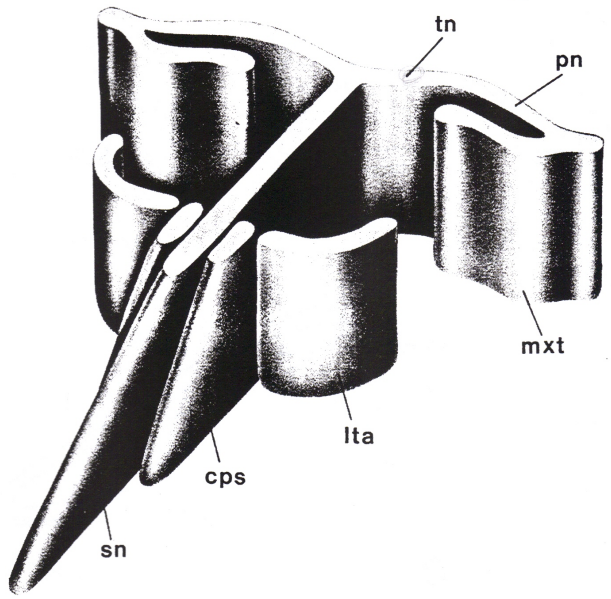

Fig. 10 : Ontogenetic displacement of the nasal structures in odontocetes. Above: early generalized pattern corresponding to terrestrial mammals. Below: typical odontocete conditions after the rotation of the nasal capsule through approximately 90 degrees. For labelling see list of abbreviations.

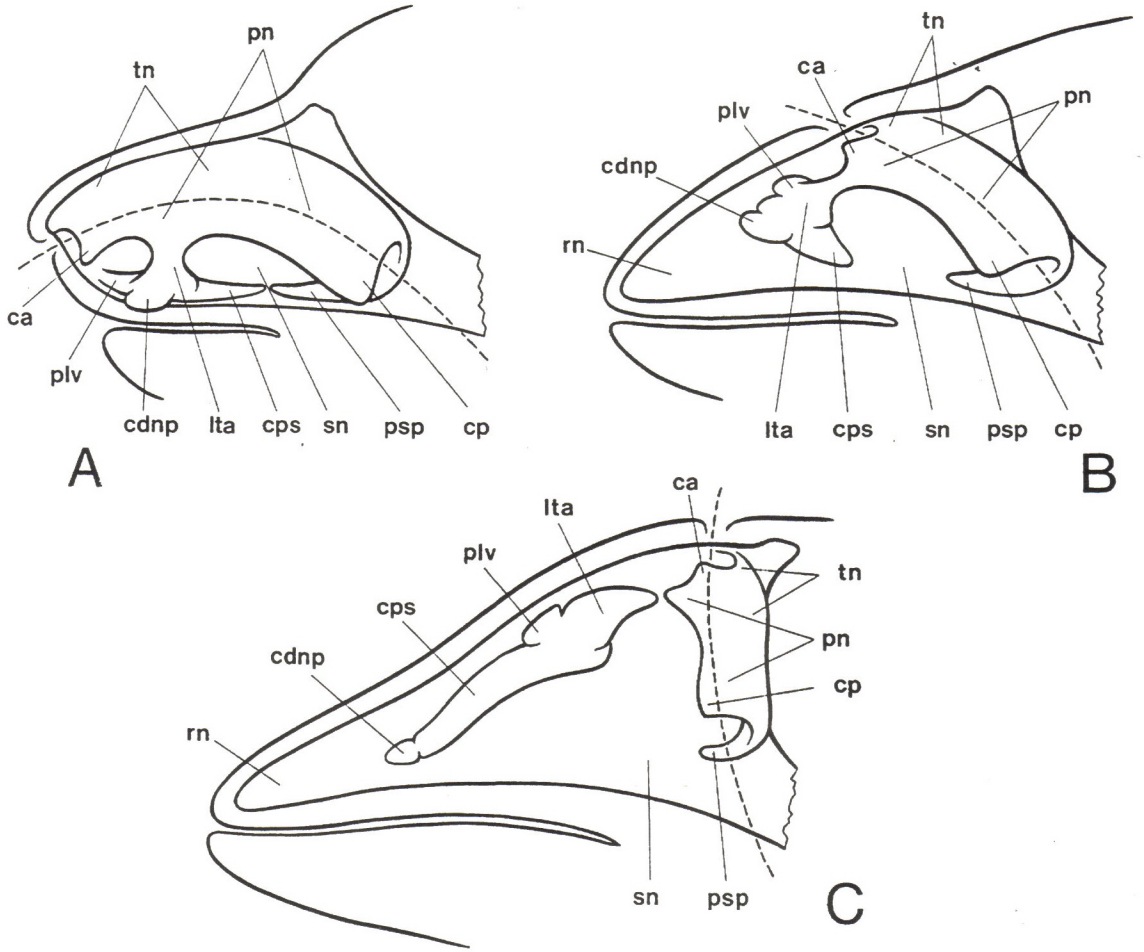

Fig. 11 : Sequence of possible evolutionary stages of the nasal capsule, starting with the generalized conditions in a terrestrial mammal (A), continuing with a hypothetical intermediate form (B), and finished with the typical capsule of odontocetes (C). For labelling see list of abbreviations.

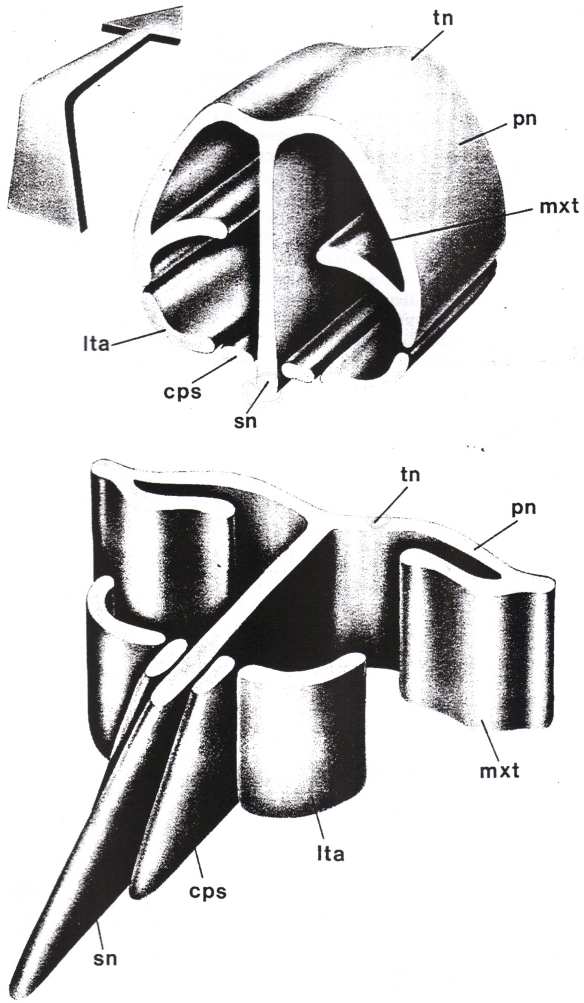

g. 10 : Ontogenetic displacement of the nasal structures in odontocetes. Above: early generalized pattern corsponding to terrestrial mammals. Below: typical odontocete conditions after the rotation of the nasal capsule rough approximately 90 degrees. For labelling see list of abbreviations.

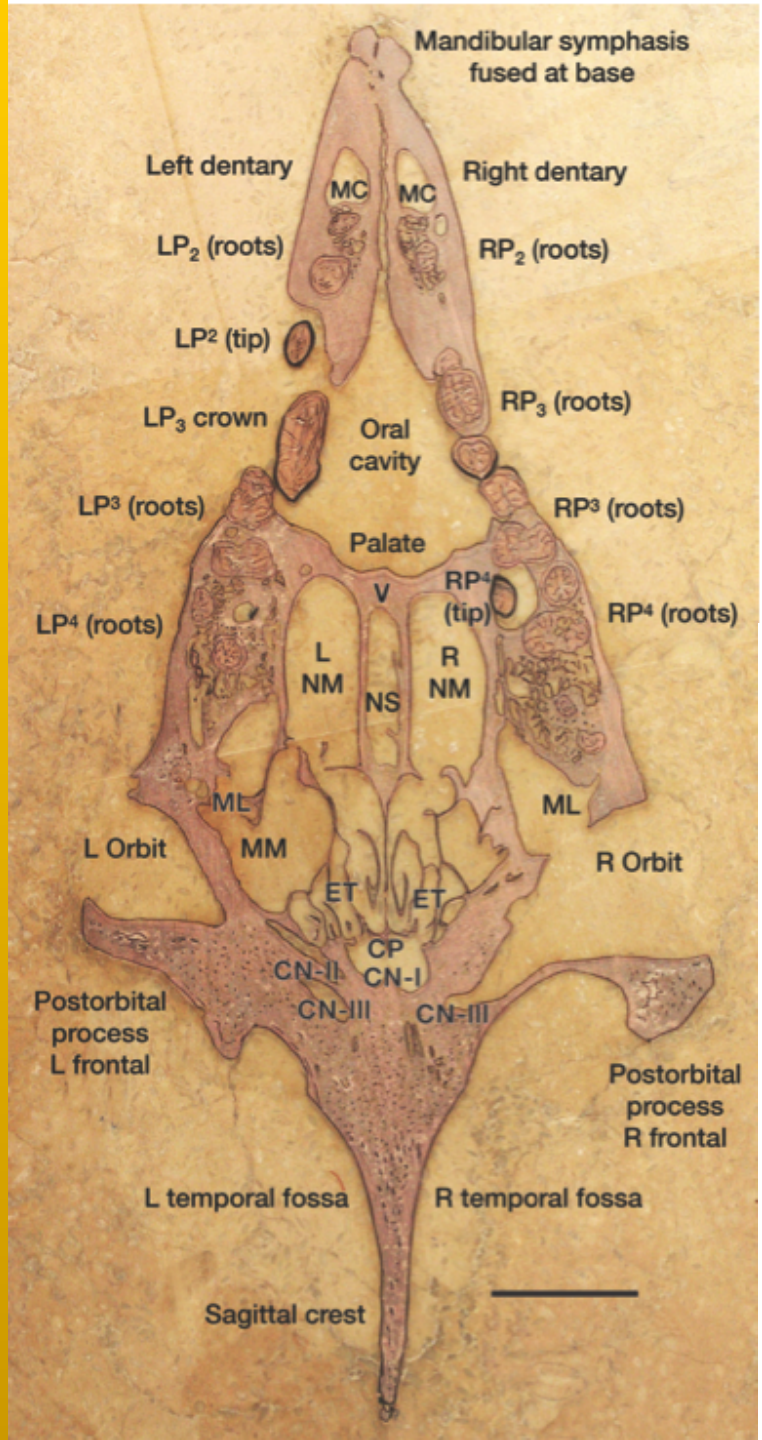

FIGURE 11. Consensus tree of nine equally parsimonious cladograms showing the relationships of *Aegyptocetus tarfa* with other archaeocetes. Tree length = 389; CI = 0.68; RI = 0.74. See Geisler et al. (2005) for description of characters and matrix, and Supplementary Data 3 for coding of characters of *Aegyptocetus tarfa* and for description of the nine equally parsimonious cladograms.

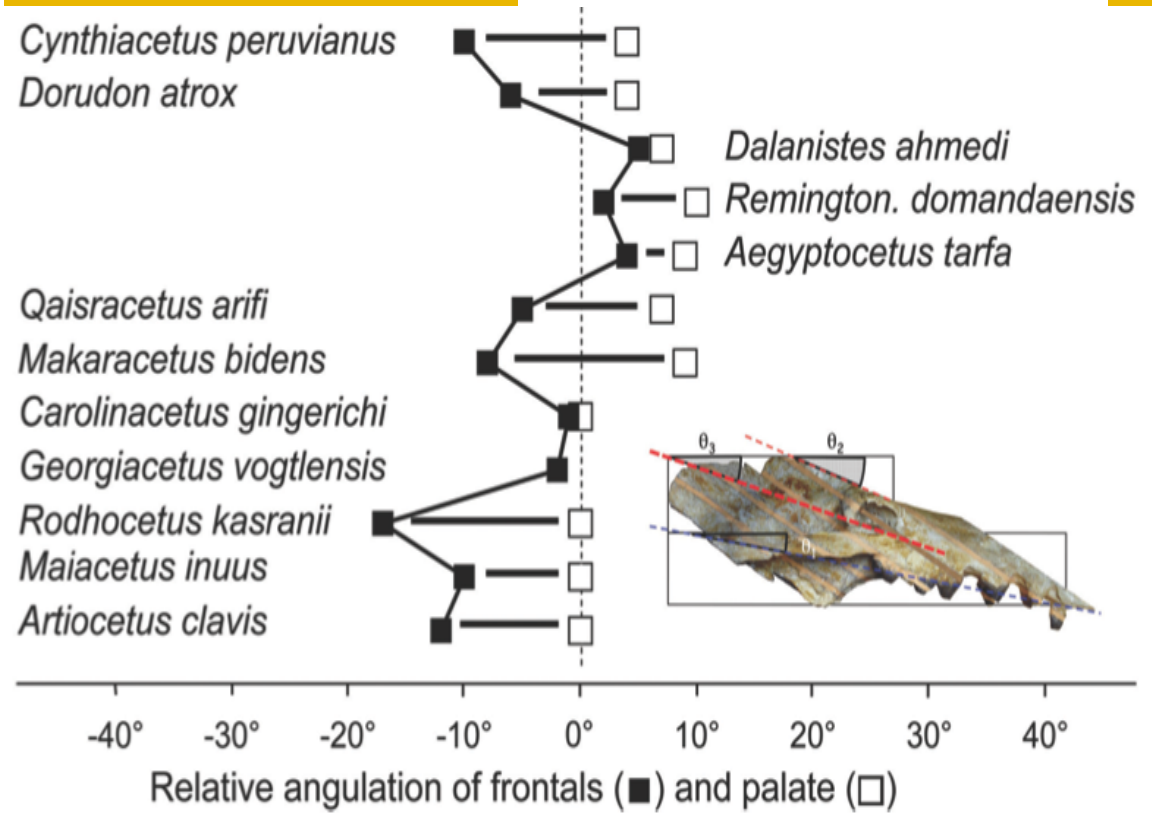

Región ótica: Paquiostosis

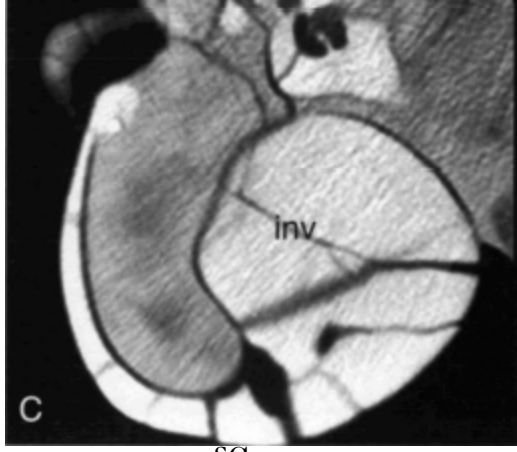

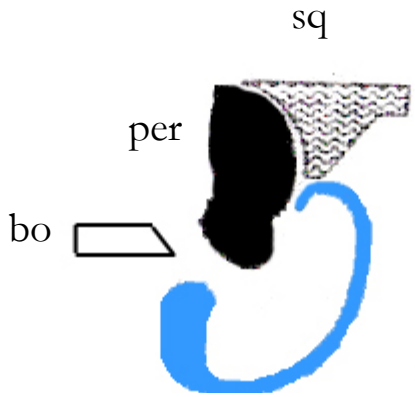

Basilosaurideos

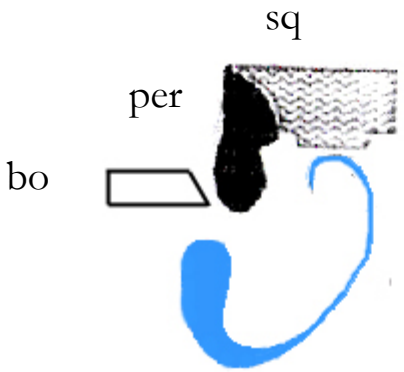

Paquicetideos

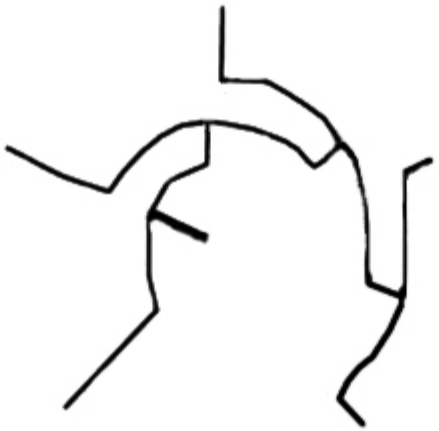

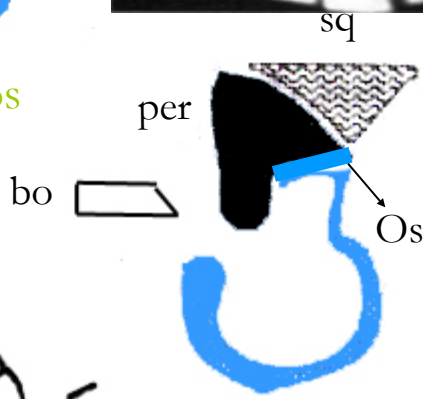

Baleanopterideos

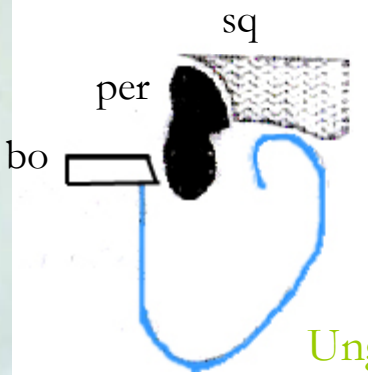

Ungulados

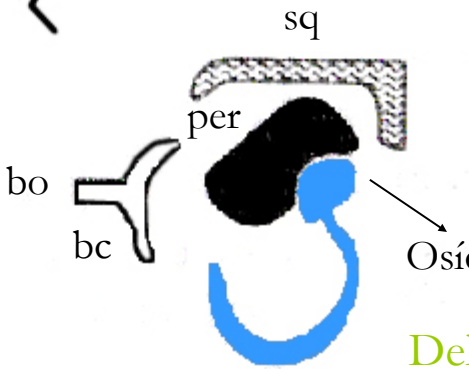

Delfinideos

LETTER

doi:10.1038/nature13086

A new fossil species supports an early origin for toothed whale echolocation

Jonathan H. Geisler[1], Matthew W. Colbert[2] & James L. Carew[3]

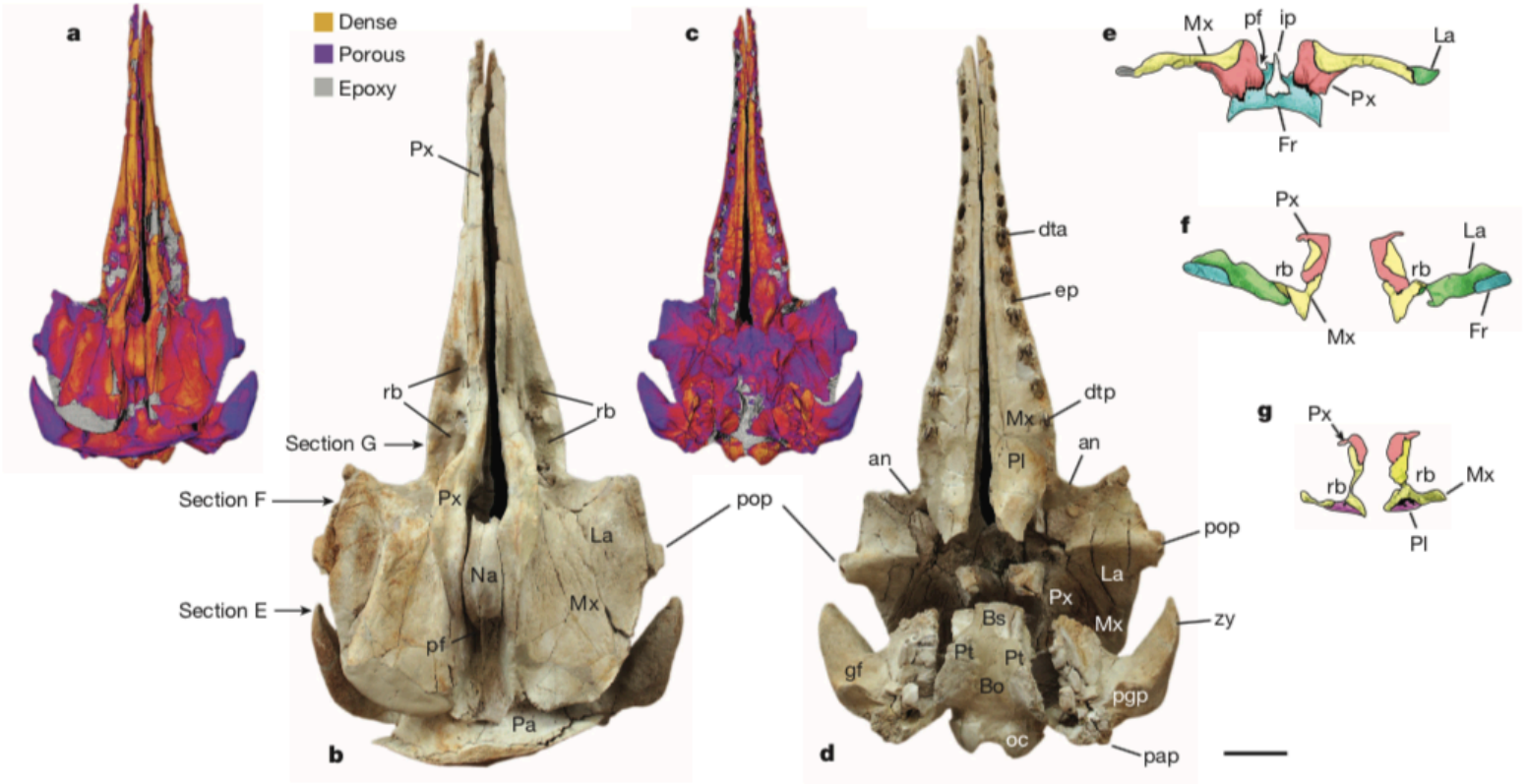

Figure 1 | Holotype skull of *Cotylocara macei* (CCNHM-101), including cross-sections and bone density. **a**, **b**, CT model and photograph of skull in dorsal view. **c**, **d**, Same as **a**, **b**, but in ventral view. **e**–**g**, CT cross-sections of skull; locations indicated in **b**. Colours in **a** and **c** reflect the relative density of bone, whereas in **e**–**g**, each bone is a separate colour as follows: blue, frontal; green, lacrimal; purple, palatine; red, premaxilla; white, interparietal; yellow, maxilla. an, antorbital notch; Bo, basioccipital; Bs, basisphenoid; dta, anteriormost double-rooted tooth; dtp, posteriormost double-rooted tooth; ep, embrasure pit; Fr, frontal; gf, glenoid fossa; ip, interparietal; La, lacrimal; Mx, maxilla; Na, nasal; oc, occipital; Pa, parietal; pap, paroccipital process; pf, postnarial fossa; pgp, postglenoid process; Pl, palatine; pop, postorbital process; Pt, pterygoid; Px, premaxilla; rb, rostral basin; zy, zygomatic process. Scale bar is 5 cm.

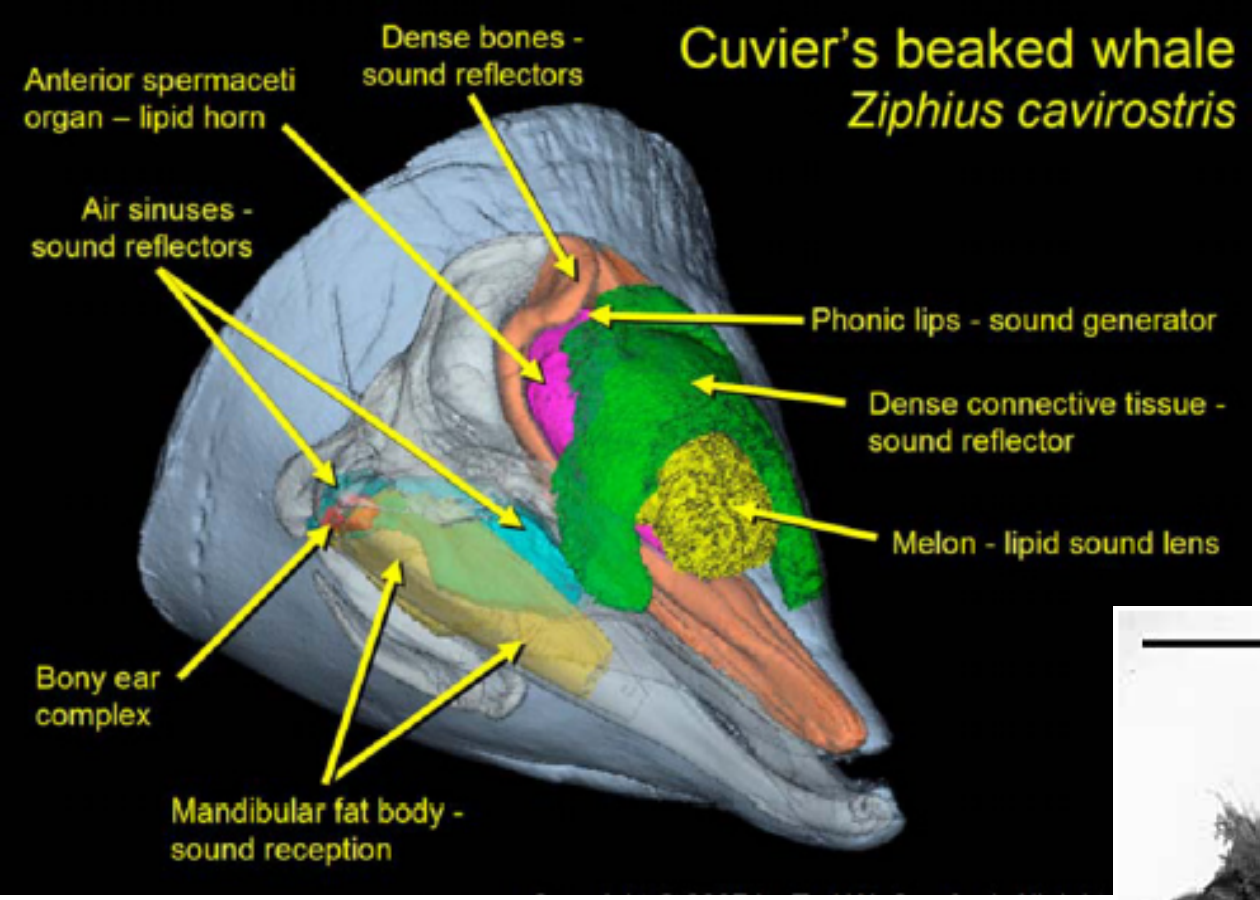

Cranford *et al.* (2008)

Clarke (2003)

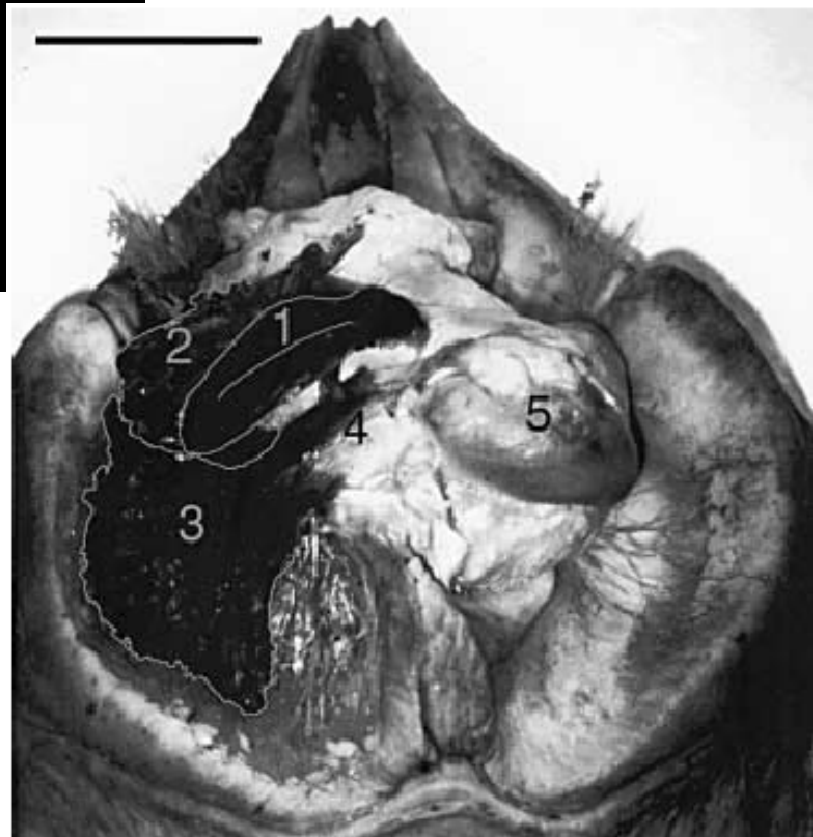

Las estructuras blandas dictan la forma de los huesos que la circundan en el caso de la anatomia facial de odontocetos (Fordyce 1994)

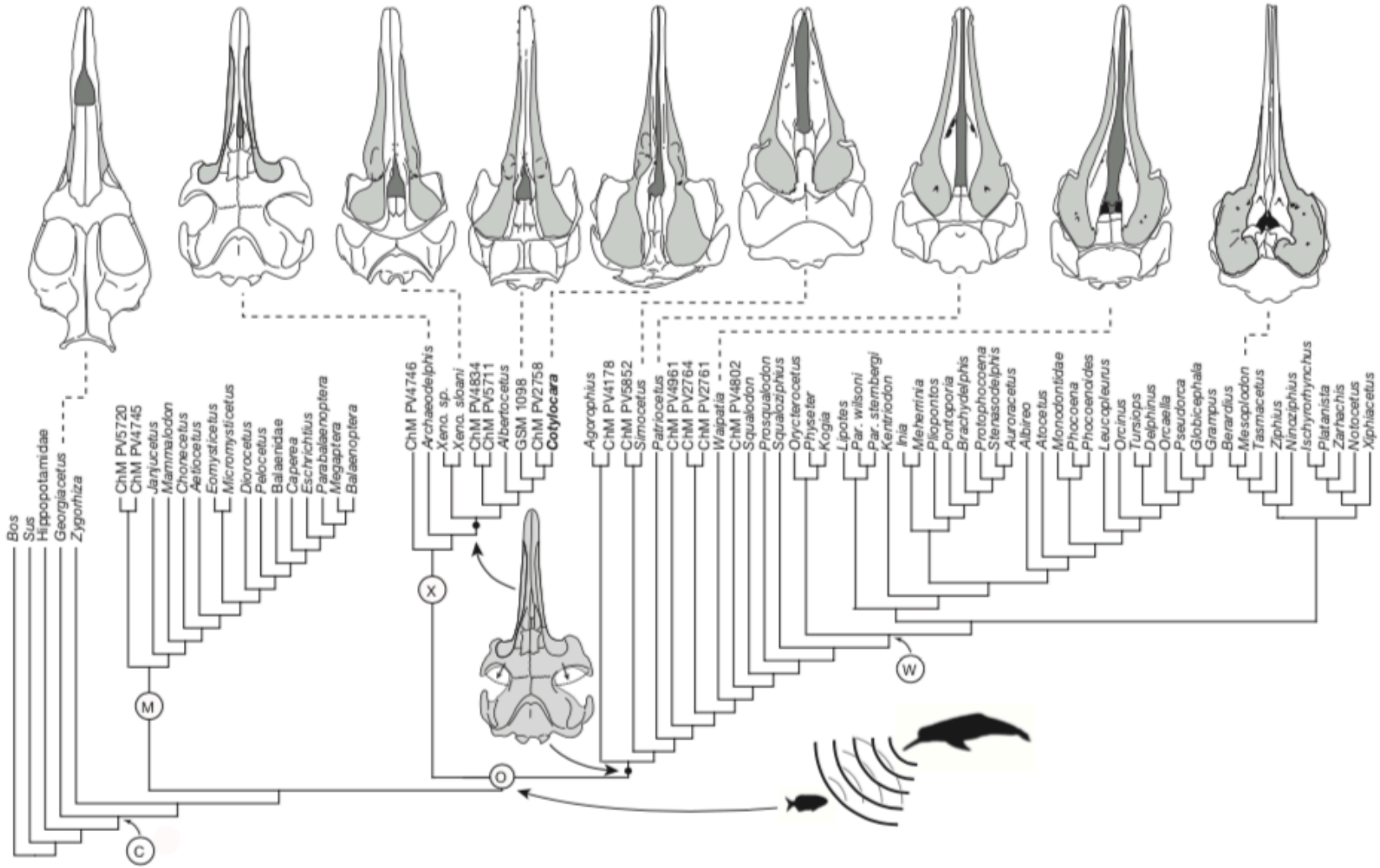

Figure 3 | Phylogeny supported by the present study, with evolution of echolocation and skull shape. Skulls are not to scale; maxilla is in grey. Solid circles indicate convergent evolution of the roof to the temporal fossa (see Supplementary Information). Aspects of the skull of *Archaeodelphis* were reconstructed, braincase of *Xenorophus sloani* based on CCNHM-168, and three skulls redrawn from published figures[10,29,30], adapted with permission from ref. 10 (Smithsonian Institution Scholarly Press) and ref. 29 (San Diego Society of Natural History). C, Cetacea; CCNHM, College of Charleston Natural History Museum, South Carolina; ChM PV, The Charleston Museum, Vertebrate Paleontology Collection, South Carolina; GSM, Georgia Southern Museum; M, Mysticeti; O, Odontoceti; *Par.*, *Parapontoporia*; X, Xenorophidae; *Xeno.*, *Xenorophus*; W, crown Odontoceti.



Variabilidad morfologica Distribución geográfica, temporal, ambiental




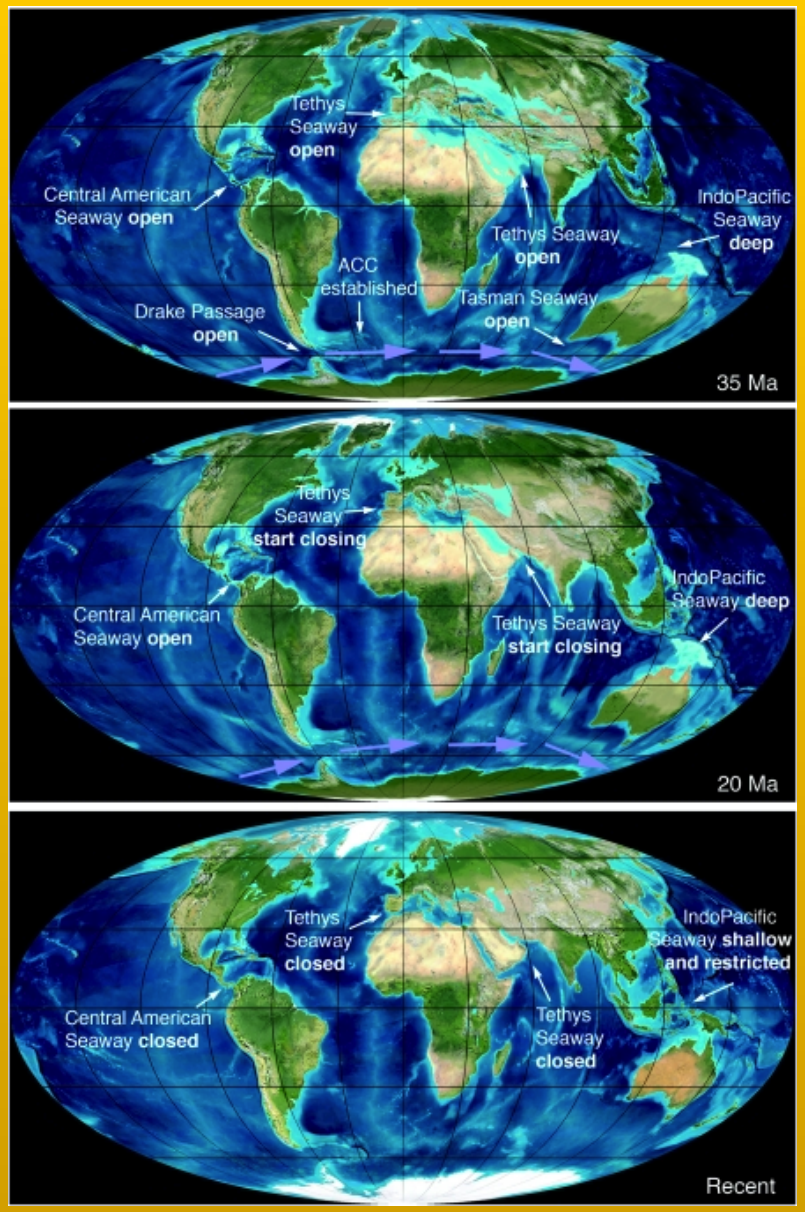

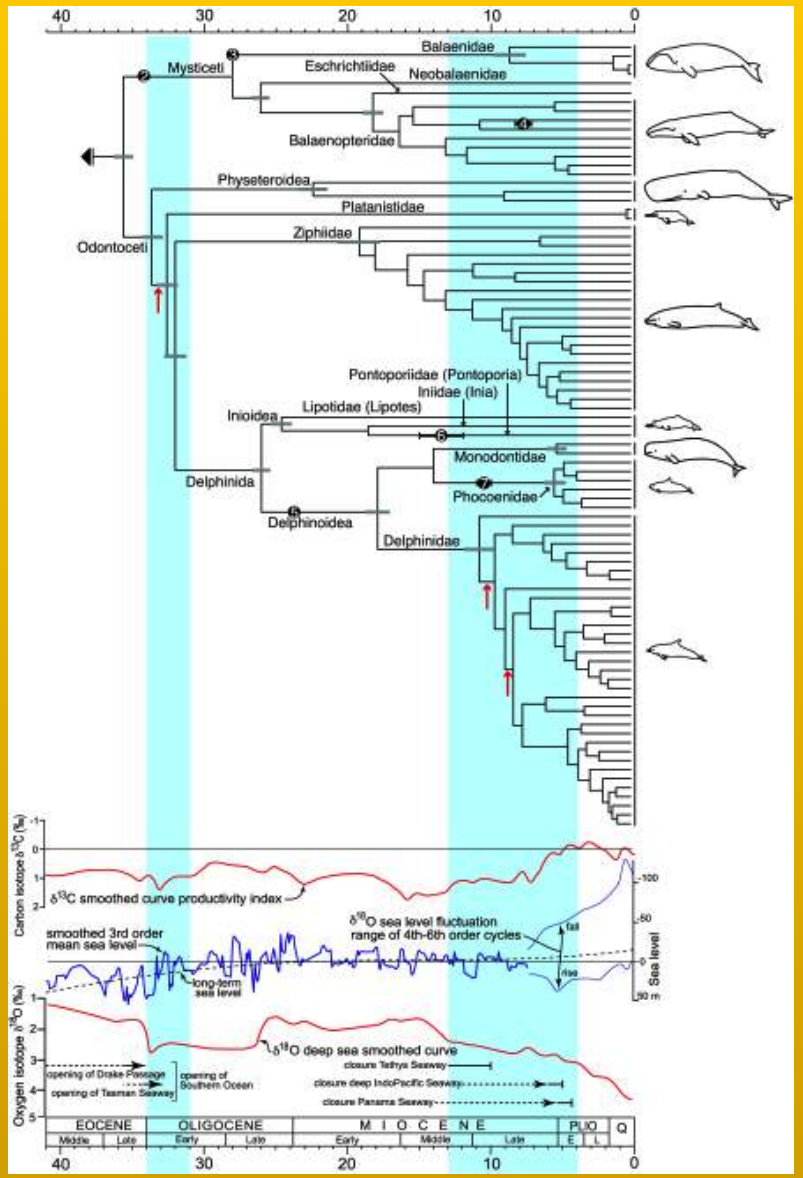

Steeman et al. 2009.
Radiation of Extant Cetaceans Driven by Restructuring of the Oceans. Syst. Biol. 58: 573-585

Odontoceti – tandwalvissen.
Squalodon. Oligoceen tot vroeg-Mioceen. ±22 miljoen jaar geleden. Lengte ±2,5 meter.

Eurhinodelphis
Mioceno

Odontoceto

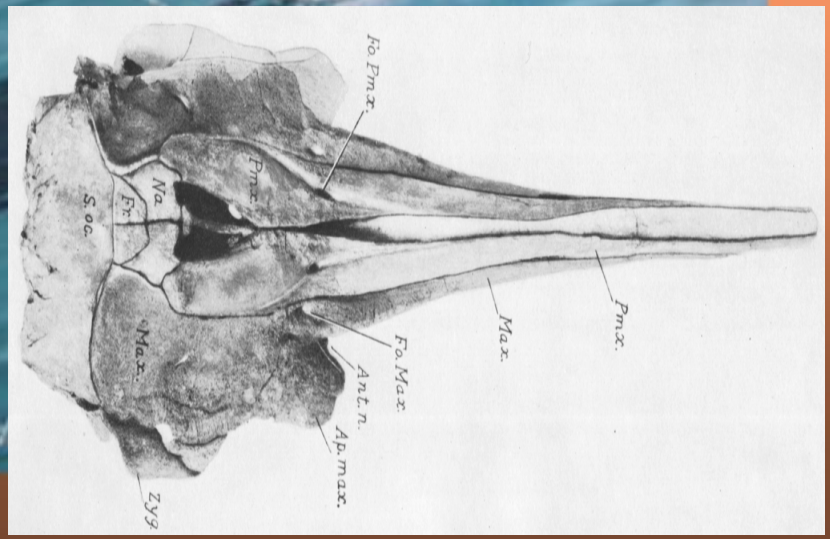

Origin and Evolution of Large Brains in Toothed Whales

LORI MARINO,[1]* DANIEL W. MCSHEA,[2] AND MARK D. UHEN[3]
[1]Neuroscience and Behavioral Biology Program, Emory University, Atlanta, Georgia
[2]Department of Biology, Duke University, Durham, North Carolina
[3]Cranbrook Institute of Science, Bloomfield Hills, Michigan

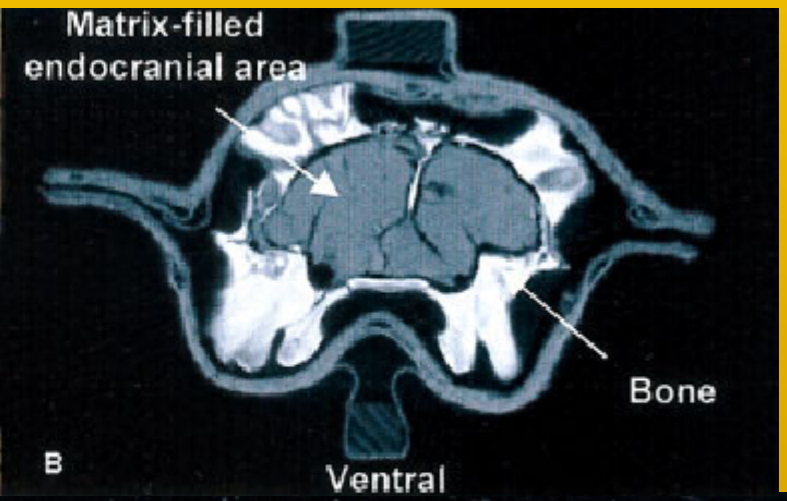

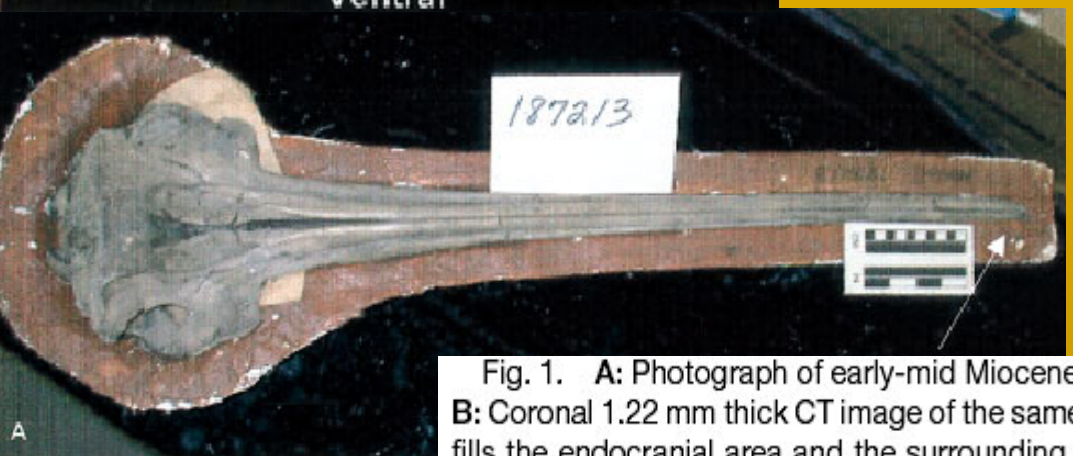

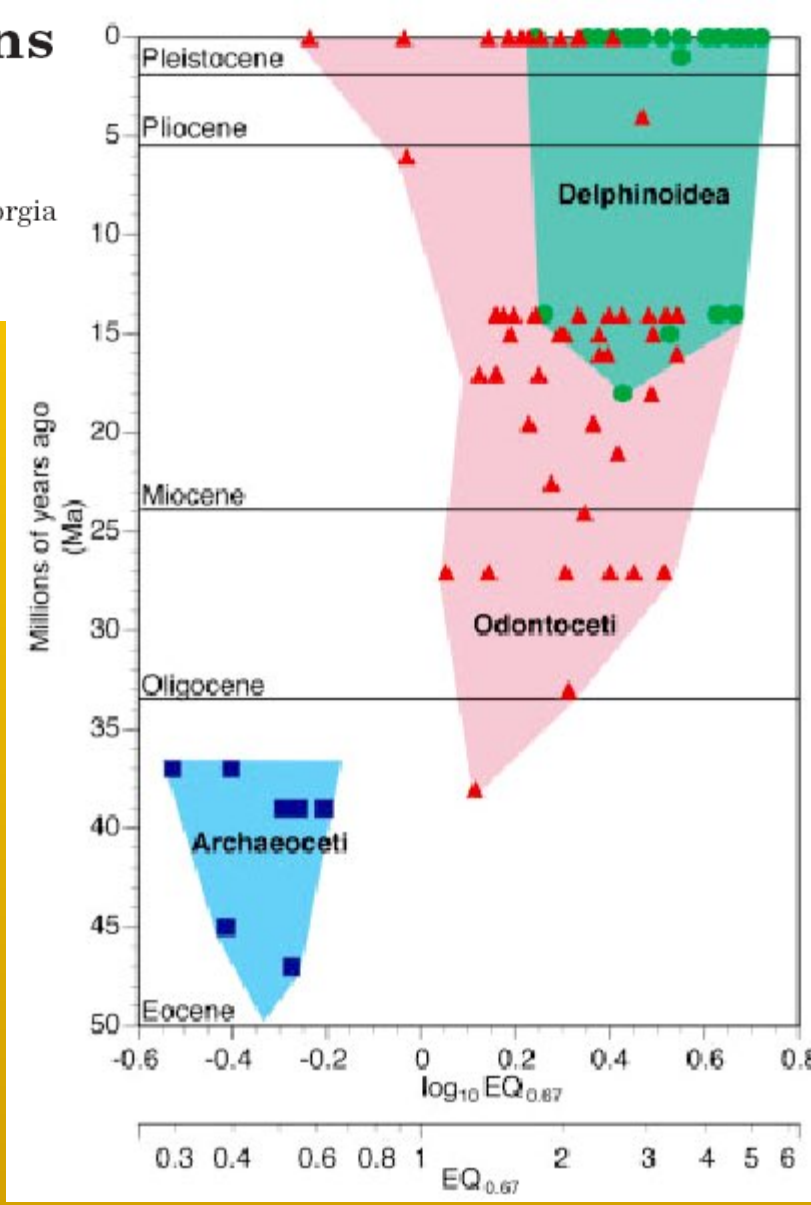

Fig. 1. **A:** Photograph of early-mid Miocene fossil odontocete (*Rhabdosteus longirostris*, USNM 187213). **B:** Coronal 1.22 mm thick CT image of the same specimen showing differentiation of the hardened matrix that fills the endocranial area and the surrounding bone.

Brain Behav Evol 2000;56:204–211

Relative Volume of the Cerebellum in Dolphins and Comparison with Anthropoid Primates

Lori Marino[a] James K. Rilling[b] Shinko K. Lin[c] Sam H. Ridgway[d]

[a]Neuroscience and Behavioral Biology Program, [b]Department of Psychiatry and Behavioral Sciences, [c]Department of Biology, Emory University, Atlanta, Ga., [d]Navy Marine Mammal Program, San Diego, Calif., USA

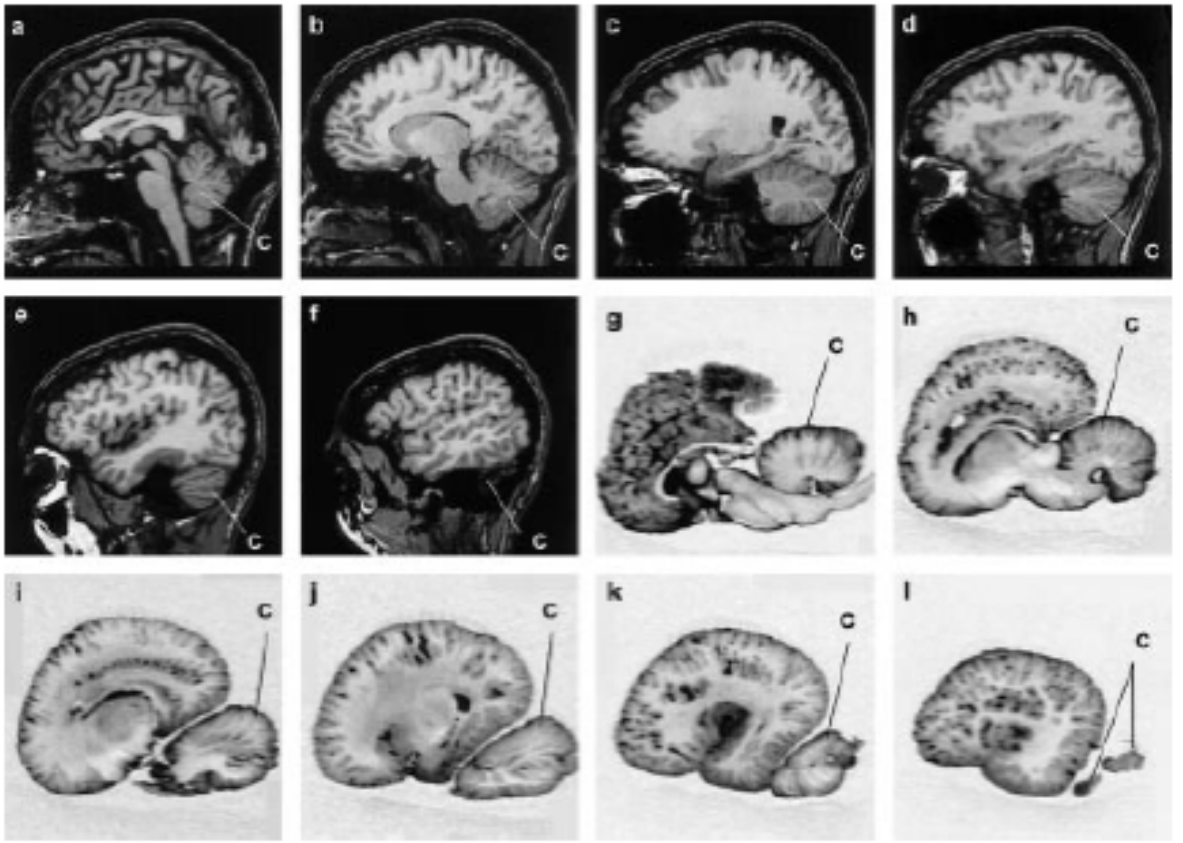

Fig. 1. Sagittal Magnetic Resonance Imaging-based slices through one hemisphere of a living human (a–f) and a post-mortem bottlenose dolphin (g–l) brain. In both brains images span the entire medial to lateral extent of the cerebellum. The 1.2 mm thick human slices (a–f) are 0 mm, 10.8 mm, 21.6 mm, 32.4 mm, 43.3 mm, and 54 mm lateral of the mid-sagittal plane, respectively. The 2 mm thick dolphin slices (g–l) are 0 mm, 12 mm, 24 mm, 36 mm, 48 mm, and 60 mm lateral of the midsagittal plane, respectively. Total brain volume for the human is 1330.00 cm^3 and for the dolphin 1420.50 cm^3. C = Cerebellum.

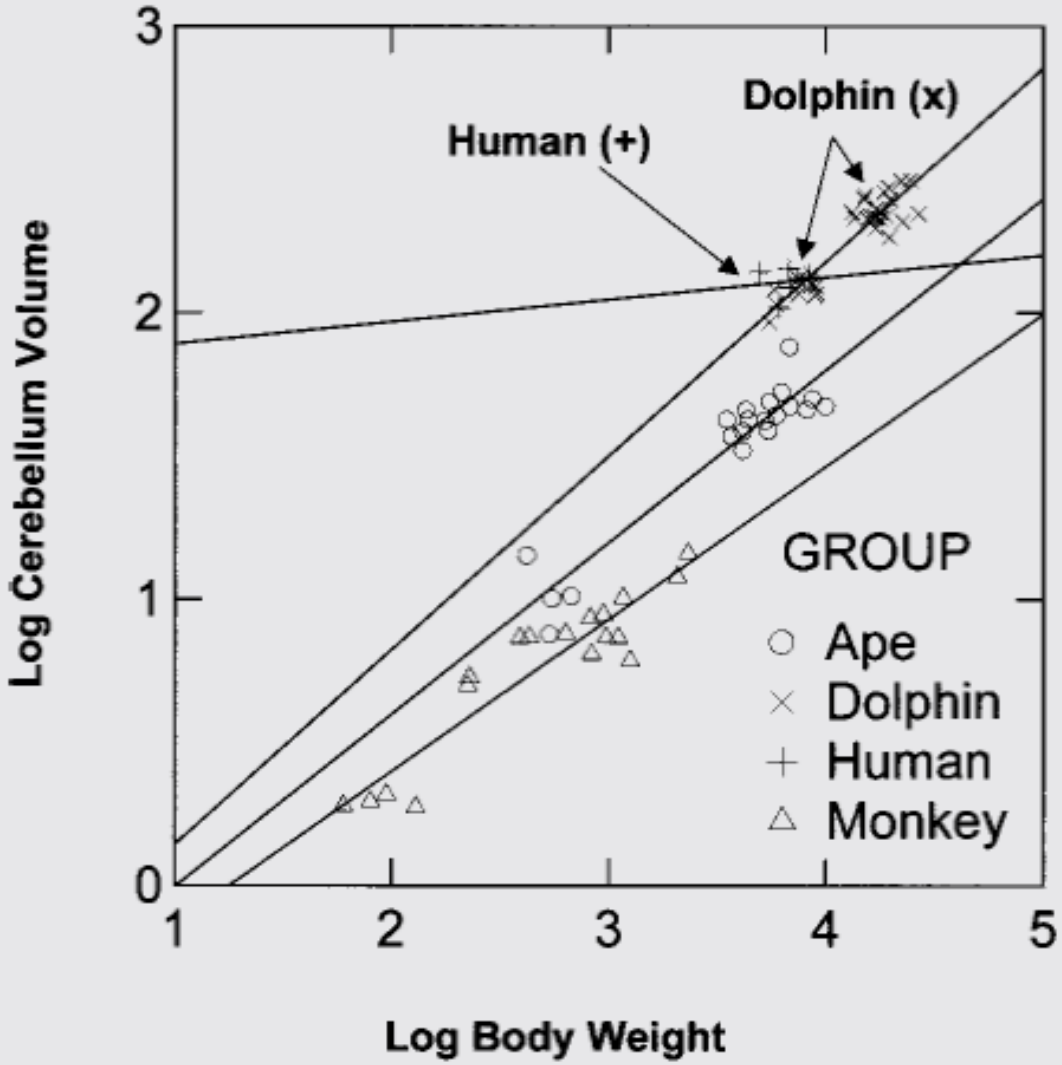

Fig. 4. Separate least squares regression lines for log cerebellum volume on log body weight for the dolphin, ape, human, and monkey groups.

- **Cerebellum 15% mayor**
- Paulin [1993] has speculated that the cerebellum is best characterized as a dynamic system for tracking the flow of incoming and outgoing sensory and motor information.
- This kind of 'dynamical state estimation' is not unlike the kind of processing that occurs during echolocation. In echolocation high frequency sound waves are emitted by the animal and the echoes from these emissions.

Physeter macrocephalus

Formación Pisco (Mioceno - Plioceno)

Images: NASA; Muizon, 1988, Lambert et al. (2008) CR Palevol; Lambert et al. (2010) Nature

Brachydelphis mazeasi

Lomacetus ginsburgi

Acrophyseter

Platanistoidea

Delphinida Ziphioidea Physeteroidea

Ziphiidae

Mesoplodon

Delphinidae

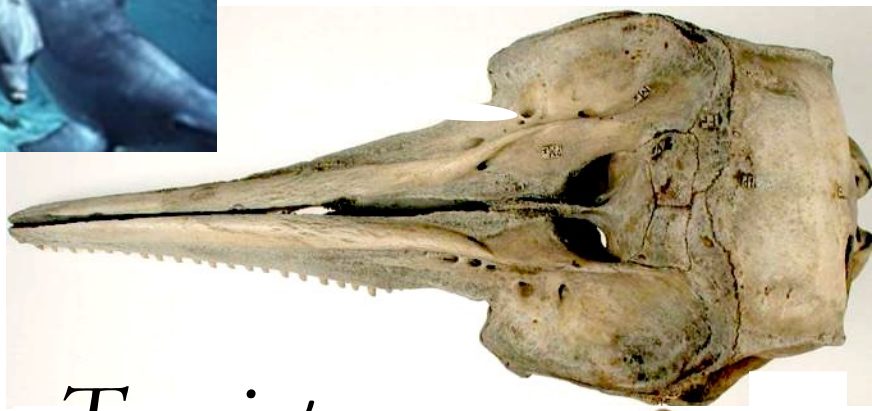

Tursiops

Hyperodon

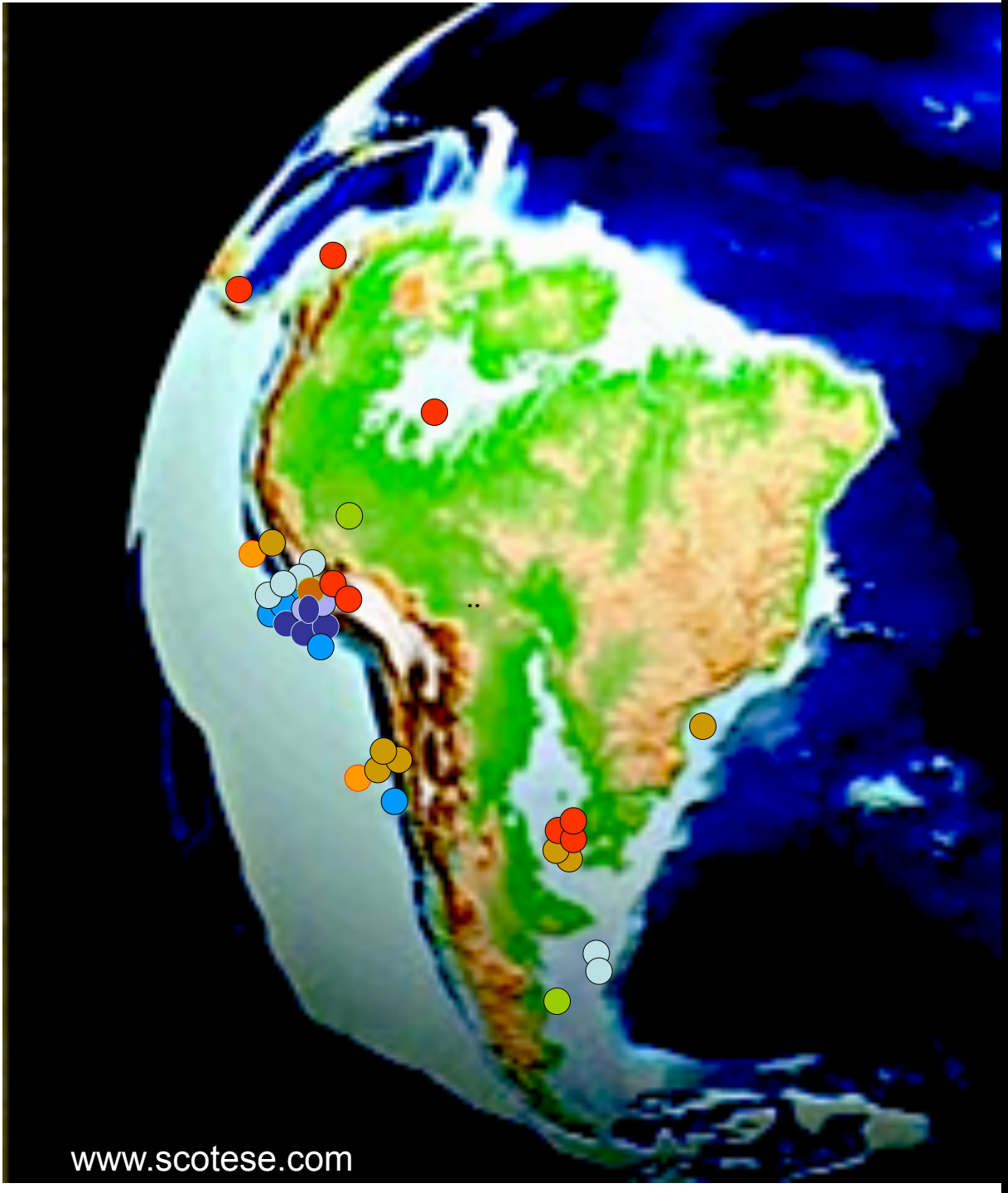

www.scotese.com

Platanistoidea

- Platanistoidea

Delphinoidea

- Phocoenidae
- Kentriodontidae
- Monodontidae
- Delphinidae

Inioidea/Lipotoidea

- Pontoporiidae
- Iniidae
- Lipotidae
- *Brachydelphis*

Pontoporiidae

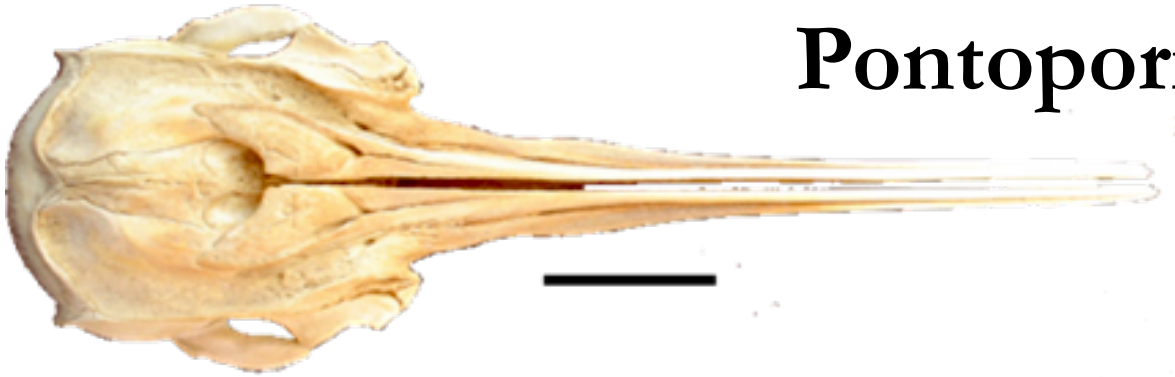

Pliopontos

Pontoporia blainvillei

delfin de la plata

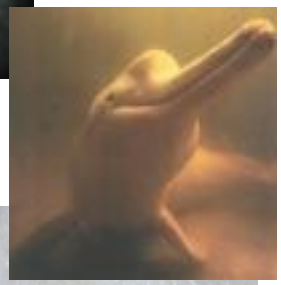

Iniidae

Inia geoffrensis

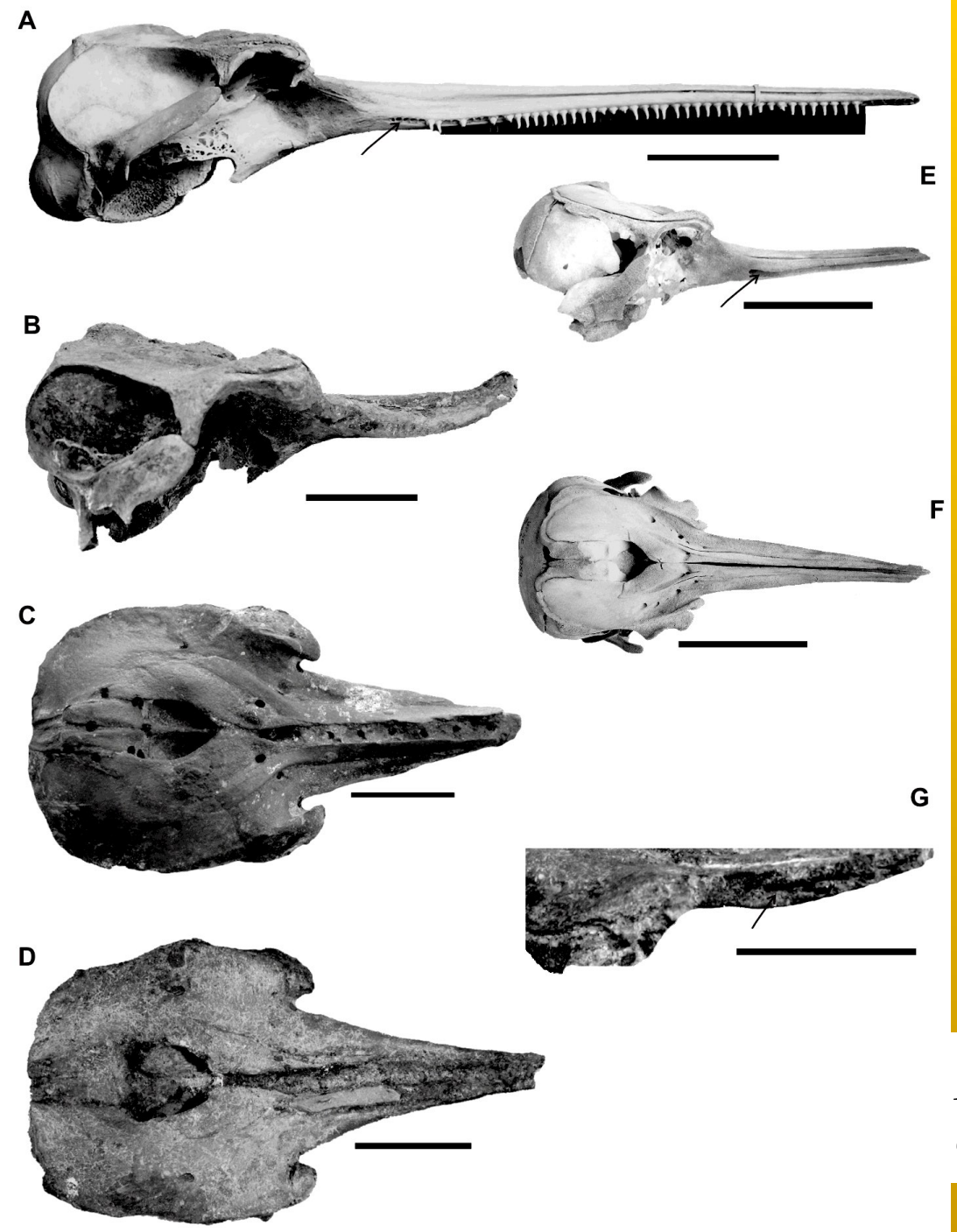

Brachydelphis mazeasi

Gutstein et al. 2009. J. Mammal.

Brachydelphis
new form

medial groove on palate that shows the premaxilla,

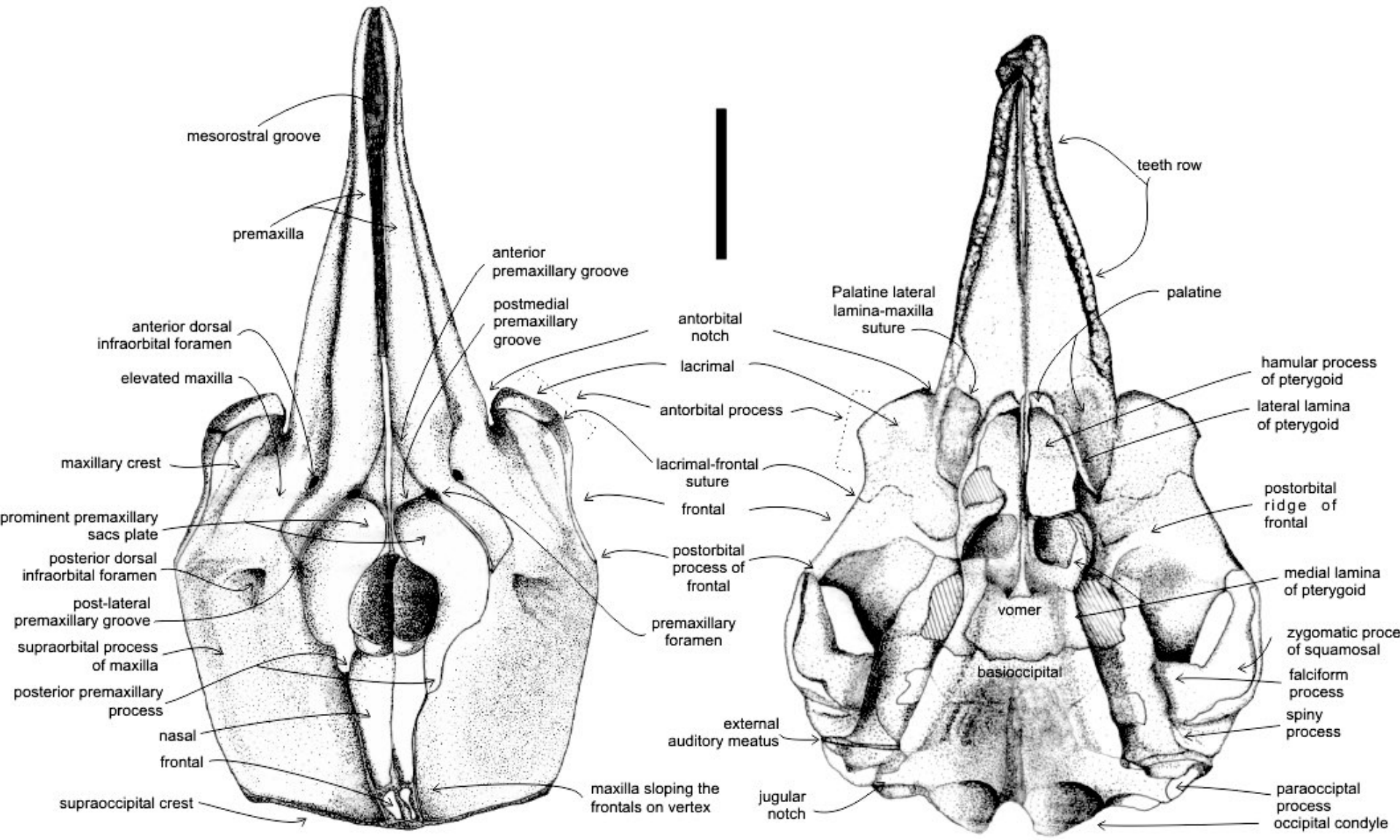

Brachydelphis mazeasi

Gutstein et al. 2009. J. Mammal.


MEERESAKROBATEN.DE

Orca

Orcinus orca
Comprimento 10 metros
Massa 8.200 kg

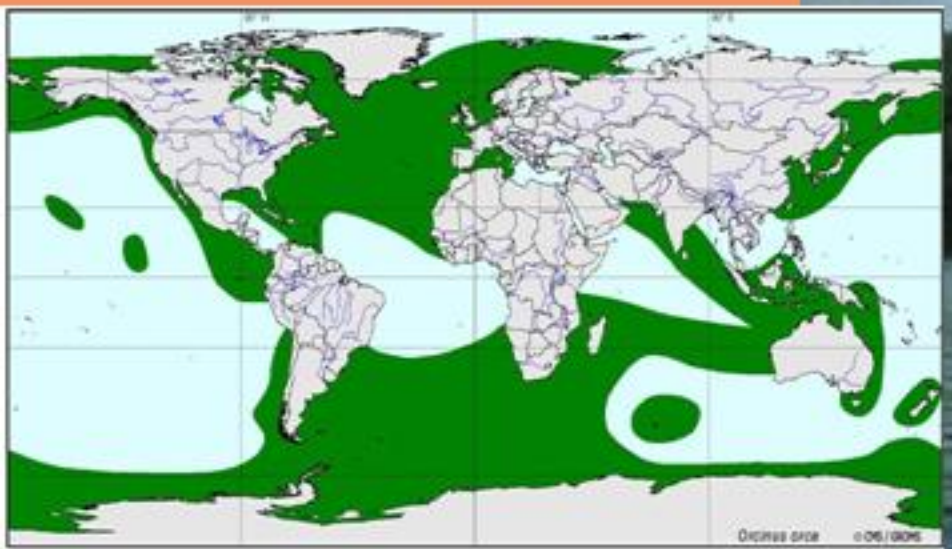

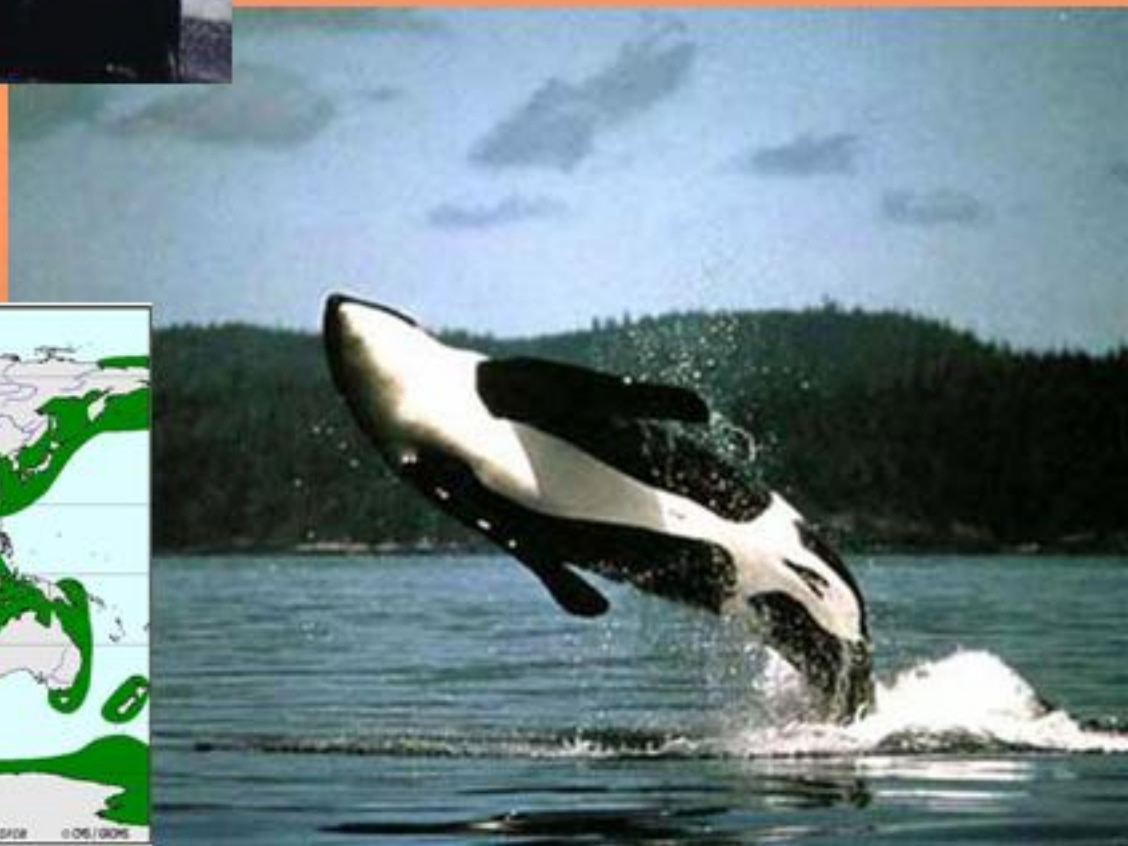


Platanista gangetica
Inia geoffrensis

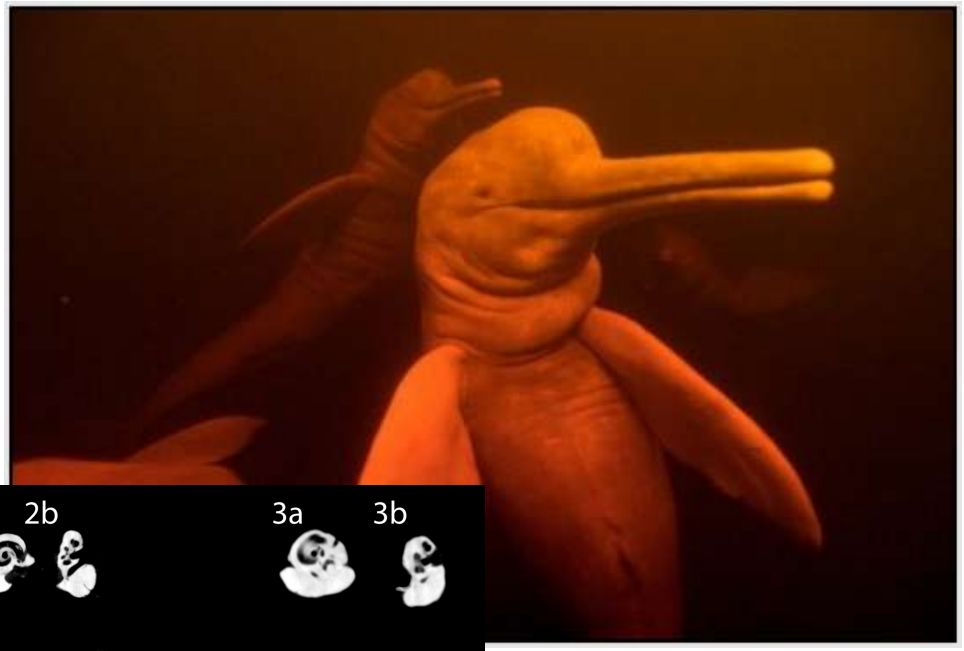

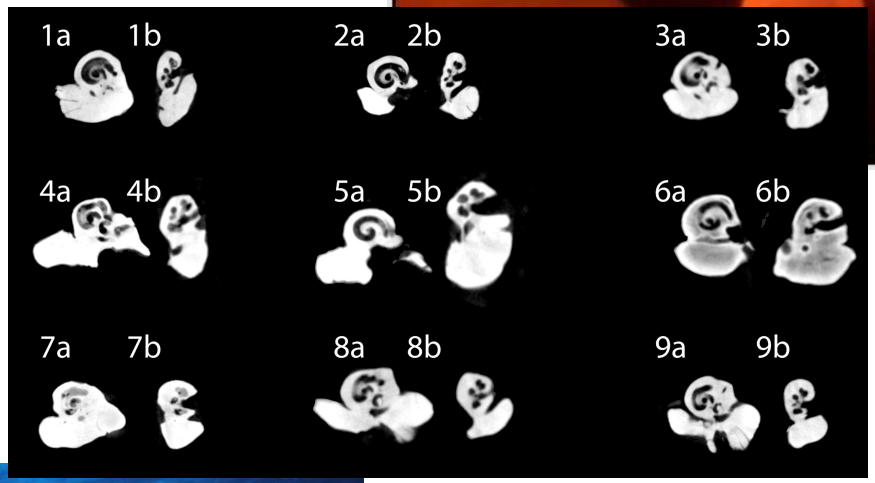
1a 1b
2a 2b
3a 3b
4a 4b
5a 5b
6a 6b
7a 7b
8a 8b
9a 9b


Brachydelphis maseazi

Odobenocetops leptodon

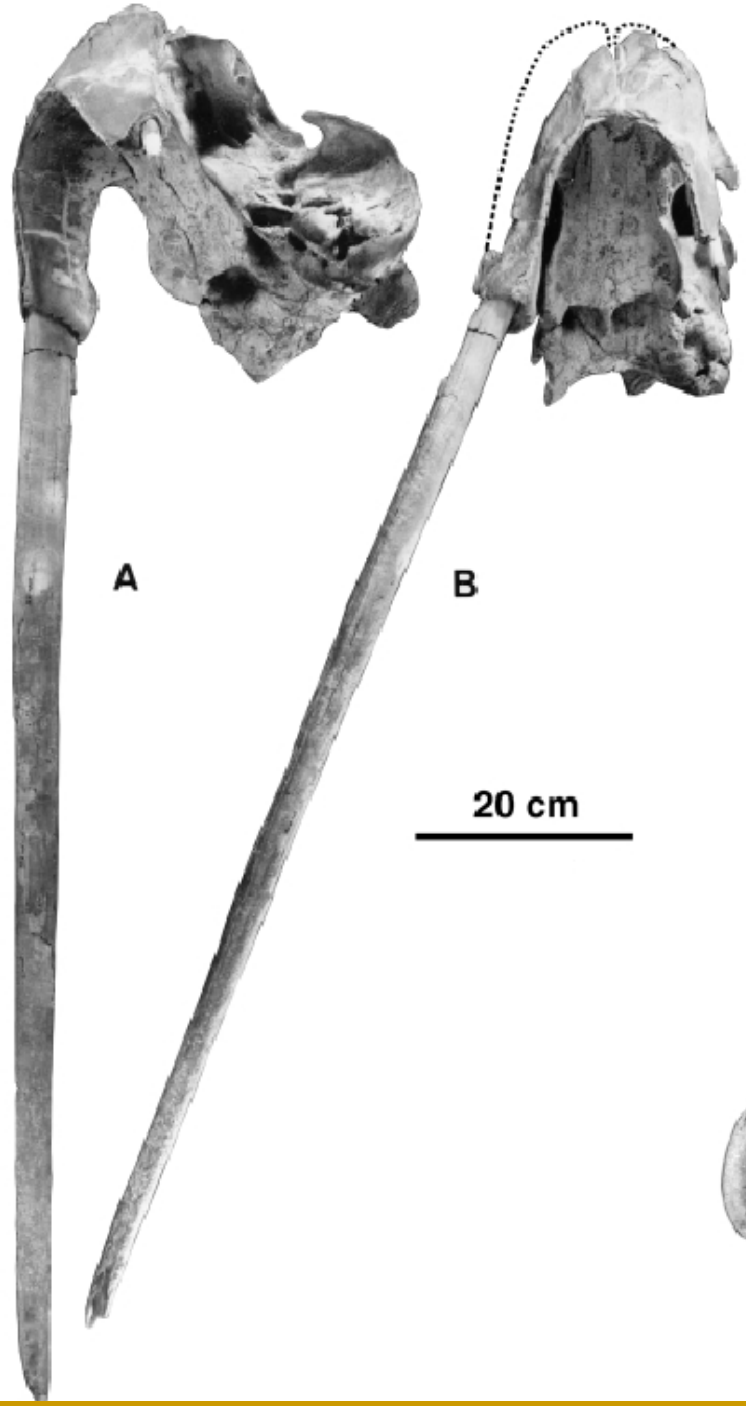
A
B
20 cm

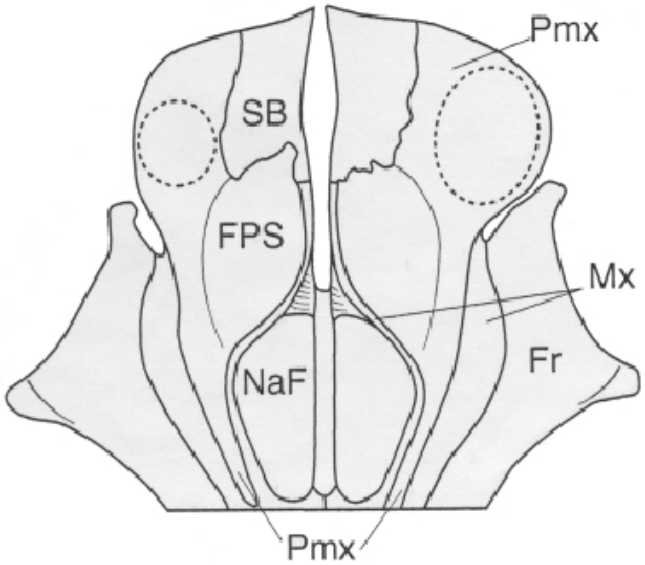
Pmx
SB
FPS
Mx
Fr
NaF
Pmx

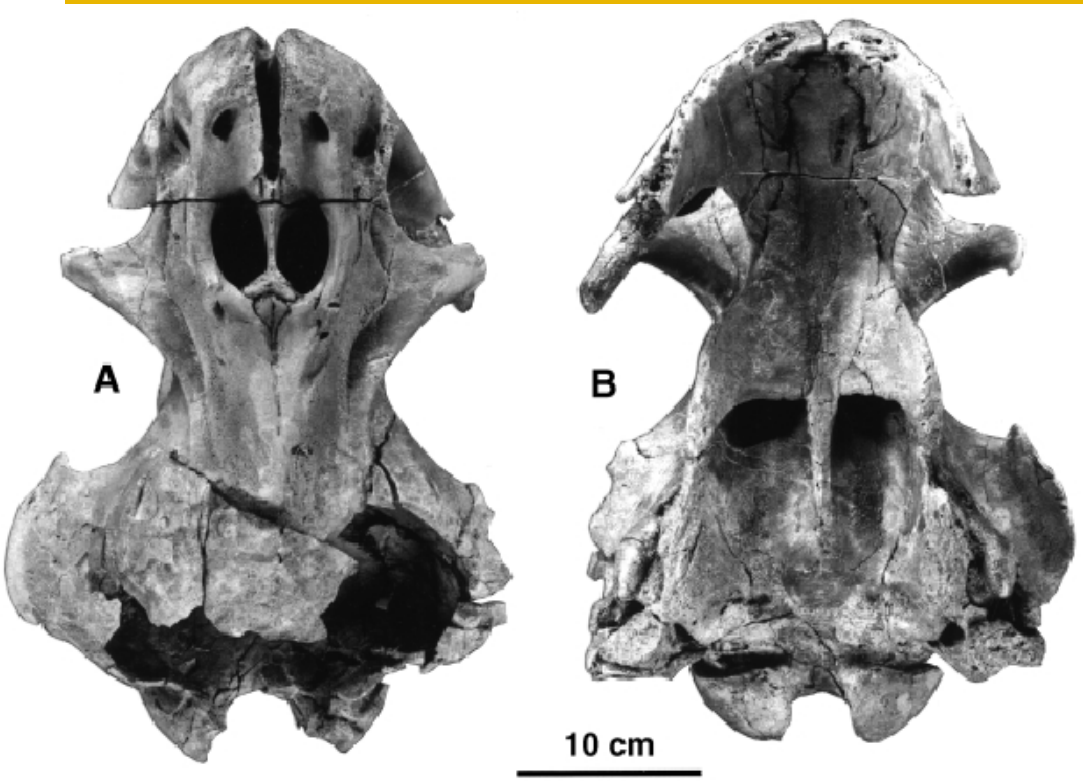
A
B
10 cm

Fin!!